Vector meson properties in a strongly interacting thermal medium

Mohammed Shahpur Mia

Department of Physics

McGill University

Montreal, Québec

CANADA

May 8, 2007

A thesis submitted to the

Faculty of Graduate Studies and Research

in partial fulfillment of the requirements

for the degree of Master of Science

© Mohammed Shahpur Mia, 2007

Library and Archives Canada

Published Heritage Branch

395 Wellington Street
Ottawa ON K1A 0N4
Canada

Bibliothèque et Archives Canada

Direction du Patrimoine de l'édition

395, rue Wellington
Ottawa ON K1A 0N4
Canada

Your file Votre référence
ISBN: 978-0-494-32754-8
Our file Notre référence
ISBN: 978-0-494-32754-8

NOTICE:
The author has granted a non-exclusive license allowing Library and Archives Canada to reproduce, publish, archive, preserve, conserve, communicate to the public by telecommunication or on the Internet, loan, distribute and sell theses worldwide, for commercial or non-commercial purposes, in microform, paper, electronic and/or any other formats.

The author retains copyright ownership and moral rights in this thesis. Neither the thesis nor substantial extracts from it may be printed or otherwise reproduced without the author's permission.

AVIS:
L'auteur a accordé une licence non exclusive permettant à la Bibliothèque et Archives Canada de reproduire, publier, archiver, sauvegarder, conserver, transmettre au public par télécommunication ou par l'Internet, prêter, distribuer et vendre des thèses partout dans le monde, à des fins commerciales ou autres, sur support microforme, papier, électronique et/ou autres formats.

L'auteur conserve la propriété du droit d'auteur et des droits moraux qui protège cette thèse. Ni la thèse ni des extraits substantiels de celle-ci ne doivent être imprimés ou autrement reproduits sans son autorisation.

In compliance with the Canadian Privacy Act some supporting forms may have been removed from this thesis.

While these forms may be included in the document page count, their removal does not represent any loss of content from the thesis.

Conformément à la loi canadienne sur la protection de la vie privée, quelques formulaires secondaires ont été enlevés de cette thèse.

Bien que ces formulaires aient inclus dans la pagination, il n'y aura aucun contenu manquant.

Canada

Acknowledgment

First and foremost I would like to thank my supervisor Professor Charles Gale for being there when it was mostly needed and for believing in me. I am grateful to Professor Guy Moore and Professor Sangyong Jeon for numerous discussions and guidances over the last couple of years. I must thank all my office mates and fellow students in the Nuclear Theory Group including Simon Turbide, Alexandre Bourque, Jean-Sebastien Gagnon and Jean Marie-Robert for being patient with my questions and providing continuous help with useful discussions. I am highly in debt to Qin Guangyou for his vital role in the numerics; without his tireless efforts, the numerical calculations would not have been possible.

Abstract

We analyze the hadronic phase of QCD using effective thermal field theory techniques. Our goal is to investigate the medium created in heavy ion collisions by calculating the electromagnetic emissivity of strongly interacting matter in the hadronic phase. We proceed through examining the vector meson properties in a thermal bath where the temperature reaches deconfinement and chiral symmetry is restored. In particular we observe the behavior of the ρ spectral function in thermal medium and use it as a probe to examine the thermal environment generated in the collision.

Résumé

Nous analysons la phase hadronique de la chromodynamique quantique (QCD) avec des méthodes de théorie des champs effective. Notre but est de characteriser le milieu créé dans les collisions relativistes d'ions lourds, en considénant l'émissivité electromagnétique. Nous examinons les propriétés du ρ dans un milieu thermique en interaction forte en calculant sa distribution spectrale. Celle-ci a un lien direct avec les mesures experimentales du spectre de paires de leptons.

Contents

1 Introduction **6**

2 Thermal Field Theory and QCD **10**

2.1 Bosons and Fermions 10

2.2 Path Integral and Operator Formalism in Imaginary Time 13

2.2.1 Frequency Sums 21

2.2.2 Self-Energy and Scattering Amplitudes 29

3 Symmetries and Currents **33**

3.1 Noether Current 33

3.2 Chiral Symmetry 34

3.2.1 Chiral Symmetry of QCD 35

3.3 Symmetry Breaking 36

3.3.1 Spontaneous Symmetry Breaking in LSM 36

3.3.2 Explicit Symmetry Breaking in LSM 38

3.3.3 Gauged LSM and Vector Meson Dominance 38

3.3.4 The Wess-Zumino-Witten Anomaly Action 41

3.4 Weinberg Sum Rules 42

3.4.1 Consequences 45

4 ρ Meson in Medium **46**

4.1 Effective Field Theory 46

4.1.1 Interaction Lagrangians 47

4.2 Self-Energies 48
4.2.1 Zero Temperature Contribution 53
4.2.2 Finite Temperature Contribution 57
4.2.3 The Parameters 58
4.2.4 Thermal Mass and Spectral Functions 60
4.2.5 Self-Energy and Scattering Amplitude for Vector Particles . . 65
4.3 Self-Energy at Higher Orders in the Interaction 68

5 Conclusions **81**

List of Figures

1.1 Phase Diagram of QCD [6] 7

4.1 Various Feynman diagrams of the ρ self-energies considered 48

4.2 Real self-energy for zero three momentum of ρ due to baryons and baryon resonances at T=120 MeV 61

4.3 Real part of self-energy for zero three momentum of ρ due to free mesons at T=120 MeV 61

4.4 Real transverse self-energy due to free mesons at ρ three momentum 300 MeV, T=120 MeV 63

4.5 Real longitudinal self-energy due to free mesons at ρ three momentum 300 MeV, T=120 MeV 63

4.6 Imaginary longitudinal self-energy due to free mesons at ρ three momentum 300 MeV, T=120 MeV 64

4.7 Transverse Spectral Function due to mesons as a function of M_ρ for various temperature and the vacuum value at ρ three momentum 300 MeV 66

4.8 Longitudinal Spectral Function due to mesons as a function of M_ρ for various temperature at ρ three momentum 300 MeV 66

4.9 Feynman Diagram for the interaction theory 69

4.10 Comparisons of a_1 spectral functions 70

4.11 Real part of transverse self-energy as a function of M for T=120 MeV including mesons with width 73

4.12 Real part of longitudinal self-energy as a function of M for T=120 MeV including mesons with width 73
4.13 Real part of transverse self-energy as a function of M for T=120 MeV including baryons with width 74
4.14 Real part of transverse self-energy as a function of M for T=120 MeV including baryons with width 74
4.15 Imaginary part of transverse self-energy as a function of M for T=120 MeV including mesons with width 75
4.16 Imaginary part of longitudinal self-energy as a function of M for T=120 MeV including mesons with width 75
4.17 Imaginary part of transverse self-energy as a function of M for T=120 MeV including baryons with width 76
4.18 Imaginary part of longitudinal self-energy as a function of M for T=120 MeV including baryons with width 76
4.19 Transverse Spectral Function including interacting mesons 78
4.20 Transverse Spectral Function including interacting mesons and baryons 78
4.21 Longitudinal Spectral Function including interacting mesons 79
4.22 Longitudinal Spectral Function including interacting mesons and baryons 79

Chapter 1

Introduction

The investigation of matter under extreme conditions is one of the most crucial fields in physics as it reveals the dynamics of the most fundamental constituents of nature. The highly dense system created by heating ordinary matter up to a trillion degrees Kelvin not only mimics our infant universe but also introduces a possible new phase of matter, a plasma of quarks and gluons[1]. In heavy ion colliders like the Relativistic Heavy Ion Collider (RHIC) and the Large Hadron Collider (LHC) such systems are generated through colliding nuclei at extremely high energies. Asymptotic freedom indicates that the strong coupling at very high energies becomes negligible thus matter generated by the collision is likely to contain deconfined free quarks and gluons right after the collision. But lattice calculations [1] predict significant deviation from the properties of an ideal gas consisting of free quarks and gluons and the new phase is referred to as the Quark-Gluon Plasma (QGP). The standard model predicts the phase diagram as shown in Fig 1.1, but questions remain about the order of the transition and precise location of the phase boundary. In particular the order depends on the number of flavors for the quarks and their masses. In addition the diagram contains the hadron gas phase, Color Flavor Locked (CFL) phase, 2SC phase, and the QGP phase.

Tantalizing problems which have generated a great deal of interest among both theoretical and experimental physicists are: what are the signatures of QGP and how distinct a phase is this from the known phases of matter? Several observable have been

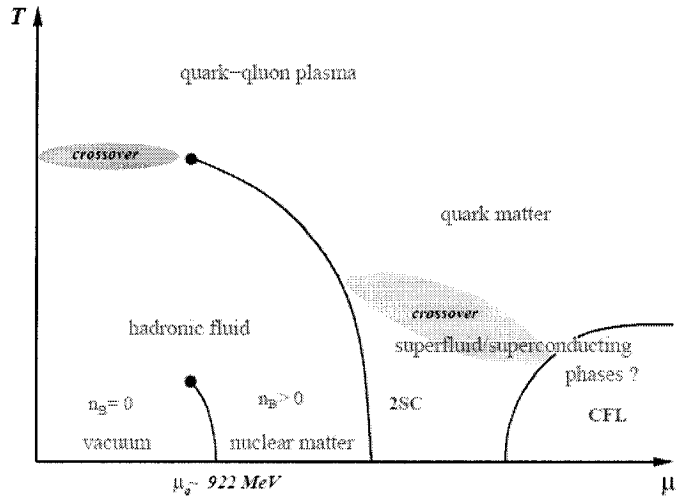

Figure 1.1: Phase Diagram of QCD [6]

proposed [2] to probe the QGP; strangeness enhancement [3], J/Ψ suppression [4] and electromagnetic radiation [5] are the leading ones. Whereas all the above are effective to some extent, the probe which has the least final state interaction is the most clear signal coming from the initial state of the created medium. As electromagnetic radiation couples least to the medium after initial production, it is a privileged probe which contains vital information about the very early stages of the collision and opens up possible windows to study the QGP. Electromagnetic radiation comprises emission of dileptons and photons. Calculations for the dileptons and photon emission rates show [7] [8] that it involves computing the photon self-energy in medium, thus the rates reflect properties of the system created in the collision. The radiation emitted from various sources in the medium created from the collision resides in the different phases of QCD. Low invariant mass dileptons emerge primarily from quark anti quark $q\bar{q}$, $\pi^+\pi^-$ or low mass hadron annihilation [9], the first one coming from possible QGP while the rest from hadronic phase. As discussed in [10] the photon signal coming from the QGP is outshined by the photons coming from hadrons at SPS energies and temperatures. Thus we are left with the dilepton signal as a probe to QGP for SPS energies and temperatures which are also the relevant range for our calculation.

In this thesis our goal is to study in medium ρ properties accessible through

measurement of the dilepton production rate coming from the hadronic phase, in particular $\pi^+\pi^-, \pi + h, N + R$ annihilation where $h = a_1, f_1, k_1, h_1, \omega, \pi'$, N is a nucleon and R is a resonance. This is insightful to the QGP as if the observed rate is different from calculated hadronic rate, it could indicate that signals are coming from QGP. As the rate calculation involves computing the imaginary part of the self-energy and thus the spectral function for the ρ propagator [11], we compute the ρ spectral function in a medium enriched with mesons and baryons.

Attempts have been made in calculating the ρ spectral function [12] [13] [14] [15][16]. In [12] [13] only $\rho\pi\pi$ interaction is considered and the π self-energy is accounted for by using model of particle-hole excitation [17] extended to finite temperature [18]. In [14] the same is done for $\rho\pi\pi$ and ρNR interaction where N is a nucleon and R is a nucleon or a resonance. Furthermore [14] includes ρ interacting in a meson gas consisting of K, K_1, a_1 and the ρ self-energy coming from these interactions are computed through using the relation between self-energy and scattering amplitude [19][20] . In [15] interaction with the meson gas is extended by considering mesons f_1, h_1, π', ω in addition to π, K, K_1, a_1 and coupling constants are fixed to produce experimental widths.Ref.[16] uses the same relation between scattering amplitude and self-energy [19][20] to compute ρ spectral function considering ρ interacting with π and nucleons. Here, the scattering amplitudes are matched to experimental data with low energy regime modeled in terms of resonance and background while high energy regime is described by Regge model. All the approaches above are based on models and extracting self-energy from scattering amplitudes, which is only a leading order behavior of the self-energy [19]. Ours is a direct calculation of the Feynmann diagrams corresponding to the ρ self-energy, using explicit expressions for propagators and vertices. Our coupling constants reproduce experimental widths just as in [15], but unlike [15] we have considered both mesons and baryons. Thus our treatment is more formal and complete than the previous attempts.

By observing the properties of the spectral functions we can comment on the dilepton rates and indirectly on the QGP. The NA60 experiment at CERN [21] has measured dilepton spectra at invariant dilepton mass range relevant to our calculation.

Our prediction for the spectral function may turn out to be vital in understanding the results of the experiment. Furthermore, many-body effects considered in the hadronic phase aid to quantify the properties of the produced medium and thus are important in their own right. Finally, we want to learn how chiral symmetry is restored. Chiral symmetry is an exact symmetry in the vanishing quark mass limit. At low temperature it is spontaneously and explicitly broken which gives rise to massive pions. At higher temperatures when masses become negligible compared to momentum, chiral symmetry is restored. The Weinberg sum rules [22] [8] imply that in the high temperature limit where chiral symmetry is restored, the difference between axial and vector spectral functions vanishes. We study the behavior of the in medium ρ spectral function as temperature is increased up to the phase boundary of deconfinement and comment on chiral symmetry restoration using the sum rules.

The thesis is divided into five chapters. In chapter two we present a brief review of finite temperature field theory and develop the tools vital for our calculation. In chapter three, we discuss the origins of our Lagrangian with a review on chiral symmetry and also present the sum rules and their implications on the spectral functions. Chapter four describes our calculations for the spectral function in detail and contains the results obtained. We conclude the thesis with a discussion of our results and of their implications.

Chapter 2

Thermal Field Theory and QCD

In quantum field theory, elementary particles are described by field operators $\hat{\Phi}$ whose action on the vacuum state generates the particle; $\hat{\Phi}(x)|0>$ is the state of a $\hat{\Phi}$ particle at location x, where x is a four vector (of course this is not a physical state because of the uncertainty principle). In the Heisenberg picture the $\hat{\Phi}$ operator evolves in time and the evolution is governed by the Euler Lagrangian equation.

In describing the thermal medium produced in a heavy ion collision the most relevant quantity we are interested in is the amplitude $< 0|\hat{\Phi}(x)\hat{\Phi}(y)|0 >$ for particle Φ to propagate from y to x; this quantity is the propagator. Our goal is to study the medium by analyzing the amplitude and other quantities crucial in describing the heat bath. In the following sections we describe the related quantities essential for our treatment of the medium.

2.1 Bosons and Fermions

The fundamental particles in nature are divided into two groups; integer-spin bosons and half integer spin fermions. A system of N bosons are symmetric under the interchange of any pair of states whereas fermions are antisymmetric [34]. That is if P_{ij} is the permutation operator which interchanges states i, j, i.e.

$$P_{ij}|k_1\rangle_1|k\rangle_2..|k_i\rangle_i...|k_j\rangle_j.....|k_N\rangle_N \;=\; |k_1\rangle_1|k_2\rangle_2..|k_j\rangle_i...|k_i\rangle_j.....|k_N\rangle_N$$

$$P_{ij}|p_1\rangle_1|p_2\rangle_2..|p_i\rangle_i...|p_j\rangle_j.....|p_N\rangle_N = -|p_1\rangle_1|p_2\rangle_2..|p_j\rangle_i...|p_i\rangle_j.....|p_N\rangle_N$$

where $|k\rangle_l$ is l'th boson and $|p\rangle_l$ is l'th fermion state; so the permutation interchanged the state of i'th and j'th particles. Now if we have boson fields Φ's and fermion field Ψ's (2.1) implies

$$\begin{aligned} P_{12}|\Phi_1(r)\Phi_2(s)\rangle &= P_{12}\Phi_1(r)\Phi_2(s)|0\rangle|0\rangle \\ &= \Phi_1(s)\Phi_2(r)|0\rangle|0\rangle \qquad (2.1) \\ P_{12}|\Psi_1(r)\Psi_2(s)\rangle &= P_{12}\Psi_1(r)\Psi_2(s)|0\rangle|0\rangle \\ &= -\Psi_1(s)\Psi_2(r)|0\rangle|0\rangle \qquad (2.2) \end{aligned}$$

where (r, s) is either position (x, y) or momentum (p, k). Now for identical particles $\Phi_i = \Phi$, $\Psi_i = \Psi$ and we have the commutation or anti-commutation relation for bosons or fermions

$$[\Phi(r), \Phi(s)] = 0 \qquad (2.3)$$

$$\{\Psi(r), \Psi(s)\} = 0 \qquad (2.4)$$

The relativistic relation between energy (k_0) and momentum $(\vec{k})$ is given by $k_0^2 = \vec{k}^2 + m^2$; in terms of quantum mechanical operator with $k_\mu = -i\partial_\mu$ with $\mu = 0, 1, 2, 3$ this equation turns into the Klein-Gordon equation

$$(\partial^2 + m^2)\xi(\mathbf{x}, t) = 0 \qquad (2.5)$$

where $\xi(\mathbf{x}, t)$ is any field. Note that any field must satisfy the Klein-Gordon equation as it is just the relativistic definition of energy. In quantum field theory we replace the field $\xi(\mathbf{x}, t)$ with the field operator $\hat{\xi}(\mathbf{x}, t)$ and denote the eigenstate of the field operator to be $|\xi\rangle$

$$\hat{\xi}(\mathbf{x}, \mathbf{t})|\xi\rangle = \xi(\mathbf{x}, \mathbf{t})|\xi\rangle \qquad (2.6)$$

where the quantum field states $|\xi\rangle$ obey the orthogonality and completeness relations[8]

$$\begin{aligned} \int d\xi(\mathbf{x})|\xi\rangle\langle\xi| &= 1 \\ \langle\xi_a|\xi_b\rangle &= \delta[\xi_a(\mathbf{x}) - \xi_\mathbf{b}(\mathbf{x})] \qquad (2.7) \end{aligned}$$

where the index a is to distinguish different ξ fields. $t = 0$ represents the Schroedinger operator while the time dependent operator is the Heisenberg operator

$$\hat{\xi}(t, \mathbf{x}) = e^{i\hat{H}t}\hat{\xi}(\mathbf{x})e^{-i\hat{H}t} \tag{2.8}$$

As physics should be unchanged under boost or rotation of frames, Lorentz invariance is required; this forces our Lagrangian to be a Lorentz scalar. Using Lorentz-scalar Lagrangian and commutation relations (2.3) we find the fields describing the bosons and fermions. A Lorentz-invariant Lagrangian for the scalars gives the Klein-Gordon equation with $\xi = \phi$ the scalar field. For spin one vectors A^μ we have the subsidiary condition

$$\begin{aligned} (\partial^2 + m_A^2)A^\mu &= 0 \\ \partial_\mu A^\mu &= 0 \end{aligned} \tag{2.9}$$

where $\mu = 0, 1, 2, 3$ and A^μ is a rank one tensor with four components, three of them being independent, describing three spin degrees of freedom.

The Lorentz group has representation in $n = 2s+1$ dimensions where s is the spin of the particle [36]. One representation of the Lorentz group in n dimension are $n \times n$ Dirac matrices γ^μ where $\mu = 0, 1, 2, 3$ are space-time index. These Dirac matrices satisfy Dirac algebra

$$\{\gamma^\mu, \gamma^\nu\} = 2g^{\mu\nu} \times \mathbf{1}_{n\times n} \tag{2.10}$$

For four dimensional Minkowski space and spin half fermions we expect four 2×2 Dirac matrices satisfying the algebra (2.10). Choosing Pauli matrices to be three of them $\gamma^l \equiv i\sigma^l$, $l = 1, 2, 3$ we see that there is no fourth 2×2 matrix which can satisfy (2.10) [36]. Thus we must have 4×4 matrices representing Dirac algebra corresponding to spin half Dirac fermions. Thus Lorentz invariance demands spin half ψ field to be a four component spinor which satisfies the Dirac equation

$$(i\gamma^\mu\partial_\mu - m)\psi(x) = 0 \tag{2.11}$$

which also satisfy the Klein-Gordon equation. For higher spin $k + 1/2$ fermions we use the Rarita-Schwinger fields $\Psi_{\mu_1\ldots\mu_k}$ which have mixed transformation properties

of four component Dirac spinor and rank k tensor [35]. Each component of the tensor is a four component Dirac spinor. The Rarita-Schwinger fields satisfy the equation [35]

$$\begin{aligned}(i\gamma^{\nu}\partial_{\nu} - m_{\Psi})\Psi_{\mu_1\ldots\mu_k} &= 0 \\ \gamma_{\alpha}\Psi_{\alpha\mu_2\ldots\mu_k} &= 0\end{aligned} \tag{2.12}$$

2.2 Path Integral and Operator Formalism in Imaginary Time

In order to compute propagation amplitude there are two methods which can be applied. Our goal is to evaluate the expectation value of product of operators in a thermal medium. At nonzero temperature the probability of an observable s with energy E_s appearing in a system is proportional to the Boltzmann factor $e^{-E_s/T}$ and the proportionality constant is the inverse of the partition function. In quantum field theory we replace observables with expectation values of field operators; then the thermal average of a field operator $\hat{O}$ becomes [31]

$$\begin{aligned}\langle\hat{O}\rangle_{\beta} &= \frac{\mathrm{Tr}(\hat{O}e^{-\beta\hat{H}})}{Z(\beta)} \\ Z(\beta) &= \mathrm{Tr}e^{-\beta H} = \sum_n e^{-\beta E_n}\end{aligned} \tag{2.13}$$

where $Z(\beta)$ is the partition function, $\beta = 1/T$ and E_n are eigenvalues of energy eigenstates $|n\rangle$ of the Hamiltonian $\hat{H}$; that is $\hat{H}|n\rangle = E_n|n\rangle$. We can write the partition function as a path integral as follows. We find the matrix representation of $\hat{H}$ using eigenstates $|\xi\rangle$ of the field operator $\hat{\xi}$ as basis in the Schroedinger picture.

As we can have continuous number of fields in field space, the trace in the partition function is an integral

$$Z(\beta) = \int d\xi\langle\xi|e^{-\beta\hat{H}}|\xi\rangle \tag{2.14}$$

Now $e^{-\beta\hat{H}} = e^{-i(-i\beta)\hat{H}}$ is the time evolution operator in imaginary time which evolves a state by $t = -i\beta$. For bosons we have $\xi = \phi$ and the integrand is the amplitude of

a ϕ particle at $\mathbf{x}, t = 0$ coming back to $\mathbf{x}$ at $t = -i\beta$. This amplitude can be written as a path integral. First we define the conjugate momentum of the classical ϕ field by $\pi(\mathbf{x}) \equiv \frac{\partial \mathcal{L}}{\partial \dot{\phi}(\mathbf{x},\mathbf{t})}$ with the field operator $\hat{\pi}$ and the conjugate momentum states $|\pi\rangle$ having properties

$$\begin{aligned} \hat{\pi}(\mathbf{x},\mathbf{0})|\pi\rangle &= \pi(\mathbf{x})|\pi\rangle \\ \int \frac{d\pi(\mathbf{x})}{2\pi}|\pi\rangle\langle\pi| &= 1 \\ \langle\pi_a|\pi_b\rangle &= \delta[\pi_a(\mathbf{x}) - \pi_{\mathbf{b}}(\mathbf{x})] \end{aligned} \tag{2.15}$$

To compute the amplitude $\langle\phi_a|e^{-\beta H}|\phi_a\rangle$ we divide the pure imaginary interval$(0, -i\beta)$ into N equal subintervals $\triangle t = -i\beta/N$, use the property that $\lim_{N\to\infty}(e^{A/N}e^{B/N})^N = e^{A+B}$, then alternatively insert a complete set of conjugate momentum and field states in between every subinterval to get [8]

$$\begin{aligned} &\langle\phi_a|e^{-i\hat{H}(-i\beta)}|\phi_a\rangle = \lim_{N\to\infty}\int\left(\prod_{i=1}^{N}\frac{d\pi_i d\phi_i}{2\pi}\right) \\ &\times\langle\phi|\pi_N\rangle\langle\pi_N|e^{-i\hat{H}\triangle t}|\phi_N\rangle\langle\phi_N|\pi_{N-1}\rangle \\ &\times\langle\pi_{N-1}|e^{-i\hat{H}\triangle t}|\phi_{N-1}\rangle\times .. \\ &\times\langle\phi_2|\pi_1\rangle\langle\pi_1|e^{-i\hat{H}\triangle t}|\phi_1\rangle\langle\phi_1|\phi\rangle \\ &= \lim_{N\to\infty}\int\left(\prod_{i=1}^{N}\frac{d\pi_i d\pi_i}{2\pi}\right)\delta(\phi_1-\phi)\times \\ &\exp\left(i\triangle t\sum_{j=1}^{N}\int d^3x\left[\pi_j(\phi_(j+1)-\phi_j)/\triangle t - \mathcal{H}(\phi_j,\pi_j)\right]\right) \end{aligned} \tag{2.16}$$

where $\phi_{N+1} = \phi_1 = \phi_a$, $\chi_j = \chi(\mathbf{x}, (j-1)\triangle t)$, $\chi = \phi$ or π. In (2.16) we used the amplitude $\langle\phi|\pi\rangle = \exp[i\int d^3x\pi(\mathbf{x})\phi(\mathbf{x})]$, orthogonality of the fields and expanded the exponential [8]

$$\langle\pi_i|e^{-i\hat{H}\triangle t}|\phi\rangle \simeq (1 - i\hat{H}\triangle t)\exp\left[-i\int d^3x\pi_1(\mathbf{x})\phi_{\mathbf{i}}(\mathbf{x})\right] \tag{2.17}$$

Now in the continuous limit and with $t = -i\tau$ we have for the partition function

$$\begin{aligned} Z(\beta) &= \int[d\pi]\int_{\text{periodic}} d[\phi]\times\exp\Bigg[\int_0^\beta d\tau\int d^3x \\ &\left(i\pi\frac{\partial\phi}{\partial\tau} - \mathcal{H}(\pi,\phi)\right]\Bigg) \end{aligned} \tag{2.18}$$

where $\int[d\pi]\int_{\text{periodic}} d[\phi]$ is the path integral defined as in (2.16), $\mathcal{H}$ is the Hamiltonian density and the ϕ path is a closed one with endpoints being equal. This is required as the amplitude is between same states as discussed earlier. We can evaluate propagators using the partition function with source j which we define to be

$$\begin{aligned} Z(\beta, j=0) &= Z(\beta) \\ Z(\beta, j) &= \int[d\pi]\int_{\text{periodic}} d[\phi] \times \exp[\int_0^\beta d\tau \int d^3x (i\pi\frac{\partial\phi}{\partial\tau} - \mathcal{H}(\pi,\phi) \\ &\quad + j(\mathbf{x},\tau)\phi(\mathbf{x},\tau))] \end{aligned} \tag{2.19}$$

We define the time ordered propagator in imaginary time to be $\langle T\Big(\hat{\phi}(-i\tau_1,\mathbf{x})\,\hat{\phi}(-i\tau_2,\mathbf{x})\Big)\rangle_\beta$ where now field operators are time dependent Heisenberg operators (2.8) and 'T' ordering means

$$\begin{aligned} T\left(\hat{\phi}(-i\tau_1,\mathbf{x})\hat{\phi}(-i\tau_2,\mathbf{x})\right) &= \hat{\phi}(-i\tau_1,\mathbf{x})\hat{\phi}(-i\tau_2,\mathbf{x}),\ \text{If } \tau_1 > \tau_2 \\ &= \hat{\phi}(-i\tau_1,\mathbf{x})\hat{\phi}(-i\tau_2,\mathbf{x}),\ \text{If } \tau_2 > \tau_1 \end{aligned} \tag{2.20}$$

Now, functional differentiation of the partition function (2.19) relative to the source gives the time ordered propagator

$$\begin{aligned} \frac{1}{Z(\beta)}\frac{\delta^2 Z(\beta,j)}{\delta j(\tau_1,\mathbf{x})\delta j(\tau_2,\mathbf{x})}|_{j=0} &= \frac{1}{Z(\beta)}\int[d\pi]\int_{\text{periodic}} d[\phi]\exp(-S)\phi(\mathbf{x},\tau_1)\phi(\mathbf{x},\tau_2) \\ &= \langle T\left(\hat{\phi}(-i\tau_1,\mathbf{x})\hat{\phi}(-i\tau_2,\mathbf{x})\right)\rangle_\beta \\ S &= \int_0^\beta d\tau\int d^3x\left(i\pi\frac{\partial\phi}{\partial\tau} - \mathcal{H}(\pi,\phi)\right) \end{aligned} \tag{2.21}$$

The above relation can be easily seen by using the expression for thermal average of Heisenberg operators (2.8,2.13) and inserting complete set of field states at time τ_1, τ_2 to express the expectation value as path integral. Using the periodicity of the path $\phi(0,\mathbf{x}) = \phi(-i\tau,\mathbf{x}) = \phi(\mathbf{x})$ and (2.21) we see that propagator for the boson at imaginary time is periodic i.e.

$$T\left(\hat{\phi}(-i\beta,\mathbf{x})\hat{\phi}(-i\tau,\mathbf{x})\right) = T\left(\hat{\phi}(0,\mathbf{x})\hat{\phi}(-i\tau,\mathbf{x})\right) \tag{2.22}$$

Also for later use we define the imaginary time propagator for scalars to be

$$\triangle(\tau,\mathbf{x}) = \langle T\left(\hat{\phi}(-i\tau,\mathbf{x})\hat{\phi}(0,\mathbf{x})\right)\rangle_\beta \tag{2.23}$$

Using operator formalism we can also compute propagators. The rest of this section closely follows the approach considered in [31], [8]. We define the scalar theory propagators

$$\begin{aligned} D^{>}(t,t') &= \langle\hat{\phi}(t,\mathbf{x})\hat{\phi}(t',\mathbf{x})\rangle_\beta \\ D^{<}(t,t') &= \langle\hat{\phi}(t',\mathbf{x})\hat{\phi}(t,\mathbf{x})\rangle_\beta = D^{>}(t,t') \end{aligned} \tag{2.24}$$

where t is complex i.e. $t = a + ib$, operators are Heisenberg operators. We also note

$$\triangle(\tau) = D^{>}(-i\tau, 0) \tag{2.25}$$

Using (2.13) and inserting a complete set of eigenstates $|n\rangle$ of the Hamiltonian $\hat{H}$ with eigenvalue E_n, we have

$$D^{>}(t,t') = \frac{1}{Z(\beta)}\sum_{n,m} e^{-\beta E_n} e^{iEn(t-t')} \times e^{-iE_m(t-t')}|\langle n|\hat{\phi}(0,\mathbf{x})|m\rangle|^2 \tag{2.26}$$

Thus all we need to know are the energy eigenvalues and the action of the field operator on the states $|n\rangle$. This is done through writing the field operator $\hat{\phi}$ and the Hamiltonian in terms of creation and annihilation operators $a^\dagger, a$ of quantum mechanics.

In the case when the convergence of (2.26) depends on the arguments of the exponentials, we see that $D^{>}, D^{<}$ converge for $-\beta \leq \mathrm{Im}(t-t') \leq 0$ and $\beta \geq \mathrm{Im}(t-t') \geq 0$ respectively. This says that on the complex plane of time, $D^{>}(t,t')(D^{<}(t,t'))$ is only meaningful within a boundary. Using the cyclicity of trace i.e. $\mathrm{Tr}(AB) = \mathrm{Tr}(BA)$ and Heisenberg operator description $e^{-\beta\hat{H}}\phi(\hat{t},\mathbf{x})e^{\beta\hat{H}} = \phi(t+\hat{i}\beta,\mathbf{x})$ we have the Kubo-Martin-Schwinger relation

$$D^{>}(t,t') = D^{<}(t+i\beta,t') \tag{2.27}$$

Denoting $D^{>(<)}(t,0) = D^{>(<)}(t)$ we write the Fourier modes

$$\begin{aligned} D^{>}(k_0) &= \int_{-\infty}^{\infty} dt e^{ik_0 t} D^{>}(t) \\ D^{<}(k_0) &= \int_{-\infty}^{\infty} dt e^{ik_0 t} D^{<}(t) = \int_{-\infty}^{\infty} dt e^{ik_0 t} D^{>}(t-i\beta) \end{aligned} \tag{2.28}$$

where in the last step we used (2.27). Now using the first equation in (2.28) we get $\int_{-\infty}^{\infty} dt e^{ik_0 t} D^{>}(t-i\beta) = e^{-\beta k_0}\int_{-\infty-i\beta}^{\infty-i\beta} dt e^{ik_0 t} D^{>}(t) = e^{-\beta k_0} D^{>}(k_0)$, where the Fourier

integral is in complex t within the domain of convergence of $D^{>}(t)$. Thus we have from the second equation in (2.28)

$$D^{<}(k_0) = e^{-\beta k_0} D^{>}(k_0) \tag{2.29}$$

We define the spectral function for the scalars to be

$$\rho(k_0) = D^{>}(k_0) - D^{<}(k_0) \tag{2.30}$$

Using (2.26), (2.29) for $D^{>(<)}$ and plugging back into (2.30) we get

$$\begin{aligned} \rho(k_0) &= -\rho(-k_0) \\ \epsilon(k_0)\rho(k_0) &> 0 \end{aligned} \tag{2.31}$$

We can write $D^{>(<)}$ using (2.29)

$$\begin{aligned} D^{>}(k_0) &= (1 + f(k_0))\rho(k_0) \\ D^{<}(k_0) &= f(k_0)\rho(k_0) \\ f(k_0) &= \frac{1}{e^{\beta k_0} - 1} \end{aligned} \tag{2.32}$$

Also from the equal time commutation relation of the $\hat{\phi}$ field operator and it's conjugate momentum $[\hat{\phi}(t), \frac{\partial \mathcal{L}}{\partial \dot{\phi}(x,t')}]|_{t'=t} = i$ we have the sum rule for scalar spectral function

$$\int_{-\infty}^{\infty} \frac{dk_0}{2\pi} k_0 \rho(k_0, \overrightarrow{k}) = 1 \tag{2.33}$$

Again for free theory writing $D^{>(<)}$ in terms of creation and annihilation operators $a, a^\dagger$ and using $[a, a^\dagger] = 1$ gives free spectral function for scalars

$$\rho_F(k_0, \overrightarrow{k}) = 2\pi\epsilon(k_0)\delta(k_0^2 - \overrightarrow{k}^2 - m_\phi^2) \tag{2.34}$$

with $\epsilon(k_0)$ being the sign function.

Now for fermions, using the Dirac Lagrangian we see that the conjugate momentum to $\hat{\psi}$ field is $\hat{\Pi} = i\hat{\psi}^\dagger$, thus $\hat{\psi}$ and $\hat{\psi}^\dagger$ are independent fields. Also as fermions anti commute (2.4), we need to consider that the fermion fields $\psi(t, \mathbf{x})$ anti commute when we do the path integral to represent the partition function. For this we need to

construct a mathematical framework where integration variables anti commute. This difficulty is remedied by using Grassman algebra $\mathcal{A}$. An n dimensional Grassman algebra consists of n generators $\eta_1, ..., \eta_n$ where elements of the algebra are complex numbers. The algebra has the properties

A $\{\eta_i, \eta_j\} = \{\eta_i, \eta_j^\dagger\} = \{\eta_i^\dagger, \eta_j^\dagger\}$=0

B if $\eta_i, \eta_j \epsilon \mathcal{A}$ then $\mu\eta_i + \gamma\eta_j \epsilon \mathcal{A}$ with μ, γ being complex numbers.

C if $\eta_i, \eta_j \epsilon \mathcal{A}$ then so is $\eta_i\eta_j$.

With this algebra in hand we now consider creation and annihilation operators $a_i(p), a_i^\dagger(p)$ (p is momentum and i spin index) which generates and annihilates fermion energy eigenstate $|n\rangle$ of momentum p and spin i. We can think of Grassman variables as fields and demand that they anti commute with the operators $\hat{a}, \hat{a}^\dagger$. For simplicity we suppress spin index and momentum dependence and consider only one pair of operators and a two dimensional Grassman algebra generated by η, η^*. We define

$$|\eta\rangle = e^{-\eta a^\dagger}|0\rangle = |0\rangle - \eta|1\rangle \tag{2.35}$$

where $|0\rangle$ is the vacuum state, $|1\rangle = \hat{a}^\dagger|0\rangle$. Thus the Grassman state is a superposition of fermion states and we can consider the Grassman fields as fermion fields. With this definition following identities arise

$$\begin{aligned} \langle\eta|0\rangle = \langle 0|\eta\rangle &= 1 \\ \langle 1|\eta\rangle = \langle\eta|1\rangle^* &= -\eta \\ \langle\eta'|\eta\rangle &= \exp(\eta'^*\eta) \end{aligned} \tag{2.36}$$

The completeness relation follows from (2.36)

$$\int d\eta^* d\eta \exp(-\eta^*\eta)|\eta\rangle\langle\eta| = 1 \tag{2.37}$$

Rule for integration over Grassman variables is

$$\int \prod_{i=1}^{n} d\eta_i^* d\eta_i \exp\left(-\sum_{i,j=1}^{n} \eta_i^* M_{ij}\eta_j\right) = detM \tag{2.38}$$

Using (2.36) we have a relation between trace of an operator $\hat{O}$ in the basis of energy eigenstates $|n\rangle$and Grassman integral

$$\begin{aligned}\int d\eta^* d\eta \exp(-\eta^*\eta)\langle -\eta|\hat{O}|\eta\rangle &= \langle 0|\hat{O}|0\rangle + \langle 1|\hat{O}|1\rangle \\ &= \mathrm{Tr}(\hat{O}) \end{aligned} \tag{2.39}$$

Note that now the amplitude in the integrand is taken between $|\eta\rangle$ and $\langle -\eta|$ unlike boson case where the states were identical.

We generalize these properties to N dimensional Grassman algebra. The Grassman algebra now correspond to N dimensional Hilbert space for energy eigenstates of fermion fields and describe fermion field theory on the limit $N \to \infty$. We want to give a path integral representation of the partition function. First we write the Hamiltonian in terms of creation-annihilation operators $\hat{H}(\hat{a}_i(p), \hat{a}_j^\dagger(q), \hat{b}_m(k), \hat{b}_n^\dagger(l))$ where $\hat{a}^\dagger, \hat{a}$'s are fermion creation (annihilation) operators and $\hat{b}^\dagger, \hat{b}$'s are anti fermion creation (annihilation) operators, i, j, m, n are spin index and p, q, k, l are momentum [36]. The fermion anti fermion field operators are written in terms of $\hat{a}$'s and $\hat{b}$'s [31], [36] and anti commutation relation of the fermion field operators impose anti commutation relations on $\hat{a}$'s and $\hat{b}$'s. With $\hat{O} = \exp\Big[-\beta\hat{H}\Big(\hat{a}_i(p), \hat{a}_j^\dagger(q), \hat{b}_m(k), \hat{b}_n^\dagger(l)\Big)\Big]$ in (2.39) we divide the $\tau = -it$ interval $(0, \beta)$ in N subintervals, insert complete set of Grassman states (2.37) in between each subinterval, expand the exponential like (2.17); in the continuum limit we obtain

$$\begin{aligned} Z(\beta) &= \int_{\eta(\beta)=-\eta(0)} [d\eta^*][d\eta] \times \exp\Bigg(-\int_0^\beta d\tau \int d^3x \Big[\eta^*(\tau,\mathbf{x})\partial_\tau \eta(\tau,\mathbf{x}) \\ &\quad +\mathcal{H}(\eta^*(\tau,\mathbf{x}), \eta(\tau,\mathbf{x}))\Big]\Bigg) \end{aligned} \tag{2.40}$$

where $[d\eta^*], [d\eta]$ are analogously defined as in the boson case. The anti periodicity in the path indicated by $\eta(\beta) = -\eta(0)$ rises as the amplitude in (2.39) is between states of opposite eigenvalue η and $-\eta$. The path integral above is computed using (2.38) and result is a simple determinant. With the Grassman fields being fermion fields, (2.40) is the partition function for fermions with $\eta(\tau,\mathbf{x}) = \psi_j(\tau,\mathbf{x}), \eta^*(\tau,\mathbf{x}) = \psi_j^*(\tau,\mathbf{x})$. Here $\psi_j^*(\tau,\mathbf{x}), \psi_j(\tau,\mathbf{x})$ are the fermion fields corresponding to fermion field operators $\hat{\psi}_j^\dagger(\tau,\mathbf{x}), \hat{\psi}_j(\tau,\mathbf{x})$, where j is spin index. We can add a current term in (2.40)

in analogy with (2.19) to get $Z(\beta, \mathcal{J})$ for fermions and then functional differentiation with respect to current $\mathcal{J}$ would give the time ordered propagator for fermions $\langle T(\hat{\psi}_i(x)\hat{\psi}_j(y))\rangle_\beta$ (x, y four vectors) in exactly the same way as (2.21). Our expression for the path integral (2.21) and the analogous expression for fermions can be used to derive Feynman rules at finite temperature and imaginary time as found in the texts [31] [8].

We can find properties of fermion propagators using operator formalism. For Dirac fermions we define, just like the scalar theory, propagators [31]

$$\begin{aligned} S^{>}_{\alpha\gamma}(x, x') &= \langle \hat{\psi}_\alpha(x)\hat{\bar{\psi}}_\gamma(x')\rangle_\beta \\ S^{<}_{\alpha\gamma}(x, x') &= -\langle \hat{\bar{\psi}}_\gamma(x')\hat{\psi}_\alpha(x)\rangle_\beta \end{aligned} \tag{2.41}$$

where α, γ are spin index. Using the cyclicity of the trace and noting $e^{-\beta\hat{H}}$ is time evolution operator in imaginary time, we find, just like in the scalar case, the KMS relations

$$S^{>}_{\alpha\gamma}(t, \mathbf{x}; t, \mathbf{x}') = -S^{<}_{\alpha\gamma}(t + i\beta, \mathbf{x}; t, \mathbf{x}') \tag{2.42}$$

which in momentum space becomes[31]

$$S^{<}_{\alpha\gamma}(p_0) = -e^{-\beta p_0} S^{>}_{\alpha\gamma}(p_0) \tag{2.43}$$

Using above relations between $S^{>}, S^{<}$, defining spectral function exactly the same way as in the bosons, we have [31]

$$\begin{aligned} \tilde{\rho}_{\alpha\gamma}(p) &= S^{>}_{\alpha\gamma}(p) - S^{<}_{\alpha\gamma}(p) \\ S^{>}_{\alpha\gamma}(p) &= (1 - \tilde{f}(p_0))\tilde{\rho}_{\alpha\gamma}(p) \\ S^{<}_{\alpha\gamma}(p) &= -\tilde{f}(p_0)\tilde{\rho}_{\alpha\gamma}(p) \\ \tilde{f}(p_0) &= \frac{1}{1 + e^{\beta p_0}} \end{aligned} \tag{2.44}$$

We also define the Matsubara propagator for Dirac fermions

$$S_{\alpha\gamma}(\tau, \mathbf{x}; \tau', \mathbf{x}') = \langle T\big(\hat{\psi}_\alpha(-i\tau, \mathbf{x})\hat{\bar{\psi}}_\gamma(-i\tau', \mathbf{x})\big)\rangle_\beta \tag{2.45}$$

Now looking at (2.39) we see that the thermal average of an operator is taken between Grassman states (which are fermion states) of opposite eigenvalue.Thus the thermal

average in (2.45) is taken between fermion fields which are anti periodic $\psi(\tau-\beta)=-\psi(\tau)$. This implies that the field operators must also be anti periodic which makes the Matsubara propagator (2.45) anti periodic

$$S_{\alpha\gamma}(\tau-\beta,\mathbf{x};\tau',\mathbf{x}')=-S_{\alpha\gamma}(\tau,\mathbf{x};\tau',\mathbf{x}') \tag{2.46}$$

2.2.1 Frequency Sums

For computational convenience we compute the propagator obtained in (2.21) in momentum space. For this we define the Fourier modes of the imaginary time propagator (2.23) in mixed representation to be

$$\begin{aligned}\triangle(iw,\vec{k}) &= \int d^3x\int_0^\beta d\tau e^{iw\tau+i\vec{k}\cdot\mathbf{x}}\triangle(\tau,\mathbf{x})\\ &= \int_0^\beta d\tau e^{iw\tau}\triangle(\tau,\vec{k})\end{aligned} \tag{2.47}$$

where $\triangle(\tau,\vec{k})=\int d^3x e^{i\vec{k}\cdot\mathbf{x}}\triangle(\tau,\mathbf{x})$ is periodic in time with period β. We are required to take the interval of τ integration finite for modes to be finite. We choose the interval to be the period as that contains the whole behavior of the function and thus is sufficient. Now for bosons, consistency with this definition and the periodicity of $\triangle(\tau,\vec{k})$ makes the inverse Fourier transform to be

$$\begin{aligned}\triangle(\tau,\vec{k}) &= \frac{1}{\beta}\sum_{w_n}e^{-iw\tau}\triangle(iw,\vec{k})\\ w_n &= \frac{2n\pi}{\beta}\end{aligned} \tag{2.48}$$

where n is an integer. These frequencies are called 'Matsubara frequencies'.

For spin one bosons, just like in the case of scalar theory, the Fourier modes of $\triangle^{\mu\nu}(\tau,\mathbf{x})$ are defined as

$$\begin{aligned}\triangle^{\mu\nu}(iw,\vec{k}) &= \int d^3x\int_0^\beta d\tau e^{iw\tau+i\vec{k}\cdot\mathbf{x}}\triangle^{\mu\nu}(\tau,\mathbf{x})\\ &= \int_0^\beta d\tau e^{iw\tau}\triangle^{\mu\nu}(\tau,\vec{k})\end{aligned} \tag{2.49}$$

with w defined as before.

The Fourier modes of the imaginary time Dirac propagator are defined (2.45) in exactly the same way for scalars with mixed representation, denoting $\tilde{\triangle}(t, \overrightarrow{k}; 0) = \tilde{\triangle}(t, \overrightarrow{k})$ and treating $\tilde{\triangle}$ as matrices

$$\tilde{\triangle}(iw', \overrightarrow{k}) = \int_0^\beta d\tau e^{iw'\tau} \tilde{\triangle}(\tau, \overrightarrow{k}) \tag{2.50}$$

$$\begin{aligned} \tilde{\triangle}(\tau, \overrightarrow{k}) &= \frac{1}{\beta} \sum_w{}' e^{-iw'\tau} \tilde{\triangle}(iw', \overrightarrow{k}) \\ w' &= w'_n = \frac{(2n+1)\pi}{\beta} \end{aligned} \tag{2.51}$$

where anti periodicity fixes w'_n.

For computing loop diagrams in the coming sections we will encounter frequency sums of the form

$$\begin{aligned} S &= T \sum_n \triangle(iw_n, E) \\ S_l^{\pm}(w) &= T \sum_n (iw_n)^l \triangle(iw_n, E_1) \triangle(i(w_n \pm w), E_2) \\ \tilde{\mathbf{S}}_l^{\pm}(w') &= T \sum_n (iw'_n)^l \tilde{\triangle}(iw'_n, E'_1) \tilde{\triangle}(i(w'_n \pm w'), E'_2) \end{aligned} \tag{2.52}$$

$$\begin{aligned} S_l^{\pm\mu\nu}(w) &= T \sum_n (iw_n)^l \triangle(iw_n, E_1) \triangle^{\mu\nu}(i(w_n \pm w), E_2) \\ S_l^{\pm\alpha\beta\mu\nu}(w) &= T \sum_n (iw_n)^l \triangle^{\alpha\beta}(iw_n, E_1) \triangle^{\mu\nu}(i(w_n \pm w), E_2) \end{aligned} \tag{2.53}$$

with $\tilde{\mathbf{S}}$ being a matrix, $E_i = \sqrt{\overrightarrow{k_i}^2 + m_i^2}$. The first sum in (2.52) is easily computed using contour integral in the complex plane and the result is [31]

$$S = \frac{1}{2E}(1 + 2n(E)) \tag{2.54}$$

where

$$n(E) = \frac{1}{e^{\beta E} - 1} \tag{2.55}$$

To compute this we first write the Fourier modes as integrals. For the scalars we note that for $\tau \epsilon [0, \beta]$

$$\begin{aligned} \triangle(\tau, \overrightarrow{k}) &= D^>(-i\tau, \overrightarrow{k}) = \int \frac{dk_0}{2\pi} e^{-k_0\tau} D^>(k_0, \overrightarrow{k}) \\ &= \int \frac{dk_0}{2\pi} e^{-k_0\tau} (1 + f(k_0)) \rho(k_0, \overrightarrow{k}) \end{aligned} \tag{2.56}$$

with the propagator written in terms of the spectral function (2.30). Also using (2.47) we have

$$\triangle(iw_n, \overrightarrow{k}) = -\int_{-\infty}^{\infty} \frac{dk_0}{2\pi} \frac{\rho(k_0, \overrightarrow{k})}{iw_n - k_0} \tag{2.57}$$

The above is the desired integral representation of the propagator. We can obtain the spectral function from the above relation by analytic continuation of $\triangle(iw_n, \overrightarrow{k})$ with $iw_n \rightarrow k_0' \pm i\epsilon, \epsilon \rightarrow 0^+$. This continuation is valid and gives unique propagator in real frequency provided [31]

I. $|\triangle(z)| \rightarrow 0$ if $|z| \rightarrow \infty$

II. $|\triangle(z)|$ is analytic outside the real axis

Thus we have the analytic propagator

$$\triangle(z, \overrightarrow{k}) = -\int_{-\infty}^{\infty} \frac{dk_0}{2\pi} \frac{\rho(k_0, \overrightarrow{k})}{z - k_0} \tag{2.58}$$

With $z = k_0' \pm i\epsilon, \epsilon \rightarrow 0^+$ (2.58) is the real frequency propagator. The choice $\pm i\epsilon$ gives the retarded or advanced propagator [31]

$$\begin{aligned} D_R(k_0, \overrightarrow{k}) &= -i\triangle(k_0 + i\epsilon, \overrightarrow{k}) = -i\triangle_R(k_0, \overrightarrow{k}) \\ D_A(k_0, \overrightarrow{k}) &= i\triangle(k_0 - i\epsilon, \overrightarrow{k}) = i\triangle_A(k_0, \overrightarrow{k}) \end{aligned} \tag{2.59}$$

Using (2.58) we finally find an expression for the spectral function[32]

$$i\rho(k_0, \overrightarrow{k}) = \triangle(z = k_0 + i\epsilon, \overrightarrow{k}) - \triangle(z = k_0 - i\epsilon, \overrightarrow{k}) \tag{2.60}$$

We can see from (2.58) that $\triangle_A(k_0, \overrightarrow{k}) = (\triangle_R(k_0, \overrightarrow{k}))^*$ and with that we have

$$\rho(k_0, \overrightarrow{k}) = 2\ \mathrm{Im}\triangle_R(k_0, \overrightarrow{k}) \tag{2.61}$$

For spin one bosons, using operator formalism or path integral formalism we have the most general imaginary time free propagator obeying rotational and gauge invariance in Minkowski space[8]

$$\begin{aligned} \triangle_F^{\mu\nu}(iw_n, \overrightarrow{k}) &= \Big(-g^{\mu\nu} + \frac{k^\mu k^\nu}{k^2}\Big)\frac{1}{w_n^2 + \overrightarrow{k}^2 + m^2} + \frac{r}{k^2}\frac{k^\mu k^\nu}{k^2} \\ &= \Big(-g^{\mu\nu} + \frac{k^\mu k^\nu}{k^2}\Big)\triangle_0^v(k) + \frac{r}{k^2}\frac{k^\mu k^\nu}{k^2} \end{aligned} \tag{2.62}$$

where $k_0 = iw_n$, with defining $\triangle_0^v(iw_n, \overrightarrow{k}) \equiv 1/(w_n^2 + \overrightarrow{k}^2 + m^2)$ and r is the gauge parameter. Depending on the gauge choice, as $D^{>\mu\nu}, D^{<\mu\nu}$ is not always well defined for μ or $\nu = 0$ and we cannot define the spectral function as the difference between them. Our goal is to find an integral representation of the propagator in (2.62); we proceed as follows. Note that $\triangle_0^v(iw_n, \overrightarrow{k})$ is the free scalar theory propagator for which (2.56) and (2.57) are valid. Setting the gauge parameter $r = -k^2/m^2$ and using the integral representation (2.57) for $\triangle_0^v(iw_n, \overrightarrow{k})$ we have

$$\begin{aligned} \triangle_F^{\mu\nu}(iw_n, \overrightarrow{k}) &= \Big(-g^{\mu\nu} + \frac{k^\mu k^\nu}{m^2}\Big)\triangle_0^v(iw_n, \overrightarrow{k}) \\ &= -\int_{-\infty}^{\infty} \frac{dk_0'}{2\pi} \frac{\rho_0^v(k_0', \overrightarrow{k})}{iw_n - k_0'}\Big(-g^{\mu\nu} + \frac{k^\mu k^\nu}{m^2}\Big) \end{aligned} \tag{2.63}$$

This is the desired integral representation for spin one boson.

Similarly, using operator or path integral formalism we have the free spin half fermion propagators [32] in matrix form

$$\begin{aligned} \tilde{\triangle}_F(iw_n', \overrightarrow{k}) &= (\not{k} + m)\frac{1}{w_n'^2 + \overrightarrow{k}^2 + m^2} \\ &= (\not{k} + m)\tilde{\triangle}_0^f \end{aligned} \tag{2.64}$$

where $k_0 = iw_n'$, $\not{k} = k^\mu\gamma_\mu$ and defining $\tilde{\triangle}_0^f(iw_n', \overrightarrow{k}) \equiv 1/(w_n'^2 + \overrightarrow{k}^2 + m^2)$. Again $\tilde{\triangle}_0^f(iw_n', \overrightarrow{k})$ having properties of scalar theory propagator, we write the integral representation in matrix form

$$\tilde{\triangle}_F(iw_n', \overrightarrow{k}) = -\int_{-\infty}^{\infty} \frac{dk_0'}{2\pi} \frac{\rho_0^f(k_0', \overrightarrow{k})(\not{k} + m)}{iw_n' - k_0'} \tag{2.65}$$

Using these integral representations (2.57, 2.62, 2.65) into (2.52, 2.53) and taking appropriate trace for the case of fermions, we obtain expressions of the form with now writing $S^{\mu\nu\alpha\beta}(\mathrm{Tr}(\tilde{\mathbf{S}})) = S(\tilde{S})$

$$\begin{aligned} S_l^{\pm}(w) &= T\sum_n \int_{-\infty}^{\infty} \frac{dk_0}{2\pi} \int_{-\infty}^{\infty} \frac{dk_0'}{2\pi} \\ &\quad \times (iw_n)^l \frac{\rho_0^v(k_0, E_1)\rho_0^v(k_0', E_2)}{(iw_n - k_0)(i(w_n \pm w) - k_0')} \end{aligned}$$

$$\begin{aligned}\tilde{S}_l^{\pm}(w') &= T\sum_n \int_{-\infty}^{\infty}\frac{dk_0}{2\pi}\int_{-\infty}^{\infty}\frac{dk_0'}{2\pi} \\ &\quad \times(iw_n)^l \frac{\rho_0^f(k_0,E_1)\rho_0^f(k_0',E_2)}{(iw_n-k_0)(i(w_n\pm w')-k_0')}\end{aligned} \tag{2.66}$$

Now as $\triangle_0^v, \tilde{\triangle}_0^f$ satisfy condition I and II, we use (2.61) to obtain

$$\rho_0^{v,f}(k) = \epsilon(k_0)2\pi\delta(k_0^2 - \overrightarrow{k}^2 - m^2) \tag{2.67}$$

Then performing the frequency sum using contour integrals in the complex plane [8], (2.66) becomes for $l = 0, 1$

$$\begin{aligned}S_0^{\pm} &= \sum_{s_1,s_2=\pm}\frac{-s_1s_2}{4E_XE_R}\frac{1+n(s_1E_X)+n(s_2E_R)}{iw-s_1E_X-s_2E_R} \\ S_1 &= \sum_{s_1,s_2=\pm}\pm\frac{s_2}{4E_R}\frac{1+n(s_1E_X)+n(s_2E_R)}{iw-s_1E_X-s_2E_R} \\ \tilde{S}_0 &= \sum_{s_1,s_2=\pm}\frac{-s_1s_2}{4E_NE_R}\frac{1+\tilde{n}(s_1E_N)+\tilde{n}(s_2E_R)}{iw-s_1E_X-s_2E_R} \\ \tilde{S}_1 &= \sum_{s_1,s_2=\pm}\pm\frac{s_2}{4E_R}\frac{1+\tilde{n}(s_1E_X)+\tilde{n}(s_2E_R)}{iw-s_1E_X-s_2E_R}\end{aligned} \tag{2.68}$$

where $n(E)$ is as in (2.55) and

$$\tilde{n}(E) = \frac{1}{e^{\beta E}+1} \tag{2.69}$$

with $E_X(R) = \sqrt{\overrightarrow{p}_X(R)^2 + M_X(R)^2}$, $\overrightarrow{p}$ is a three-momentum.

For higher spin fermions, free theory spectral functions and propagators can be written in exactly the same way as for spin half case with $\triangle^{\mu\nu} = \triangle_0^f T^{\mu\nu}$, $\rho^{\mu\nu} = \rho_0^f T^{\mu\nu}$ and with $\triangle_0^f, \rho_0^f$ defined as before; but now $T^{\mu\nu}$ is a matrix tensor as the fields are spinor tensors.

Using the exact same arguments we can get frequency sums for all spin particles in interaction theory. In considering interaction we define the self-energy Π through the Schwinger-Dyson equation

$$G^{-1} - G_0^{-1} = \Pi \tag{2.70}$$

where G is interacting theory propagator and G_0 is free propagator in real or imaginary time formalism. In imaginary time formalism (2.70) reads $\triangle(\tau)^{-1} - \triangle_o(\tau)^{-1} =$

$\Pi(\tau)$. Defining Π_R, Π_A through (2.70) with $G = \triangle_R, \triangle_A$ given by (2.59) and using the expression for free scalar propagators $\triangle_F(iw_n) = -1/((iw_n)^2 - w^2)$we have

$$\triangle_R(k_0, E_k) = \frac{-1}{(k_0 + i\epsilon)^2 - E_k^2 - \Pi_R} \tag{2.71}$$

with $E_k^2 = \overrightarrow{k}^2 + m^2$.

Thus from (2.61) we have

$$\rho(k_0, E_k) = \frac{-2\ \mathrm{Im}\Pi_R(k_0, E_k)}{(k_0^2 - (E_k^2 + \mathrm{Re}\Pi_R(k_0, E_k)))^2 + (\mathrm{Im}\Pi_R(k_0, E_k))^2} \tag{2.72}$$

with $\mathrm{Im}\Pi_R$ being negative, guaranteeing the positivity of spectral function.

For our calculation, spin one boson self energies are four dimensionally transverse. Thus it can be written in Minkowski space as sum of three dimensionally transverse and longitudinal parts as follows:

$$\Pi_{\mu\nu}(k, T) = F(k, T)P_{\mu\nu}^L + G(k, T)P_{\mu\nu}^T \tag{2.73}$$

where $P_{\mu\nu}^L$ and $P_{\mu,\nu}^T$ are standard transverse and longitudinal projection tensors,

$$\begin{aligned} P_{00}^T = P_{0i}^T &= P_{i0}^T = 0 \\ P_{ij}^T &= \delta_{ij} - \frac{k_i k_j}{\overrightarrow{k}^2} \\ P_{\mu\nu}^L &= \frac{k_\mu k_\nu}{k^2} - g_{\mu\nu} - P_{\mu,\nu}^T \end{aligned} \tag{2.74}$$

where $i, j = 1, 2$ or 3, $\mu, \nu = 0, 1, 2$ or 3. These tensors have the property

$$\begin{aligned} P_\mu^{\mu L} &= -1 \\ P_\mu^{\mu T} &= -2 \\ Q_{\mu\nu} &= P_{\mu\nu}^L + P_{\mu\nu}^T \end{aligned} \tag{2.75}$$

At finite temperature, there is a frame-dependent four-vector u denoting the temperature. We can move frames so that $u = (1, 0, 0, 0)$. Every vector is defined in this new frame where $u = (1, 0, 0, 0)$. The four momentum of the particle for which we are computing the self-energy can be arbitrary k'; but we can rotate frames such that

the nonzero three momentum of the particle is in the z direction i.e. $\overrightarrow{k} = (0, 0, |\overrightarrow{k}|)$. With this choice we note that

$$\begin{aligned} G(k,T) &= \Pi_{11}(k,T) = \Pi_{22}(k,T) \\ F(k,T) &= \Pi_{33}\frac{k^2}{k_0^2} \end{aligned} \tag{2.76}$$

By evaluating $F(k,T)$ and $G(k,T)$ and putting them back to (2.73) the tensor structure of the self energies are apparent. To obtain quantities relative to the frame $u = (1,0,0,0)$ we rotate back to the frame $u = (1,0,0,0)$ i.e. we write k in terms of k'.

Now using (2.70) and (2.62) with the specified gauge choice, we get the interaction theory propagator

$$\triangle^{\mu\nu}(iw_n, \overrightarrow{k}) = -\frac{P_L^{\mu\nu}}{k^2 - m^2 - F} - \frac{P_T^{\mu\nu}}{k^2 - m^2 - G} - \frac{k^\mu k^\nu}{m^2 k^2} \tag{2.77}$$

where $k_0 = iw_n$. Now writing $-1/(k^2 - m^2 - F) \equiv \triangle_L(k_0, \overrightarrow{k}), -1/(k^2 - m^2 - G) \equiv \triangle_L(k_0, \overrightarrow{k})$ as integrals we define ρ_L, ρ_T by the following equations:

$$\begin{aligned} \frac{-1}{k^2 - m^2 - F} &= -\int_{-\infty}^{\infty} \frac{dk_0'}{2\pi} \frac{\rho_L(k_0', \overrightarrow{k})}{k_0 - k_0'} \\ \frac{-1}{k^2 - m^2 - G} &= -\int_{-\infty}^{\infty} \frac{dk_0'}{2\pi} \frac{\rho_T(k_0', \overrightarrow{k})}{k_0 - k_0'} \end{aligned} \tag{2.78}$$

As $\triangle_{L,T}(k_0)$ in the complex plane of k_0 satisfies condition I and II, we find $\rho_{L,T}$ using (2.61), to be

$$\begin{aligned} \rho_L &= \frac{-2\,\mathrm{Im}F}{(k^2 - m^2 - \mathrm{Re}F)^2 + (\mathrm{Im}F)^2} \\ \rho_T &= \frac{-2\,\mathrm{Im}G}{(k^2 - m^2 - \mathrm{Re}G)^2 + (\mathrm{Im}G)^2} \end{aligned} \tag{2.79}$$

Then (2.77) becomes

$$\begin{aligned} \triangle^{\mu\nu}(iw_n, \overrightarrow{k}) &= -\int_{-\infty}^{\infty} \frac{dk_0'}{2\pi} \frac{-P_L^{\mu\nu}(iw_n, \overrightarrow{k}) 2\,\mathrm{Im}F_R(k_0', \overrightarrow{k})}{(iw_n - k_0')(k_0'^2 - \overrightarrow{k}^2 - m^2 - \mathrm{Re}F_R(k_0', \overrightarrow{k})^2 + (\mathrm{Im}F_R(k_0', \overrightarrow{k}))^2)} \\ &- \int_{-\infty}^{\infty} \frac{dk_0'}{2\pi} \frac{-P_T^{\mu\nu}(iw_n, \overrightarrow{k}) 2\,\mathrm{Im}G_R(k_0', \overrightarrow{k})}{(iw_n - k_0')(k_0'^2 - \overrightarrow{k}^2 - m^2 - \mathrm{Re}G_R(k_0', \overrightarrow{k})^2 + (\mathrm{Im}G_R(k_0', \overrightarrow{k}))^2)} \\ &- \frac{k^\mu k^\nu}{m^2 k^2} \end{aligned} \tag{2.80}$$

with $F_R(k_0, \vec{k}) \equiv F(k_0 + i\epsilon, \vec{k})$, $G_R(k_0, \vec{k}) \equiv G(k_0 + i\epsilon, \vec{k})$, $\epsilon \to 0^+$. For our calculation in chapter four, we consider the case $G = F$ and write $\rho_L = \rho_T = \rho_A$. With this we have

$$\begin{aligned}
\triangle^{\mu\nu}(iw_n, \vec{k}) &= -\int_{-\infty}^{\infty} \frac{dk_0'}{2\pi} \frac{-Q^{\mu\nu}(iw_n, \vec{k}) 2\,\mathrm{Im}F_R(k_0', \vec{k})}{(iw_n - k_0')(k_0'^2 - \vec{k}^2 - m^2 - \mathrm{Re}F_R(k_0', \vec{k})^2 + (\mathrm{Im}F_R(k_0', \vec{k}))^2)} \\
&- \frac{k^\mu k^\nu}{m^2 k^2} \\
&= -\int_{-\infty}^{\infty} \frac{dk_0'}{2\pi} \frac{-2\left(\frac{k_\mu k_\nu}{m^2} - g_{\mu\nu}\right)\mathrm{Im}F_R(k_0', \vec{k})}{(iw_n - k_0')(k_0'^2 - \vec{k}^2 - m^2 - \mathrm{Re}F_R(k_0', \vec{k})^2 + (\mathrm{Im}F_R(k_0', \vec{k}))^2)} \\
&+ C^{\mu\nu}(iw_n, \vec{k}) \qquad (2.81)
\end{aligned}$$

with $C^{\mu\nu}$ defined by the above equation. Of course for $F \to 0$ we end up with free theory and $C^{\mu\nu} = 0$. For our calculation we will see that F is small and thus it is a good approximation to ignore $C^{\mu\nu}$ in the above expression.

Just like the boson case we find interaction theory fermion propagator and it's integral representation in matrix notation

$$\begin{aligned}
\tilde{\triangle}(iw_n', \vec{k}) &= \mathbf{M}(k,m) \frac{1}{w_n'^2 + \vec{k}^2 + m^2 + \Pi(iw_n', \vec{k})} \\
&= -\int_{-\infty}^{\infty} \frac{dk_0'}{2\pi} \frac{\rho^f(k_0', \vec{k})\mathbf{M}(k,m)}{(iw_n' - k_0')} \qquad (2.82)
\end{aligned}$$

with $\rho^f(k_0', \vec{k})$ defined as in (2.72), $\mathbf{M}(k,m)$ is a matrix depending on the nature of the fermion. For instance $\mathbf{M}(k,m) = \not{k} + m$ for spin one half.

Also in computing the self-energy we consider one propagator to be free and the other to be dressed; this leads us to expressions of the form (2.53). Using (2.81, 2.82) for dressed propagators, taking appropriate traces and using (2.57, 2.62, 2.65) for the free propagators we obtain

$$\begin{aligned}
S_l^{\pm}(w) &= T\sum_n \int_{-\infty}^{\infty} \frac{dk_0}{2\pi} \int_{-\infty}^{\infty} \frac{dk_0'}{2\pi} \\
&\times (iw_n)^l \frac{\rho_A(k_0, E_1)\rho_0^v(k_0', E_2)}{(iw_n - k_0)(i(w_n \pm w) - k_0')}
\end{aligned}$$

$$\tilde{S}_l^{\pm}(w') = T\sum_n \int_{-\infty}^{\infty}\frac{dk_0}{2\pi}\int_{-\infty}^{\infty}\frac{dk_0'}{2\pi} \times(iw_n)^l \frac{\rho^f(k_0,E_1)\rho_0^f(k_0',E_2)}{(iw_n-k_0)(i(w_n\pm w')-k_0')} \tag{2.83}$$

Now performing the frequency sum using contour integrals in complex plane and using $\rho_0^{v,f}(k) = \epsilon(k_0)2\pi\delta(k_0^2 - \overrightarrow{k}^2 - m^2)$, we obtain the temperature dependent part of (2.83)

$$\begin{aligned} S^{\pm}_{l(T)}(w) = \frac{1}{2E_1}\Big[\int_0^{\infty}\frac{dy}{\pi}\rho_A(y,E_2)\Big(\frac{n(y)(y-(\pm iw))^l - n(E_1)E_1^l}{\pm iw+E_1-y} \\ - \frac{n(y)(y-(\pm iw))^l + (-1)^l n(E_1)E_1^l}{\pm iw-E_1-y}\Big) + \int_{-\infty}^{0}\frac{dy}{\pi}\rho_A(y,E_2)\Big(\frac{n(-y)(y-(\pm iw))^l + n(E_1)E_1^l}{\pm iw+E_1-y} \\ - \frac{n(-y)(y-(\pm iw))^l - (-1)^l n(E_1)E_1^l}{\pm iw-E_1-y}\Big)\Big] \end{aligned} \tag{2.84}$$

with $n(x)$ given by (2.69), E_i as defined in (2.52). In exact analogous way we obtain temperature dependent part of $\tilde{S}_l^{\pm}(w')$; the result is (2.84) with $n(x) \to -\tilde{n}(x)$ and $\rho_A \to \rho^f$

2.2.2 Self-Energy and Scattering Amplitudes

There is a close relationship between imaginary part of self-energy and matrix elements of different scattering processes contained in the self-energy loop. This relationship is a consequence of unitarity and implies that the imaginary part of retarded self-energy is proportional to the sum of matrix elements squared.

For free theory we can easily show this relationship. We use spectral representation of frequency sums (2.66) that appear in a loop. Consider a scalar Φ interacting with two scalars ϕ_1, ϕ_2 with coupling strength g. Then self-energy for Φ reads [33] [31]

$$\begin{aligned} \Pi(iw_a,\overrightarrow{q}) &= -g^2T\sum_n\int\frac{d^3p}{(2\pi)^3}\triangle(iw_n,\overrightarrow{p})\triangle(i(w_n+w_a),\overrightarrow{k}) \\ &= -g^2\int\frac{d^3p}{(2\pi)^3}\int_{-\infty}^{\infty}\frac{dp_0}{2\pi}\int_{-\infty}^{\infty}\frac{dk_0}{2\pi} \\ &\quad\times(1+f(p_0)+f(k_0))\frac{\rho(p_0)\rho^{\pm}(k_0)}{iw_a+p_0+k_0} \end{aligned} \tag{2.85}$$

where $k = p + q$ is four momentum of ϕ_2. We note that as a function of complex variable iw_a, Π is hermitian analytic with cuts along the real axis [33]

$$(\Pi(w))^* = \Pi(w^*)$$

Thus the discontinuity is simply related to it's imaginary part [33] [31]

$$\begin{aligned} \mathrm{Disc}\Pi(q_0) &= \Pi(q_0 + i\epsilon) - \Pi(q_0 - i\epsilon) \\ &= 2i\mathrm{Im}\Pi(q_0 + i\epsilon) = 2i\mathrm{Im}\Pi_R(q_0) \end{aligned}$$

where q_0 is real. Now using the free spectral function

$$\rho_{F,\phi_i} = 2\pi\epsilon(h_0)\frac{1}{2w_h}[\delta(h_0 - w_h) + \delta(h_0 + w_h)] \tag{2.86}$$

where $h = k, p$, $w_h = \sqrt{\vec{h}^2 + m_{\phi_i}}$, we have through analytic continuation of $\Pi(iw_a)$ in (2.85) and using (2.86)

$$\begin{aligned} &\mathrm{Im}\Pi(q_0 + i\epsilon) = -g^2\pi \int \frac{d^3p}{(2\pi)^3} \int_{-\infty}^{\infty} dp_0 \int_{-\infty}^{\infty} dk_0 \frac{1}{4w_k w_p} \varepsilon(p_0)\varepsilon(k_0) \\ &(\delta(q_0 - p_0 - k_0)\delta(p_0 - w_p)\delta(k_0 - w_k)(1 + f(p_0) + f(k_0)) \\ &+\delta(q_0 - p_0 - k_0)\delta(p_0 - w_p)\delta(k_0 + w_k)(1 + f(p_0) + f(k_0)) \\ &+\delta(q_0 - p_0 - k_0)\delta(p_0 + w_p)\delta(k_0 - w_k)(1 + f(p_0) + f(k_0)) \\ &+\delta(q_0 - p_0 - k_0)\delta(p_0 + w_p)\delta(k_0 + w_k)(1 + f(p_0) + f(k_0))) \\ = \; &-\pi \int \frac{d^3p}{(2\pi)^3} \int d^3k \int_{-\infty}^{\infty} dp_0 \int_{-\infty}^{\infty} dk_0 \frac{1}{4w_k w_p} \varepsilon(p_0)\varepsilon(k_0) \\ &(M^2_{\Phi\to\phi_1\phi_2}\delta^4(q - p - k)\delta(p_0 - w_p)\delta(k_0 - w_k)(1 + f(p_0) + f(k_0)) \\ &+M^2_{\Phi\phi_1\to\phi_2}\delta^4(q + p - k)\delta(p_0 + w_p)\delta(k_0 + w_k)(-f(p_0) + f(k_0)) \\ &-M^2_{\Phi\phi_1\phi_2\to 0}\delta^4(q + p + k)\delta(-p_0 + w_p)\delta(k_0 + w_k)(1 + f(p_0) + f(k_0)) \\ &+M^2_{\Phi\phi_2\to\phi_1}\delta^4(q - p + k)\delta(p_0 + w_p)\delta(-k_0 + w_k)(f(p_0) - f(k_0))) \\ = \; &-\pi \int \frac{d^3p}{(2\pi)^3} \frac{1}{4w_k w_p} (M^2_{\Phi\to\phi_1\phi_2}\delta(q_0 - w_p - w_k)(1 + n(w_k) + n(w_p)) \\ &+M^2_{\Phi\phi_2\to\phi_1}\delta(q_0 - w_p + w_k)(-n(w_p) + n(w_k)) \\ &+M^2_{\Phi\phi_1\to\phi_2}\delta(q_0 + w_p - w_k)(n(w_p) - n(w_k)) \\ &+M^2_{\Phi\phi_2\phi_1\to 0}\delta(q_0 + w_p + w_k)(-1 - n(w_p) - n(w_k))) \end{aligned} \tag{2.87}$$

where each coefficient of the matrix elements $M^2 = g^2$ in the last expression contributes positively.

For interaction theory, the effect of interaction can be accounted using interaction spectral function. We can demonstrate optical theorem using spectral representation of the frequency sums (2.66). For the spectral functions of the particles in the loop we replace $\rho_0^{v,f}$ in (2.66) by ρ given by (2.72); note that the spectral function has peaks at the location of positive or negative energy of the particle with renormalized mass and it flattens out quite fast provided $\mathrm{Im}\Pi$ is small. Thus the δ functions which appear in (2.87) from the free spectral function are replaced by Lorentzian like distributions with nonzero width and also the peaks are at renormalized energy instead of bare energy. Those are the only differences between interaction theory and free theory.

For illustration, we consider scalar theory interaction spectral function. Also we can ignore the real part of the self-energy in the denominator as mass renormalization usually is not that large and effects the spectral function insignificantly. With this we have

$$\rho(k_0, E_k) = \frac{-2\ \mathrm{Im}\Pi_R(k_0, E_k)}{(k_0^2 - E_k^2)^2 + (\mathrm{Im}\Pi_R(k_0, E_k))^2} \tag{2.88}$$

This is a Lorentzian like distribution with varying width $|\mathrm{Im}\Pi_R(k_0, E_k)/2|$. Now we can Taylor expand $k_0^2 - E_k^2$ around it's zeroes and for $\rho(k_0, E_k)$ decaying fast, we have approximately

$$\begin{aligned}\rho(k_0, E_k) \simeq \quad & \frac{-2\ \mathrm{Im}\Pi_R}{(2E_k)^2(k_0 - E_k)^2 + (\mathrm{Im}\Pi_R)^2} \\ & + \frac{-2\ \mathrm{Im}\Pi_R}{(2E_k)^2(k_0 + E_k)^2 + (\mathrm{Im}\Pi_R)^2}\end{aligned} \tag{2.89}$$

The approximation gets better as $\rho(k_0, E_k)$ decays faster away from the zero of $k_0^2 - E_k^2$ and we get closer to the free theory spectral function. We denote $L(k_0 \pm E_k) = \frac{-2\ \mathrm{Im}\Pi_R}{(2E_k)^2(k_0 \pm E_k)^2 + (\mathrm{Im}\Pi_R)^2}$, then we have analogous expressions to (2.87) for scalar interaction theory

$$\mathrm{Im}\Pi(q_0 + i\epsilon) = -\pi \int \frac{d^3p}{(2\pi)^3} \int d^3k \int_{-\infty}^{\infty} dp_0 \int_{-\infty}^{\infty} dk_0 \frac{1}{4w_k w_p} \varepsilon(p_0)\varepsilon(k_0)$$

$$
\begin{aligned}
&(M^2_{\Phi\to\phi_1\phi_2}\delta^4(q-p-k)L(p_0-w_p)L(k_0-w_k)(1+f(p_0)+f(k_0))\\
&+M^2_{\Phi\phi_1\to\phi_2}\delta^4(q+p-k)L(p_0+w_p)L(k_0+w_k)(-f(p_0)+f(k_0))\\
&+M^2_{\Phi\phi_1\phi_2\to 0}\delta^4(q+p+k)L(-p_0+w_p)L(k_0+w_k)(-1-f(p_0)-f(k_0))\\
&+M^2_{\Phi\phi_2\to\phi_1}\delta^4(q-p+k)L(p_0+w_p)L(-k_0+w_k)(f(p_0)-f(k_0)))
\end{aligned}
\tag{2.90}
$$

and again we have the desired relation.

In summary, we have discussed the path integral formalism crucial in deriving partition functions (2.18,2.19,2.40) and propagator(2.21) which will be the foundation of our calculation in chapter 4. Using various relations between propagators and spectral functions, we have derived frequency sums for free theory (2.54,2.68) and interaction theory (2.84), which will be the key expressions for computing Feynmann diagrams of interest in chapter 4. We have also demonstrated the crucial relationship between imaginary part of the self-energies and matrix elements (2.87,2.90), which can serve to check the sign of imaginary part of self-energy and gives physical meaning to self-energy.

Chapter 3

Symmetries and Currents

In this chapter we will discuss the concepts vital in deriving Lagrangians, which in turn describe vector mesons in strongly interacting thermal medium. Furthermore, we briefly examine the relationship between vector meson and axial vector meson spectral functions. This relationship may shed light in our understanding of how chiral symmetry is restored at high temperature.

3.1 Noether Current

Symmetry is said to exist in a system when change in variables of the system renders the physics of the system unchanged. In classical field theory, symmetry is realized through the invariance of the action with the variation of the field [36], $\phi(x) \rightarrow \phi'(x) = \phi(x) + \alpha\triangle\phi(x)$. For this continuous field transformation to show symmetry the invariance of the action requires the Lagrangian to be invariant up to a 4-divergence, i.e.

$$\mathcal{L}(x) \rightarrow \mathcal{L}(x) + \alpha\partial_\mu \mathcal{J}^\mu(x)$$

for arbitrary $\mathcal{J}^\mu$. Then using the Euler Lagrangian equation for $\mathcal{L}(x)$ we find

$$\partial_\mu j^\mu = 0$$

where

$$j^{\mu} = \frac{\partial \mathcal{L}}{\partial(\partial_{\mu}\phi)} \triangle\phi - \mathcal{J}^{\mu}$$

Thus for a given continuous symmetry we have a conserved current j^{μ} called the Noether current. This conservation law is expressed through defining the charge

$$Q = \int_{\text{all space}} j^{0} d^{3}x$$

which stays constant in time due to the above definition.

3.2 Chiral Symmetry

QCD matter has various symmetries relevant to different part of the phase diagram. Here we discuss chiral symmetry and the consequences of it's restoration.

Consider a massless Dirac fermion field $\psi(x)$ with equation of motion,

$$i\ \partial\!\!\!/\psi = 0$$

Multiplying this equation with the γ_5 matrix leaves it invariant,

$$i\ \partial\!\!\!/\gamma_5\psi = 0$$

Thus both ψ and $\gamma_5\psi$ satisfy the Dirac equation and so does their linear combination

$$\begin{aligned} \psi_L &= \frac{1}{2}(1-\gamma_5)\psi \\ \psi_R &= \frac{1}{2}(1+\gamma_5)\psi \end{aligned} \tag{3.1}$$

These combinations are said to be of definite 'chirality'. With these fields having definite momentum, ψ_L corresponds to the particle having it's momentum aligned with it's spin and ψ_R being anti-aligned with it's spin; thus for massless particles 'chirality' coincides with the notion of helicity.

Chirality can be incorporated in the Lagrangian formalism with Lagrangian splitting into 'Left' and 'Right' chiral components, each of which being invariant under

the global chiral phase transitions

$$\begin{aligned} \mathcal{L} &= i\overline{\psi}\ \partial\!\!\!/\psi = \mathcal{L}_L + \mathcal{L}_R \\ \mathcal{L}_{L,R} &= i\overline{\psi}_{L,R}\ \partial\!\!\!/\psi_{L,R} \end{aligned} \tag{3.2}$$

$$\psi_{L,R}(x) \rightarrow \exp(-i\alpha_{L,R})\psi_{L,R}(x) \tag{3.3}$$

where $\alpha_{L,R}$ are arbitrary constant phases. As the Lagrangians are invariant we have chiral symmetry and corresponding conserved Noether currents and charges

$$\begin{aligned} J^{\mu}_{L,R} &= \overline{\psi}_{L,R}\gamma^{\mu}\psi_{L,R} \\ \partial_{\mu}J^{\mu}_{L,R} &= 0 \\ Q_{L,R} &= \int d^3x J^0_{L,R} \end{aligned} \tag{3.4}$$

Using these combinations of the left and right currents we can form 'vector' and 'axial-vector' currents and corresponding charges

$$\begin{aligned} V^{\mu} &= J^{\mu}_L + J^{\mu}_R \\ A^{\mu} &= J^{\mu}_L - J^{\mu}_R \\ Q &= \int d^3x V^0(x) = Q_R + Q_L \\ Q_5 &= \int d^3x A^0(x) = Q_R - Q_L \end{aligned} \tag{3.5}$$

3.2.1 Chiral Symmetry of QCD

With vanishing quark masses the QCD Lagrangian has left and right independent chiral components

$$\mathcal{L}_{QCD,m=0} = -\frac{1}{4}F^a_{\mu\nu}F^{a\mu\nu} + \sum_f \left(\overline{\psi}_L\ \not{D}\psi_L + \overline{\psi}_R\ \not{D}\psi_R\right) \tag{3.6}$$

which separately show chiral invariance with symmetry operators L and R defined to be

$$\begin{aligned} \psi_L &\rightarrow \exp(-i\theta_L \cdot \tau)\psi = L\psi_L \\ \psi_R &\rightarrow \exp(-i\theta_R \cdot \tau)\psi = R\psi_R \end{aligned} \tag{3.7}$$

where τ are the $SU(N_f)$ Pauli matrices, N_f being the number of flavors. In terms of the vector and axial-vector transformation corresponding to the vector and axial-vector currents, we have

$$\begin{aligned} \psi &\rightarrow \exp(-i\theta_V \cdot \tau)\psi \\ \psi &\rightarrow \exp(-i\theta_A \cdot \tau\gamma_5)\psi \\ \theta_V &= (\theta_L + \theta_R)/2 \\ \theta_A &= (\theta_L - \theta_R)/2 \end{aligned} \tag{3.8}$$

These invariances are referred to as chiral $SU(N_f)$, $SU(N_f)_L \times SU(N_f)_L$ or $SU(N_f)_V \times SU(N_f)_A$ transformation. For massive quarks the separate chiral symmetry is broken but the vector and axial-vector isospin symmetry remains.

3.3 Symmetry Breaking

In quantum field theory the notion of symmetry breaking is crucial as it describes the existence and mass of mesons and baryons. Here we discuss spontaneous and explicit symmetry breaking and it's consequences.

3.3.1 Spontaneous Symmetry Breaking in LSM

The most insightful field theory model describing symmetry breaking and the resulting implications, is the Linear Sigma Model (LSM) consisting of massless fermions ψ, scalar σ and triplet of pion field π [29]

$$\begin{aligned} \mathcal{L} = \quad & \overline{\psi} i \not{\partial} \psi + \frac{1}{2}\partial_\mu \pi \cdot \partial^\mu \pi + \frac{1}{2}\partial_\mu \sigma \partial^\mu \sigma \\ & -g\overline{\psi}(\sigma - i\tau \cdot \pi\gamma_5)\psi + \frac{\mu^2}{2}(\sigma^2 + \pi^2) - \frac{\lambda}{4}(\sigma^2 + \pi^2)^2 \end{aligned} \tag{3.9}$$

This Lagrangian exhibits chiral symmetry for the massless fermions and for the symmetry to hold, requires the π, σ field to transform in a particular way. Defining the matrix field $\Sigma = \sigma + i\tau \cdot \pi$ and the chiral transformations

$$U_{L,R} \quad = \quad \exp(-i\alpha_{L,R} \cdot \tau/2)$$

$$\begin{aligned} \psi_{L,R} &\rightarrow \psi'_{L,R} = U_{L,R}\psi_{L,R} \\ \Sigma &\rightarrow L\Sigma R^{\dagger} \end{aligned} \tag{3.10}$$

where $\alpha_{L,R}$ is arbitrary constant, we have the following currents

$$J^k_{L\mu} = \overline{\psi}_L \gamma_\mu \frac{\tau^k}{2} \psi_L - \frac{1}{2}\left(\sigma \partial_\mu \pi^k - \pi^k \partial_\mu \sigma\right) + \frac{1}{2}\epsilon^{klm}\pi^l \partial_\mu \pi^m \tag{3.11}$$

We have the potential energy for the Lagrangian (3.9)

$$V(\sigma, \pi) = -\frac{\mu^2}{2}(\sigma^2 + \pi^2) + \frac{\lambda}{4}(\sigma^2 + \pi^2)^2 \tag{3.12}$$

With μ^2 being positive minimizing this potential gives a set of degenerate ground states with

$$\sigma^2 + \pi^2 = \frac{\mu^2}{\lambda} \tag{3.13}$$

From this solution set we pick one field configuration

$$\begin{aligned} \langle \sigma \rangle_0 &= \sqrt{\frac{\mu^2}{\lambda}} = v \\ \langle \pi \rangle_0 &= 0 \end{aligned} \tag{3.14}$$

From the form of the potential, with this ground state we see that fluctuations in the π direction do not change the potential thus require no energy; thus by Goldstone theorem, π's are Goldstone Bosons. We can redefine the σ field, $\tilde{\sigma} = \sigma - v$ leaving the physics of the π field unchanged to give mass to the fermions ψ and $\tilde{\sigma}$. With this redefinition the Lagrangian in (3.9) becomes

$$\begin{aligned} \mathcal{L} = \quad & \overline{\psi}(i \not{\partial} - gv)\psi + \frac{1}{2}\left[\partial_\mu \tilde{\sigma} \partial^\mu \tilde{\sigma} - 2\mu^2 \tilde{\sigma}^2\right] + \frac{1}{2}\partial_\mu \pi \cdot \partial^\mu \pi \\ & - g\overline{\psi}(\tilde{\sigma} - i\tau \cdot \pi\gamma_5)\psi - \lambda v \tilde{\sigma}(\tilde{\sigma}^2 + \pi^2) - \frac{\lambda}{4}\left[(\tilde{\sigma}^2 + \pi^2)^2 - v^4\right] \end{aligned} \tag{3.15}$$

From (3.15) we see that the π is massless whereas the fermions Ψ and $\tilde{\sigma}$ are massive. Thus the original symmetry between the masses of π and σ (both mass being the same) is broken. This happens 'spontaneously' with π, σ acquiring vacuum configuration. The chiral partners π and σ no longer have degenerate mass and we have spontaneous chiral symmetry breaking. This in fact explains the existence of the π. For π to get a mass we need explicit symmetry breaking.

3.3.2 Explicit Symmetry Breaking in LSM

Through adding a linear term $a\sigma$ in (3.9), we break the symmetric nature of the potential, where now the lowest energy field configuration in (3.14) changes to

$$\begin{aligned} \langle\sigma\rangle_0 &= \sqrt{\frac{\mu^2}{\lambda}} + \frac{a}{2\mu^2} = v' \\ \langle\pi\rangle_0 &= 0 \end{aligned} \tag{3.16}$$

where only first order terms in a are considered, which is reasonable for small a. Now with $\tilde{\sigma}' = \sigma - v'$, the modified (3.9) [adding $a\sigma$ to it] gives a mass term for the π with

$$m_\pi^2 = \frac{a}{v} \tag{3.17}$$

3.3.3 Gauged LSM and Vector Meson Dominance

Hadrons with electromagnetic interaction can be incorporated in the sigma model using the principle of Vector Meson Dominance. This principle states that the entire hadronic electromagnetic current operator can be well approximated with a linear combination of the meson resonance field operators ρ, w, ϕ[11]. To motivate, we note that electromagnetic charge can be thought of as the coupling constant between the charged field and electromagnetic gauge field [23]. Just like electromagnetic photon field is introduced by requiring local gauge invariance of the lepton fields, we can introduce electromagnetic vector fields B_μ associated with the charged hadrons Φ by requiring local gauge invariance of the charged fields. For this electromagnetic process we have the Lagrangian

$$\begin{aligned} \mathcal{L} &= \frac{1}{2}|(\partial_\mu - i\tilde{g}B_\mu)\phi|^2 - \frac{1}{2}m_\Phi^2|\Phi|^2 - \frac{1}{4}B_{\mu\nu}B^{\mu\nu} + \frac{1}{2}m_B^2 B_\mu B^\mu \\ B^{\mu\nu} &= \partial^\mu B^\nu - \partial^\nu B^\mu \end{aligned} \tag{3.18}$$

where $\tilde{g}$ is the charge. With J^μ being the Noether current of the gauge transformation, we have the equation of motion for the B field to be [23]

$$-m_B^2 \partial^\mu B_\mu = \tilde{g}\partial^\mu J_\mu \tag{3.19}$$

We assume that the B field is divergentless (as the free B field) which implies the current is conserved by the above equation (3.19). This current is the electromagnetic

current associated with the hadrons (Φ) and from (3.19) the current field identity follows

$$J^{EM}_{\mu,B} = -\frac{m_B^2}{\tilde{g}} B_\mu \tag{3.20}$$

In general B can represent any hadronic vector fields coupled to charged hadronic fields and the total current is the sum of all the fields. But Vector Meson Dominance states that all the hadronic EM current is well approximated by ρ, w, ϕ fields

$$J^{EM}_{\mu} = -\frac{e}{g_\rho} m_\rho^2 \rho_\mu - -\frac{e}{g_\phi} m_\phi^2 \phi_\mu - -\frac{e}{g_w} m_w^2 w_\mu \tag{3.21}$$

We include vector and axial-vector mesons in the linear sigma model where they behave as the gauge particles for the fundamental $\Phi = \sigma t^0 + i\pi \cdot \overrightarrow{t}$ fields where $t^0 = 1/2$ and t^a are such that $\mathrm{Tr}(t^a t^b) = \delta^{ab}$. By VMD this inclusion will account for all the EM interactions of the hadrons. The gauge fields $A^\mu_{L,R}$ obey global chiral symmetry, $SU(2)_L \times SU(2)_R$ and are linear combinations of the vector and axial-vector mesons (w, ρ and a_1, f_1) [24]

$$A^\mu_{L,R} = (w^\mu \pm f_1^\mu) t^0 + (\overrightarrow{\rho}^\mu \pm \overrightarrow{a_1}^\mu) \cdot \overrightarrow{t} \tag{3.22}$$

The gauge transformation on the Φ forces the gauge fields to locally transform in a certain way to make the Lagrangian invariant. This local transformation on the gauge fields can now be considered as the chiral transformation and thus we have raised global chiral transformation to a local one [9]. In making this chiral gauge transformation on the gauge fields we restrict the form of the interaction Lagrangian involving Φ and vector and axial vector mesons. Denoting the vector meson dominance coupling by g, we have the effective Lagrangian

$$\begin{aligned} \mathcal{L} = \quad & tr(|D^\mu \Phi|^2 - \mu^2 |\Phi|^2 + \lambda(|\Phi|^2)^2 - 2ht^0 \Phi \\ & + \frac{1}{4}(F_L^{\mu\nu})^2 + \frac{1}{4}(F_R^{\mu\nu})^2 + \frac{m^2}{2}[(A_L^\mu)^2 + (A_R^\mu)^2]) \end{aligned} \tag{3.23}$$

where

$$\begin{aligned} D^\mu \Phi &= \partial^\mu \Phi - ig(A_L^\mu \Phi - \Phi A_R^\mu) \\ F^{\mu\nu}_{L,R} &= \partial^\mu A^\nu_{L,R} - \partial^\nu A^\mu_{L,R} - ig[A^\mu_{L,R}, A^\nu_{L,R}] \end{aligned} \tag{3.24}$$

and we have the gauge current [9]

$$J^{\mu(EM)}_{A_{L,R}} = -\frac{m^2_{A_{L,R}}}{\tilde{g}} A^{\mu}_{L,R} \tag{3.25}$$

In (3.24) μ^2 is the parameter responsible for the mass of the Φ and generates spontaneous symmetry breaking. The parameter h generates explicit symmetry breaking and gives the π mass, while m^2 produces mass for vector and axial-vectors. By the methods of the preceding section we have spontaneous and explicit symmetry breaking in Lagrangian (3.23) by introducing fields $\tilde{\sigma} = \sigma + \langle\sigma\rangle_0$. Also from the form of the covariant derivative in (3.24) we see that we will have the vertex of the form $A^{\mu}\partial_{\mu}\Phi$. To get rid of the vertex we redefine the Φ field and the axial field so that there is no such vertex. With this redefinition we generate mass terms for ρ, w, a_1, f_1 and the π

$$\begin{aligned}
m^2_{\rho} &= m^2_{w} = m^2 \\
m^2_{a_1} &= m^2_{f_1} = m^2 + (g\langle\sigma\rangle_0)^2 \\
f_{\pi} &= \frac{m_{\rho}}{m_{a_1}}\langle\sigma\rangle_0 \\
m^2_{\pi} &= \frac{m_{a_1}}{m^2_{\rho}}\frac{h}{\langle\sigma\rangle_0} \\
m^2_{\sigma} &= \frac{h}{\langle\sigma\rangle_0} + 2\lambda\langle\sigma\rangle_0
\end{aligned} \tag{3.26}$$

where all quantities above are bare. By observation on the Lagrangian (3.23) we see that it includes four point self interaction vertex for the axial and vector mesons. Noting that the spin 1 Euclidean propagator in momentum space is $\triangle^{\mu\nu} = (\delta^{\mu\nu} + P^{\mu}P^{\nu})/(P^2 + m^2)$, a straight forward calculation for the self-energy at finite temperature gives [24]

$$\Pi^{\mu\nu} = (\delta^{\mu\nu} - P^{\mu}P^{\nu}/P^2)(g^2T^2/6) \tag{3.27}$$

This indicates that renormalized mass increases as temperature increase. We will comment on this in the later chapters. Also note that the (3.23) Lagrangian after redefinition of fields includes $V\Phi\Phi$ and $AV\Phi$ interaction terms.

3.3.4 The Wess-Zumino-Witten Anomaly Action

When a symmetry current is not conserved thus the symmetry is violated, an 'anomaly' is said to exist. Without the appearance of the mass term for the chiral fields $A_{L,R}$, (3.23) obeys chiral symmetry. But there exists hadronic processes ($w \rightarrow \rho\pi \rightarrow 3\pi$, $K\overline{K} \rightarrow 3\pi$) which break chiral symmetry. Thus we have chiral anomaly whose description was first given by Wess and Zumino, with Wess-Zumino term. Witten [39] subsequently gave an elegant representation of the anomaly action, Γ_{WZW}. This is a gauge invariant action which produces the interaction terms responsible for parity violating processes. Here we give a brief but formal presentation of the action following [37] [38].

We consider a unitary matrix field $U = \exp(2i\phi/F_\pi)$ containing pseudo scalar nonet mesons $\phi = \phi^a\tau^a/\sqrt{2}$. In terms of differential one form we define

$$\begin{aligned} L &= (\partial_\mu U)U^\dagger dx^\mu = (dU)U^\dagger \\ R &= U^\dagger dU = U^\dagger L U \\ \Gamma_{WZW}(U) &= C\int_{M^5} tr[L^5] = C\int_{M^5} tr[R^5] \end{aligned} \tag{3.28}$$

where $\Gamma_{WZW}(U)$ is the action without gauge fields, M^5 is the five dimensional manifold whose boundary is the four dimensional Minkowski space, i.e. $\partial M^5 = M^4$. The constant $C = -iN_c/240\pi^2$ is determined by Witten [39]. Now we gauge it with trial and error method; first consider the the variation

$$\delta U = i\epsilon[Q, U] \tag{3.29}$$

where ϵ is arbitrary, Q is $SU(3)$ charge i.e. $Q = diag(\frac{2}{3}, -\frac{1}{2}, -\frac{1}{2})$. Under variation (3.29), the action (3.28) varies as

$$\delta\Gamma_{WZW} = -5Ci\int_{M^4} d\epsilon tr[Q(L^3 + R^3)] \tag{3.30}$$

In order to make this variation zero we need to add a gauge field $A = A_\mu dx^\mu$ with transformation property $\delta A = d\epsilon$ to our action $\Gamma_{WZW}(U)$

$$\begin{aligned} \Gamma^{(1)}(U, A) &= \Gamma_{WZ}(U) - \delta\Gamma(U) \\ &= \Gamma_{WZ}(U) + 5Ci\int_{M^4} Atr[Q(L^3 + R^3)] \end{aligned} \tag{3.31}$$

We again vary U, A and compute the variation on $\Gamma^{(1)}$. If it is zero, we are done; if not we define another action $\Gamma^{(2)}$ by subtracting $\delta\Gamma^{(1)}$ from $\Gamma^{(1)}$. We keep on repeating until we get a gauge invariant action.

This process generates the anomalous action for chiral gauge fields $A_{L,R}$ of the previous section. The action generated $\Gamma(U, A_L, A_R)$ breaks chiral symmetry as well as both vector and axial vector symmetry corresponding to the currents. But in nature only the axial current is the anomalous one. One can shift the anomaly residing in both vector and axial sector to only axial sector as was shown by Bardeen [40]. Then the action Γ^B_{WZW} breaks $U(3)_L \times U(3)_R$ symmetry to $U(3)_V \times U(1)_A$ and contains all the vertices involving $VV\phi$ and VVA necessary for the anomalous processes.

3.4 Weinberg Sum Rules

The implication of current algebra on spectral functions of vectors and axial vectors was formulated by Weinberg [22]. In the limit where chiral symmetry is exact, where the axial and vector currents are conserved the spectral functions are constrained by the 'Weinberg Sum Rules' in both zero and finite temperature.

We start with the vector and axial vector currents arising from chiral symmetry of the massless quark fields ψ, [8]

$$\begin{aligned} V^a_\mu &= \overline{\psi}\gamma_\mu(\tau^a/2)\psi \\ A^a_\mu &= \overline{\psi}\gamma_\mu\gamma_5(\tau^a/2)\psi \end{aligned} \tag{3.32}$$

where $\tau^a/2$ are isospin generators. As quark mass is zero, the symmetry is exact and currents above are conserved. Due to the commutation relations of the fermion fields the associated charge of these currents obey the equal time commutation relations

$$\begin{aligned} \left[Q^a_V, Q^b_V\right] &= i\epsilon^{abc}Q^c_V \\ \left[Q^a_V, Q^b_A\right] &= i\epsilon^{abc}Q^c_A \\ \left[Q^a_A, Q^b_A\right] &= i\epsilon^{abc}Q^c_V \end{aligned} \tag{3.33}$$

We define the vector and axial vector spectral functions, ρ_V, ρ_A at zero temperature

through the propagator

$$\begin{aligned}\langle V^a_\mu(x)V^b_\nu(0)\rangle &= \frac{\delta^{ab}}{2\pi^3}\int d^4p\theta(p^0)e^{ip\cdot x}\rho_V(-p^2)[g_{\mu\nu}-p_\mu p_\nu/p^2] \\ \langle A^a_\mu(x)A^b_\nu(0)\rangle &= \frac{\delta^{ab}}{2\pi^3}\int d^4p\theta(p^0)e^{ip\cdot x}(\rho_A(-p^2)[g_{\mu\nu}-p_\mu p_\nu/p^2] \\ &\quad +F_\pi^2\delta(p^2)p_\mu p_\nu) \end{aligned} \tag{3.34}$$

where F_π is the weak pion decay constant.

We consider the three point function

$$\begin{aligned}-i\epsilon^{abc}M_{\mu\nu\lambda}(q,p) &= \int d^4xd^4y\langle T\left(A^a_\mu(x),A^b_\nu(y),V^c_\lambda(0)\right)\rangle_0 \\ &\quad \exp[-iq\cdot x-ip\cdot y]\end{aligned} \tag{3.35}$$

With the commutation relations we have the Ward identities from (3.35)

$$\frac{1}{2}q^\mu M_{\mu\nu\lambda}(q,p) = \triangle_{V\nu\lambda}(q+p)-\triangle_{A\nu\lambda}(p) \tag{3.36}$$

$$\frac{1}{2}(q+q)^\lambda M_{\mu\nu\lambda}(q,p) = \triangle_{A\mu\nu}(q)-\triangle_{A\nu\lambda}(p) \tag{3.37}$$

where $\triangle_V, \triangle_A$ are propagators of vector and axial vector free currents. Multiplying (3.36) by $(p+q)^\lambda$ and (3.37) by q^μ we have

$$(q+p)^\lambda\triangle_{V\nu\lambda}(q+p) = q^\lambda\triangle_{A\nu\lambda}(q)+p^\lambda\triangle_{A\nu\lambda}(p) \tag{3.38}$$

As (3.38) works for all momentum q,p we must have

$$k^\lambda\triangle_{V\nu\lambda}(k) = k^\lambda\triangle_{A\nu\lambda}(q) = k^\lambda C_{\lambda\nu} \tag{3.39}$$

where C is a constant, k is arbitrary. In coordinate space we have using current conservation

$$\delta(x^0)\langle[V^{a0},V^{b0}]\rangle_0 = \delta(x^0)\langle[A^{a0},A^{b0}]\rangle_0 = -i\delta^{ab}C_{\nu\lambda}\partial^\lambda\delta^4(x) \tag{3.40}$$

Using (3.34) in (3.40) we have the first sum rule

$$\int_0^\infty[\rho_V(\mu^2)-\rho_A(\mu^2)]\mu^{-2}d\mu^2 = F_\pi^2 \tag{3.41}$$

Now set $q_\mu = 0$ in (3.36); as the left hand side has a pion pole term, only that remains and we have

$$\frac{1}{2}iF_\pi \int d^4x \langle \pi^a | T\left(A^b_\nu(y), V^c_\lambda(0)\right) |0\rangle e^{-ip\cdot y} = \triangle_{V\nu\lambda}(p) - \triangle_{A\nu\lambda}(p) \tag{3.42}$$

where $|\pi^a\rangle$ is a normalized pion state with zero energy and isospin index a. Now as we let $p^2 \to \infty$, our assumption that current is free at high momentum makes the coefficient of $g_{\nu\lambda}$ behave like $\frac{1}{p^4}$where the coefficient of $g_{\nu\lambda}$ on the right hand side approaches $\frac{1}{p^2}\int_0^\infty [\rho_V(\mu^2) - \rho_A(\mu^2)]d\mu^2$. Thus for (3.42) to be consistent we need the second sum rule

$$\int_0^\infty [\rho_V(\mu^2) - \rho_A(\mu^2)]d\mu^2 = 0 \tag{3.43}$$

The sum rules derived for zero temperature above have their counterparts at finite temperature. As mentioned in section 2.2.1, at finite temperature there is a specific frame relative to which temperature is defined and which is the rest frame of the medium. This preference of frame breaks Lorentz symmetry and thus a tensor depending on $\overrightarrow{p}$ will have distinct three dimensionally transverse and longitudinal components relative to $\overrightarrow{p}$. With this in mind we define transverse and longitudinal spectral functions as follows

$$\begin{aligned}
\langle V^a_\mu(x)V^b_\nu(0)\rangle &= \frac{\delta^{ab}}{2\pi^3}\int d^4p\theta(p^0)e^{ip\cdot x}\Big(\rho^L_V(p_0,\overrightarrow{p})P^L_{\mu\nu}(p) + \\
&\quad \rho^T_V(p_0,\overrightarrow{p})P^T_{\mu\nu}(p)\Big) \\
\langle A^a_\mu(x)A^b_\nu(0)\rangle &= \frac{\delta^{ab}}{2\pi^3}\int d^4p\theta(p^0)e^{ip\cdot x}\Big(\rho^L_A(p_0,\overrightarrow{p})P^L_{\mu\nu}(p) + \\
&\quad \rho^T_A(p_0,\overrightarrow{p})P^T_{\mu\nu}(p)\Big)
\end{aligned} \tag{3.44}$$

where $P^T_{\mu\nu}, P^L_{\mu\nu}$ is defined as before. Note that with gauge choice $r = 0$ and $m = 0$ in (2.62) we obtain the massless limit of (2.77, 2.78) which is consistent with the definition above (3.44). These spectral functions follow the sum rules [8]

$$\begin{aligned}
\int_0^\infty \frac{dww}{w^2 - \overrightarrow{p}^2}\Big(\rho^L_V(w,\overrightarrow{p}) - \rho^L_A(w,\overrightarrow{p})\Big) &= 0 \\
\int_0^\infty dww\Big(\rho^L_V(w,\overrightarrow{p}) - \rho^L_A(w,\overrightarrow{p})\Big) &= 0 \\
\int_0^\infty dww\Big(\rho^T_V(w,\overrightarrow{p}) - \rho^T_A(w,\overrightarrow{p})\Big) &= 0
\end{aligned} \tag{3.45}$$

3.4.1 Consequences

The sum rules derived above apply to the massless fields where chiral symmetry is exact. As temperature is raised, the average kinetic energy of the particles become significantly higher than their mass and ignoring mass becomes a good approximation. Thus at high temperature, in particular above some critical temperature T_c chiral symmetry is restored and the spectral functions defined in (2.78) should obey the sum rules (3.45). This restricts the high temperature behavior of the vector and axial vector spectral functions. We discuss briefly the consequences of the sum rules below [8].

One possibility is that the spectral functions mix, without changing their shapes, as follows

$$\begin{aligned} \rho_V(p_0, \overrightarrow{p}, T) &= (1-\epsilon(T))\rho_V(p,0) + \epsilon(T)\rho_A(p,0) \\ \rho_A(p_0, \overrightarrow{p}, T) &= (1-\epsilon(T))\rho_A(p,0) + \epsilon(T)\rho_V(p,0) \end{aligned} \tag{3.46}$$

When $\epsilon(T) = 1/2$, (3.45) is obeyed. Thus for this scenario $\epsilon(T) \to 1/2$ as $T \to T_c$.

Another possibility is that the pole mass (the value of invariant mass $\sqrt{k^2}$ for which first term in the denominator of (2.79) is zero) of the ρ meson and a_1 mesons move towards each other [26] or both goto zero [27] as temperature is increased. This results in exact cancellation of the spectral functions and again (3.45) are obeyed. The third possibility is that both spectral functions flatten out as temperature rises and the sum rules are satisfied.

Chapter 4

ρ Meson in Medium

4.1 Effective Field Theory

In our analysis of the ρ propagator we consider the gauged sigma model Lagrangian of 3.3.3 to describe $\rho\pi\pi, \rho A\pi$ interaction (A is an axial-vector meson) and the Wess-Zumino-Witten Lagrangian coming from the action of 3.3.4 to describe $\rho\pi w, \rho\pi f_1$ interaction. Both these Lagrangians are built from gauge-chiral symmetry principle and are discussed in the sections mentioned above. We include the interaction of the ρ with nucleons and nucleon resonances with Lagrangians obeying gauge and chiral symmetry. Our Lagrangians are effective in the sense that we fix our couplings to match with experimental decay widths; thus we obtain an effective vertex seen in experiments. The fields and couplings are renormalized for Lagrangians containing field operators in up to four dimensions thus only $\rho\pi\pi$ Lagrangian is renormalizable. We assume the issue involving Lagrangians being not renormalizable is resolved by beyond standard model physics and proceed with out effective calculation. The effective coupling we compute is the full vertex which is the sum of all the small coupling vertices in that energy regime and thus does not necessarily has to be small. We proceed with our analysis by describing the Lagrangian.

4.1.1 Interaction Lagrangians

We consider the following interaction Lagrangian for the ρ

$$\mathcal{L}_{\rho\pi\pi} = \frac{1}{2}|(\partial_\mu - ig_{\rho\pi\pi}\rho_\mu)\phi|^2 \tag{4.1}$$

$$\mathcal{L}_{\rho PA} = g_{\rho PA}A_\mu(g^{\mu\nu}q_\alpha p^\alpha - q^\mu p^{nu})p_\nu P \tag{4.2}$$

$$\mathcal{L}_{\rho PV} = g_{\rho PV}\mathcal{F}_{\rho PV}\epsilon_{\mu\nu\sigma\tau}k^\mu V^\nu q^\sigma p^\tau P \tag{4.3}$$

$$\mathcal{L}_{\rho PP'} = g_{\rho PP'}\mathcal{F}_{\rho PP'}P'(k\cdot qp_\mu - p\cdot qk_\mu)p^\mu P \tag{4.4}$$

$$\mathcal{L}_{\rho VA} = g_{\rho VA}\mathcal{F}_{\rho PA}\epsilon_{\mu\nu\sigma\tau}p^\mu V^\nu \rho^{\sigma\alpha}k_\alpha A^\tau - i\frac{\lambda}{2}(k_\beta A^\beta)^2 \tag{4.5}$$

$$\mathcal{L}_{\rho NR(N)} = \begin{cases} i\frac{f_{3/2^-}}{m_\rho}\mathcal{F}_{\rho NR^{3/2^-}}\overline{\psi}^\mu\gamma^\nu\psi F_{\mu\nu}, & J^P = \frac{3}{2}^- \\ i\frac{f_{3/2^+}}{m_\rho}\mathcal{F}_{\rho NR^{3/2^+}}\overline{\psi}^\mu\gamma^\nu\psi F_{\mu\nu}, & J^P = \frac{3}{2}^+ \\ i^2\frac{f_{5/2^+}}{m_\rho{}^2}\mathcal{F}_{\rho NR^{5/2^+}}\overline{\psi}^{\mu\nu}\gamma^5\gamma^\lambda\psi\partial_\nu F_{\mu\lambda}, & J^P = \frac{5}{2}^+ \\ f_{\rho NN}\left(\overline{\psi}\gamma^\mu\psi + i\frac{\kappa}{2m_N}\overline{\psi}\sigma^{\mu\nu}\psi\partial_\nu\right)\rho_\mu \end{cases} \tag{4.6}$$

where from (4.1) to (4.6) g_{abc} and f_{JP} are coupling constants, ϕ is the complex pion field, $P = \pi$ or K, $P' = \pi'$, A and V are axial-vector and vector mesons, respectively. Also ψ is the nucleon (N) field, ψ^μ is the spin $\frac{3}{2}$ and $\psi^{\mu\nu}$ is the spin $\frac{5}{2}$ nucleon resonance (R) field. p^μ, q^μ and k^μ denote the four momenta of the pseudo scalar ρ and the (axial) vector mesons, respectively. In (4.5) we denoted ρ field strength tensor as $\rho^{\sigma\alpha} = q^\sigma\rho^\alpha - q^\alpha\rho^\sigma$ and we have explicitly written the kinetic term of the axial vector field where λ is a constant associated with the gauge freedom of the axial vector field[41]. We have taken $\lambda = 1$ in our calculation. In (4.6) ρ field strength tensor is given by $F_{\mu\nu} = \partial_\mu\rho_\nu - \partial_\nu\rho_\mu$, $\sigma^{\mu\nu} = \frac{1}{2}[\gamma^\mu, \gamma^\nu]$, m_N is the nucleon mass, $\mathcal{F}_{\rho AB}$ are the form factors taking into account the finite size of the interaction vertex. $g_{\rho AB}, f_{\rho AB}$ are coupling constants and will be described in detail in a following subsection. The form factors are taken to be of dipole form [15]

$$\mathcal{F}_{\rho N R^{J^P}}(q_{cm}) = \left(\frac{2\Lambda^2 + m_{R^{J^P}}^2}{2\Lambda^2 + [w_\rho(q_{cm}) + w_N(q_{cm})]^2}\right)^2 \tag{4.7}$$

where q_{cm} is the three momentum of the decay product of the process $R \to N\rho$ in resonances rest frame, $w_N(q_{cm})^2 = {m_N}^2 + q_{cm}^2, w_\rho(q_{cm})^2 = {m_\rho}^2 + q_{cm}^2$.

These Lagrangian obey chiral symmetry and electromagnetic current conservation and can be derived from linear sigma model or WZW action as described in Chapter three. They also appear in [11] and [15]. Note that there is an issue in including the interaction Lagrangian (4.5) as the Born amplitude for $\rho\rho \to f_1 \to \rho\rho$ vanishes identically following the analysis based on chiral Lagrangian [43] [44]. But the later also suggests within VDM the absence of the decay $f_1 \to \rho^0\gamma$ which is empirically large. Thus we include Lagrangian (4.5) circumventing the vanishing $\rho\rho f_1$ coupling by making use of the gauge freedom by adding the additional term $-\frac{\lambda}{2}(k_\beta {f_1}^\beta)$.

4.2 Self-Energies

We use the imaginary time formalism to evaluate the self-energies with Euclidean or Minkowski metric. The ρ self-energy in Euclidean space ($\mu = 1, 2, 3, 4$) corresponding to (4.1) is [11]

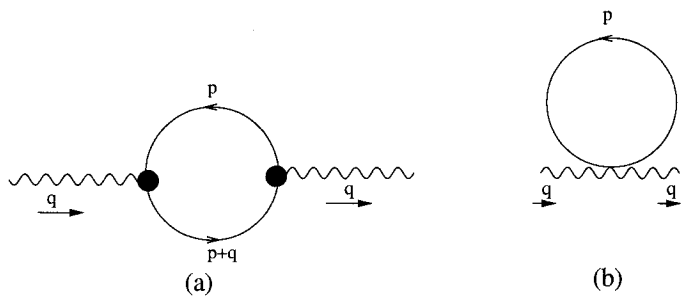

Figure 4.1: Various Feynman diagrams of the ρ self-energies considered

$$\Pi_{\mu\nu}(q) = \quad -{g_{\rho\pi\pi}}^2 T \sum_{p_4} \int \frac{d^3p}{(2\pi)^3} \frac{(2p+q)_\mu (2p+q)_\nu}{(p^2 + {m_\pi}^2)[(p+q)^2 + {m_\pi}^2)]}$$

$$+2\delta^{\mu\nu} g_{\rho\pi\pi}{}^2 T \sum_{p_4} \int \frac{d^3p}{(2\pi)^3} \frac{1}{p^2 + m_\pi^2} \tag{4.8}$$

where $p_4 = w_n = 2\pi T n = -ip_0, q_4 = w = -iq_0$.

From now on everything is in Minkowski space. ρ self-energy for (4.2) - (4.6) in Minkowski space is ($\mu = 0, 1, 2, 3$)

$$\Pi_{\mu\nu}^{J^{P(n)}}(iw, \overrightarrow{q}) = -IF\, T \sum_n \int \frac{d^3p}{(2\pi)^3} \frac{M_{\mu\nu}^{J^{P(n)}}}{[w_n^2 + E_X^2][(w_n + w)^2 + E_R^2]} \tag{4.9}$$

$$\Pi_{(J)\mu\nu}^{\pm}(iw', \overrightarrow{q}) = -IF\; T \sum_n \int \frac{d^3p}{2\pi^3} \frac{T_{(J)\mu\nu}^{\pm}(p, p+q)}{[w_n^2 + E_N^2][(w_n' + w' + \mu)^2 + E_R^2]} \tag{4.10}$$

We have drawn the Feynman diagrams for the self energies above in figure 4.1. (a) and (b) correspond to (4.8) whereas (a) correspond to (4.9, 4.10). The overall minus signs in (4.9, 4.10) come from the definition of self-energy using (2.70) and the expression for free propagator (2.63). IF is an isospin factor, $X = \pi, K$ or ρ, $w_n = 2n\pi T, w_n' = (2n+1)\pi T, w = 2m\pi T, w' = (2m+1)\pi T$, $E_{X(N)} = \sqrt{m_{X(N)}^2 + \overrightarrow{p}^2}$, $E_R = \sqrt{m_R^2 + (\overrightarrow{p} \pm \overrightarrow{q})^2}$, n, m integers, m_X are the mass of the pseudo scalar (π, K) or the vector (ρ) meson, m_R are the mass of the resonance which are the vector (w), axial-vector (h_1, a_1, K_1, f_1) or the pseudo scalar (π') or the nucleon or nucleon resonances $(N, N(1520), \triangle(1700), N(1720), \triangle(1905))$. We also use notation $M_{\mu\nu}^{J^{P(n)}}$, with $n = 1$ corresponds to (4.2) - (4.4) and $n = 2$ corresponds to (4.5).

Equation (4.8) explicitly gives the self-energy expression for $\rho\pi\pi$; whereas numerators in (4.9) are given by

$$\begin{aligned}
M_{\mu\nu}^{1^{\pm}(n=1)} &= \Gamma_{\mu\alpha}^{1^{\pm}} \left(-g^{\alpha\beta} + \frac{k^\alpha k^\beta}{m_R^2}\right) \Gamma_{\beta\nu}^{1^{\pm}} \\
M_{\mu\nu}^{0^{-}(n=1)} &= \Gamma_{\mu}^{0^{-}} \Gamma_{\nu}^{0^{-}} \\
M_{tf}^{1^{+}(n=2)} &= \Gamma_{\mu\alpha t}^{1^{+}(n=2)} \left(-g^{\mu\nu} + \frac{p^\mu p^\nu}{m_\rho^2}\right) \Gamma_{\nu\beta f}^{1^{+}(n=2)} \left(-g^{\beta\alpha} + \frac{k^\beta k^\alpha}{m_R^2}\right)
\end{aligned} \tag{4.11}$$

where the vertices can be easily obtained from the Lagrangians (4.1) - (4.5)

$$\Gamma_{\alpha\beta}^{1^{+}(n=1)} = g_{\rho PA} \mathcal{F}_{\rho PV} [g_{\alpha\beta}(p \cdot q - p_\alpha q_\beta]$$

$$\begin{aligned}
\Gamma^{1^-(n=1)}_{\alpha\beta} &= g_{\rho\pi V}\mathcal{F}_{\rho\pi V}[\epsilon_{\gamma\alpha\delta\beta}(k^\gamma q^\delta] \\
\Gamma^{0^-(n=1)}_{\alpha} &= g_{\rho\pi P'}\mathcal{F}_{\rho\pi P'}[q\cdot k p_\alpha - p\cdot q k_\alpha] \\
\Gamma^{1^+(n=2)}_{\mu\alpha t} &= g_{\rho V A}\mathcal{F}_{\rho V A}\epsilon_{a\mu b\alpha}p^a(q^b k_t - k\cdot q g^{sb}g_{ts})
\end{aligned} \tag{4.12}$$

Note that they are all real as we are working with imaginary time formalism. We can see this by looking at the partition function (2.19) which is similar to our partition function; we recognize the argument in the the exponential to be the Euclidean action with no i in front, so there is no i in the path integral and in the vertex. We also note that the Feynman rules, thus obtained, are consistent with the ones presented in [8] [31]. Using (4.11) with $k = p + q$, the exact expressions for $M^{J^{P(n)}}_{\mu\nu}$ is

$$\begin{aligned}
M^{1^+(1)}_{\mu\nu} &= -g^2_{\rho PA}\mathcal{F}_{\rho PA}[-(p\cdot q)^2 Q_{\mu\nu} + q^2\left(1 - \frac{q^2}{m_R^2}\right)K_{\mu\nu}] \\
M^{1^-(1)}_{\mu\nu} &= -g^2_{\rho\pi V}\mathcal{F}_{\rho\pi V}\left([p^2q^2 - (p\cdot q)^2]Q_{\mu\nu} + q^2 K_{\mu\nu}\right) \\
M^{0^-(1)}_{\mu\nu} &= g^2_{\rho\pi P'}\mathcal{F}_{\rho\pi P'}q^4 K_{\mu\nu} \\
M^{1^+(2)}_{tf} &= g^2_{\rho\rho f_1}\mathcal{F}_{\rho\rho f_1}\Big(- K_{tf}\left[2p^2q^2 + 2p\cdot q(q^4/m_R^2) + (p\cdot q)^2q^2/m_R^2 - 2q^4 + q^6/m_R^2\right] \\
&\quad + Q_{tf}\left[4p^2q^2 p\cdot q - 2p^2(q^4/m_R^2)p\cdot q - p^2(q^2/m_R^2)(p\cdot q)^2\right. \\
&\quad + 2p^2(p\cdot q)^2 + 2p^2q^4 - p^2(q^6/m_R^2) + (p\cdot q)^2q^4/m_R^2 \\
&\quad \left. + 2(p\cdot q)^3q^2/m_R^2 + (p\cdot q)^4/m_R^2\right]\Big)
\end{aligned} \tag{4.13}$$

where

$$Q_{\mu\nu} = \left(-g_{\mu\nu} + \frac{q_\mu q_\nu}{q^2}\right) \tag{4.14}$$

$$K_{\mu\nu} = \left(p_\mu - \frac{(p\cdot q)}{q^2}q_\mu\right)\left(p_\nu - \frac{(p\cdot q)}{q^2}q_\nu\right) \tag{4.15}$$

In order to compute the self energies in (4.10) we need to know the spin 3/2 and 5/2 free propagators i.e. the Rarita-Schwinger propagators. We can obtain them using path integral formalism or operator formalism. Writing the Heisenberg field operators as creation and annihilation operators and then writing the commutation relation in terms of the projection operator i.e. using operator formalism procedure of [45], the propagators can be computed for arbitrary spin. The spin 3/2 and 5/2 propagators

are given by [46] [47]

$$\begin{aligned}
\mathcal{R}^{\mu\nu}_{3/2}(k) &= \frac{\not{k}+m_R}{k^2-m_R^2}\Big(-g^{\mu\nu}+\frac{1}{3}\gamma^\mu\gamma^\nu+\frac{2}{3}\frac{k^\mu k^\nu}{m_R^2}-\frac{1}{3}\frac{k^\mu\gamma^\nu-k^\nu\gamma^\mu}{m_R}\Big) \\
&= \frac{1}{k^2-m_R^2}\mathcal{R}'^{\mu\nu}_{3/2}(k) \qquad (4.16) \\
\mathcal{R}^{\alpha\beta\rho\sigma}_{5/2}(k) &= \sum_{\rho\leftrightarrow\sigma,\alpha\leftrightarrow\beta}\Bigg(\frac{k^\alpha k^\beta k^\rho k^\sigma}{10m_R^4}+\frac{k^\alpha k^\beta k^\sigma\gamma^\rho-k^\rho k^\sigma k^\alpha\gamma^\beta}{10m_R^3}+\frac{k^\alpha\gamma^\beta k^\sigma\gamma^\beta}{10m_R^2} \\
&\quad +\frac{k^\alpha k^\beta g^{\sigma\rho}+k^\sigma k^\rho g^{\alpha\beta}}{20m_R^2}-\frac{2k^\alpha k^\sigma g^{\beta\rho}}{5m_R^2}-\frac{\gamma^\sigma k^\beta g^{\alpha\rho}-\gamma^\alpha k^\sigma g^{\beta\rho}}{10m_R} \\
&\quad -\frac{\gamma^\alpha\gamma^\sigma g^{\beta\rho}}{10}-\frac{g^{\alpha\beta}g^{\sigma\rho}}{20}+\frac{g^{\alpha\rho}g^{\beta\sigma}}{4}\Bigg)\frac{\not{k}+m_R}{k^2-m_R^2} \\
&= \mathcal{R}'^{\alpha\beta\rho\sigma}_{5/2}(k)\frac{1}{k^2-m_R^2} \qquad (4.17)
\end{aligned}$$

where sum over the indices $\alpha\beta\rho\sigma$ of a tensor $T^{\alpha\beta\rho\sigma}$ means

$$\sum_{\rho\leftrightarrow\sigma,\alpha\leftrightarrow\beta} T^{\alpha\beta\rho\sigma} = T^{\alpha\beta\rho\sigma}+T^{\beta\alpha\rho\sigma}+T^{\alpha\beta\sigma\rho}+T^{\beta\alpha\sigma\rho} \qquad (4.18)$$

Again note that there are no i's in the numerators, consistent with our Feynman rules.

For the baryon loop (4.10) with nonzero chemical potential, the nucleon resonances in the loop gives two diagrams, (a) of fig 4.1 and the same diagram with $q \to -q$. Whereas for zero chemical potential both are identical. We can see this as follows; the numerators in (4.10) after considering the minus sign coming from the fermion loop and noting that we have an anti fermion in the loop are

$$\begin{aligned}
T^{\pm}_{(3/2)\mu\nu}(p,k) &= -\mathrm{Tr}[(\not{p}-m_N)\Gamma^{\pm}_{\mu\alpha}(q)\mathcal{R}'^{\alpha\beta}_{3/2}(k)\Gamma^{\pm}_{\nu\beta}(-q)] \\
T^{\pm}_{(5/2)\mu\nu}(p,k) &= -\mathrm{Tr}[(\not{p}-m_N)\Gamma^{\pm}_{\mu\alpha\beta}(q)\mathcal{R}'^{\alpha\beta\rho\sigma}_{5/2}(k)\Gamma^{\pm}_{\nu\sigma\rho}(-q)] \\
T_{(1/2)\mu\nu}(p,k) &= -\mathrm{Tr}[(\not{p}-m_N)\Gamma_\mu(q)(\not{k}+m_N)\Gamma_\nu(-q)] \qquad (4.19)
\end{aligned}$$

where $k = p+q$ and we have considered anti particle nucleon propagator. Note that with μ being chemical potential, $k_0 = p_0+q_0+\mu$. But for the case $q \to -q$, $k_0 = p_0-q_0+\mu$. Thus we obtain two diagrams as the two expressions are not equal once we substitute into (4.10). On the other hand for zero chemical potential we have are identical expressions. We consider zero chemical potential and thus proceed with

the unique diagram (a) corresponding to (4.10). Also note that for the nucleon loop we drop $\pm$ sign of $T^{\pm}_{(J)\mu\nu}$ as there is a unique parity for the NN loop. The vertices above are given by

$$\Gamma^{\pm}_{\mu\alpha}(q) = \left(\frac{f_{3/2^{\pm}}}{m_\rho}\right)\mathcal{F}_{\rho N3/2^{\pm}}\gamma_5^{\frac{1\pm1}{2}}(\gamma_\mu q_\alpha - \not{q}g_{\mu\alpha}) \tag{4.20}$$

$$\Gamma^{\pm}_{\mu\alpha\beta}(q) = \left(\frac{f_{3/2^{\pm}}}{m_\rho^2}\right)\mathcal{F}_{\rho N5/2^{\pm}}\gamma_5^{\frac{1\pm1}{2}}\gamma^\delta q_\beta(q_\alpha g_{\delta\mu} - q_\delta g_{\alpha\mu}) \tag{4.21}$$

$$\Gamma_\mu(q) = \gamma_\mu - \frac{\kappa}{2m_N}\sigma^{\mu\nu}q_\nu \tag{4.22}$$

Using the expressions for the vertices and the Rarita-Schwinger propagators, we have explicit expressions for the numerator in (4.10)

$$\begin{aligned}
T^{\pm}_{(3/2)\mu\nu}(p,p+q) &= \frac{8}{3}q^2\left(\frac{f_{3/2^{\pm}}}{m_\rho}\right)^2\mathcal{F}^2_{\rho N3/2^{\pm}}\Bigg(\left[1+\frac{p^2+p\cdot q}{m_R^2}\right]K_{\mu\nu} \\
&\quad +\left[p^2 \pm (-m_N m_R) - \frac{(p\cdot q)^2}{q^2} - \frac{(p^2+p\cdot q)(q^2+p\cdot q)^2}{q^2 m_R^2}\right]Q_{\mu\nu}\Bigg) \\
T^{+}_{(5/2)\mu\nu}(p,p+q) &= \frac{8}{5}q^2\left(\frac{f_{5/2^{+}}}{m_\rho^2}\right)^2\mathcal{F}^2_{\rho N5/2^{+}}\Bigg(\Bigg[\frac{2(q^2+p\cdot q)^2+2(q^2+p\cdot q)q^2-3(p^2+p\cdot q)q^2}{4m_R^2} \\
&\quad -\left(1-\frac{m_N}{m_R}\right)q^2 + \frac{(q^2+p\cdot q)^2(p^2+p\cdot q)}{m_R^4}\Bigg]K_{\mu\nu} \\
&\quad +\Bigg[\left(\frac{3m_N}{4m_R}\right)(q^2+p\cdot q)^2 - \frac{(q^2+p\cdot q)^4(p^2+p\cdot q)}{m_R^4 q^2} - \frac{q^2}{4} \\
&\quad \left(3p^2+3m_N m_R - 2\frac{(p\cdot q)^2}{q^2} + p\cdot q\right) \\
&\quad +\frac{7(q^2+p\cdot q)^2(p^2+p\cdot q)q^2 - 2(q^2+p\cdot q)^3 p\cdot q}{4m_R^2 q^2}\Bigg]Q_{\mu\nu}\Bigg) \\
T_{(1/2)\mu\nu}(p,p+q) &= \left(8+2\frac{q^2\kappa^2}{m_N^2}\right)K_{\mu\nu} \\
&\quad +\Bigg(-4m_N^2 + \frac{p^2q^2\kappa^2}{m_N^2} + 4p^2 - \frac{p\cdot q q^2\kappa^2}{m_N^2} \\
&\quad +4p\cdot q - 2\frac{(p\cdot q)^2\kappa^2}{m_N^2} + q^2\kappa^2\Bigg)Q_{\mu\nu}
\end{aligned} \tag{4.23}$$

The self energies have vacuum and matter contributions corresponding to the zero and temperature dependent terms. We compute the vacuum part using dimensional regularization and the finite temperature part using the methods of [31] [8]. Note that we have both finite and divergent contributions for the vacuum part.

4.2.1 Zero Temperature Contribution

The tensor on the numerator of (4.8, 4.9, 4.10) can be written as a polynomial in (iw_n). Once we have that form we will arrive at the Matsubara frequency sums (2.52) as described in chapter two. For the case where all the propagators are free i.e. $\triangle(iw_n, \overrightarrow{p}) = \triangle_F(iw_n, \overrightarrow{p}) = 1/(w_n^2 + \overrightarrow{p}^2 + m^2)$ the boson and fermion propagator given by (2.63) and (2.64) we see that the temperature independent term after some algebra is of the form

$$\begin{aligned} \Pi_{\mu\nu}^{vac} &= g^2 \frac{1}{2\pi i} \int_{-i\infty}^{i\infty} dp_0 \int_{-\infty}^{\infty} \frac{d^3p}{(2\pi)^3} \frac{H_{\mu\nu}(p, p+q)}{(p_0^2 - E_X^2)((p_0+q_0)^2 - E_R^2)} \\ &= -g^2 \int_{-\infty}^{\infty} \frac{d^4p}{(2\pi)^4} \frac{H_{\mu\nu}(p, p+q)}{(p_4^2 + E_X^2)((p_4+q_4)^2 + E_R^2)} \end{aligned} \tag{4.24}$$

where $q_0 = iq_4, p_0 = ip_4$, p_4 integral runs from $-\infty$ to ∞. Introducing Feynman parameter integral to write the two denominators above as one, we have in Euclidean space with $\mathbf{p}+\mathbf{qx}=\mathbf{l}$ and $\mathbf{p}^2 = \sum_1^4 p_i$, $\mathbf{q}^2 = \sum_{i=1}^4 q_i$, $\mathbf{l}^2 = \sum_{i=1}^4 l_i$

$$\Pi_{\alpha\beta}^{vac} = -g^2 \int_0^1 dx \int_{-\infty}^{\infty} \frac{d^4\mathbf{l}}{(2\pi)^4} \frac{H_{\alpha\beta}(\mathbf{l}, \mathbf{q})}{(\mathbf{l}^2 + M^2)^2} \tag{4.25}$$

where $M^2 = \mathbf{q}^2 x(1-x) + M_X^2 + (M_R^2 - M_X^2)x$, $\alpha, \beta = 1, 2, 3, 4$. Note that we have written four vectors in 'bold' to emphasis that they are Euclidean four vectors. The $\mathbf{l}$ integral is done using dimensional regularization [49] in Euclidean space.

Looking at the explicit form of $H_{\mu\nu}(p, p+q)$ from (4.23, 4.13) the self-energy (vacuum and temperature dependent part) is transverse due to the presence of the tensors $K_{\mu\nu}, Q_{\mu\nu}$. Thus the decomposition (2.73) is valid and we have for our vacuum calculation using (2.73-2.76) with $F^{vac} = G^{vac}$

$$\begin{aligned} \Pi_{\mu\nu}^{vac}(q,T) &= Q_{\mu\nu}(q,T) F^{vac}(q,T) \\ F^{vac}(q,T) &= \frac{1}{3} Q^{\mu\nu} \Pi_{\mu\nu}^{vac} \end{aligned} \tag{4.26}$$

We can evaluate F^{vac} above in Minkowski space once the integral in (4.25) is done and by writing $iq_4 = iw = q_0$, thus converting $\Pi_{\alpha\beta}$ to $\Pi_{\mu\nu}$.For $\rho PA, \rho\pi V, \rho\pi\pi'$

interaction (4.9) we explicitly compute and the result is

$$
\begin{aligned}
F^{vac}_{\rho PA} &= -\frac{g^2_{\rho\pi A}\mathcal{F}^2_{\rho\pi A}}{(4\pi)^2}\int_0^1 dx\Big(\big(-\ln\mathcal{M}^2-\gamma-\ln(4\pi)\big)\big[3q^4x^2+(2+q^2/m_R^2)\frac{q^2\mathcal{M}^2}{2} \\
&+2(1-q^2/m_R^2)q^2\mathcal{M}^2\big]-\big[\frac{q^2\mathcal{M}^2}{2}(2+q^2/m_R^2)+2q^2\mathcal{M}^2(1-q^2/m_R^2)\big]\Big) \\
F^{vac}_{\rho\pi V} &= \frac{g^2_{\rho\pi V}\mathcal{F}^2_{\rho\pi V}}{(4\pi)^2}\int_0^1 dx q^2\mathcal{M}^2\Big(-\ln\mathcal{M}^2+\ln(4\pi)-\gamma+1\Big) \\
F^{vac}_{\rho\pi\pi'} &= \frac{g^2_{\rho\pi\pi'}\mathcal{F}^2_{\rho\pi\pi'}}{(4\pi)^2}\int_0^1 dx q^4\frac{3}{2}\mathcal{M}^2\Big(-\ln\mathcal{M}^2+\ln(4\pi)-\gamma+1\Big)
\end{aligned}
\tag{4.27}
$$

where $\mathcal{M}^2 = -q^2x(1-x)+M_X^2+(M_R^2-M_X^2)x$ and D is a constant.

So far $q_0 = iw$ was pure imaginary; we want to analytically continue to real values of energy for the ρ, i.e. $q_0 = iw \rightarrow q_0' + i\epsilon$ with $\epsilon \rightarrow 0^+$. After the continuation, the self-energy in (4.27) will have imaginary parts when $\mathcal{M}^2$ is negative which happens for $S-L<x<S+L$ where

$$
\begin{aligned}
S &= \frac{q^2+M_X^2-M_R^2}{2q^2} \\
L &= \frac{\sqrt{(q^2+M_X^2-M_R^2)^2-4q^2M_X^2}}{2q^2}
\end{aligned}
\tag{4.28}
$$

As our integration range in x is between 0 and 1 we are restricted to the region $[S-L,S+L]\epsilon[0,1]$. Note that this forces L to be real, L^2 to be positive and we are restricted in certain region in q^2 phase space. The physical interpretation is as $T=0$ implies vacuum we only have decays of ρ and the ρ invariant mass needs to be at least the sum of the mass of the decaying particles for the imaginary self-energy to be non zero. This is precisely due to the relation between imaginary self-energy and scattering amplitudes described in section 2.2.2. With $q_0 = q_0' + i\epsilon, \epsilon \rightarrow 0^+$ we have

$$
\ln\mathcal{M}^2 = \ln|\mathcal{M}^2| - i\pi, \mathcal{M}^2 < 0 \tag{4.29}
$$

where the choice $-i\pi$ is essential to avoid the branch cut of ln. Considering the q phase space restriction we have the expression for F^{vac} to be

$$
\mathrm{Re}F^{vac}_{\rho PA} = \frac{g^2_{\rho\pi A}\mathcal{F}^2_{\rho\pi A}}{(4\pi)^2}\Big[\Big(\theta(L^2)\Big(\Big[\Big[y\ln|y^2-L^2|-2y+L\ln|\frac{y+L}{y-L}|\Big]A_I
$$

$$
\begin{aligned}
&+\Big[\frac{1}{2}(y^2-L^2)\ln|y^2-L^2|-y^2\Big]A_{II}+\Big[\frac{1}{3}(y^3\ln|y^2-L^2|-\frac{2}{3}y^3-2L^2y\\
&+L^3\ln|\frac{y+L}{y-L}|)\Big]A_{III}\Big]++\theta(-L^2)\Big[\Big[y\ln(y^2-L^2)-2y+2\sqrt{-L^2}\tan^{-1}\frac{y}{\sqrt{-L^2}}\Big]A_I\\
&+\Big[\frac{1}{2}(y^2-L^2)\ln(y^2-L^2)-y^2\Big]A_{II}+\Big[\frac{1}{3}\Big(y^3\ln(y^2-L^2)-\frac{2}{3}y^3-2L^2y\\
&+2\sqrt{-L^2}^3\tan^{-1}\frac{y}{\sqrt{-L^2}}\Big)\Big]A_{III}\Big]+\ln(q^2)\Big(yA_I+\frac{y^2}{2}A_{II}+\frac{y^3}{3}A_{III}\Big)\Big)\Big)\Big|_{y=-S}^{y=1-S}\\
&+\Big[\Big(\gamma-\ln(4\pi)\Big)\Big[q^4(2-\frac{q^2}{2M_R^2})\\
&+\frac{3q^2}{2}(M_R^2-M_X^2-q^2)(1-\frac{q^2}{2M_R^2})+3M_X^2q^2(1-\frac{q^2}{2M_R^2})\Big]\\
&-3q^2(1-\frac{q^2}{2M_R^2})(\frac{q^2}{3}+\frac{(M_R^2-M_X^2-q^2)}{2}+M_X^2)+q^4C_{\rho\pi A}\Big]
\end{aligned}
$$

$$
\begin{aligned}
\mathrm{Im}F^{vac}_{\rho PA} &= -\frac{g^2_{\rho\pi A}\mathcal{F}^2_{\rho\pi A}\pi\theta(q-M_X-M_R)}{(4\pi)^2}\Big[q^4y^3+3q^2\Big(1-\frac{q^2}{2M_R^2}\Big)\\
&\Big[\frac{y^2}{2}(M_R^2-M_X^2)+M_X^2y+q^2(\frac{y^3}{3}-\frac{y^2}{2})\Big]\Big]\Big|_{y=S-L}^{y=S+L}\\
A_I &= 3S^2q^4\Big(2-\frac{q^2}{2M_R^2}\Big)+3Sq^2\Big(1-\frac{q^2}{2M_R^2}\Big)(M_R^2-M_X^2-q^2)+3q^2M_X^2\Big(1-\frac{q^2}{2M_R^2}\Big)\\
A_{II} &= 6Sq^4\Big(2-\frac{q^2}{2M_R^2}\Big)+3q^2\Big(1-\frac{q^2}{2M_R^2}\Big)(M_R^2-M_X^2-q^2)\\
A_{III} &= 3q^4\Big(2-\frac{q^2}{2M_R^2}\Big)\\
\mathrm{Re}F^{vac}_{\rho\pi V} &= \frac{g^2_{\rho\pi V}\mathcal{F}^2_{\rho\pi V}q^2}{(4\pi)^2}\Big[\frac{3(M_R^2+M_X^2)-q^2}{6}\Big)(\ln(4\pi)-\gamma+1)\\
&-\Big[\theta(L^2)\Big(\frac{1}{3}\Big(y^3\ln|y^2-L^2|-\frac{2}{3}y^3-2L^2y+L^3\mathrm{In}|\frac{y+L}{y-L}|\Big)\\
&-L^2\Big(y\ln|y^2-L^2|-2y+L\ln|\frac{y+L}{y-L}|\Big)\Big)-\theta(-L^2)\Big(\Big[\frac{1}{3}\Big(y^3\ln(y^2-L^2)\\
&-\frac{2}{3}y^3-2L^2y+2\sqrt{-L^2}^3\tan^{-1}\frac{y}{\sqrt{-L^2}}\Big)\Big]-\\
&L^2\Big[y\ln(y^2-L^2)-2y+2\sqrt{-L^2}\tan^{-1}\frac{y}{\sqrt{-L^2}}\Big]+\ln(q^2)(y^2-L^2)\Big)\Big]\Big|_{y=-S}^{y=1-S}\\
&+C_{\rho\pi V}\Big]\\
\mathrm{Im}F^{vac}_{\rho\pi V} &= \frac{g^2_{\rho\pi V}\mathcal{F}^2_{\rho\pi V}\pi\theta(q-M_X-M_R)q^2}{(4\pi)^2}\Big[\Big(M_R^2+M_X^2\Big)\frac{y^2}{2}-\frac{q^2}{6}(y^2-y^3)\Big]\Big|_{y=S-L}^{y=+L}
\end{aligned}
$$

$$
\begin{aligned}
\mathrm{Re}F^{vac}_{\rho\pi\pi'} &= \frac{g^2_{\rho\pi\pi'}\mathcal{F}^2_{\rho\pi\pi'}q^2}{2(4\pi)^2}\Bigg[\frac{3(M_R^2+M_X^2)-q^2}{6}\Big)(\ln(4\pi)-\gamma+1) \\
&\quad -\Bigg[\theta(L^2)\Bigg(\frac{1}{3}\Big(y^3\ln|y^2-L^2|-\frac{2}{3}y^3-2L^2y+L^3\mathrm{ln}|\frac{y+L}{y-L}|\Big) \\
&\quad -L^2\Big(y\ln|y^2-L^2|-2y+L\ln|\frac{y+L}{y-L}|\Big)\Bigg)-\theta(-L^2)\Bigg(\Big[\frac{1}{3}\Big(y^3\ln(y^2-L^2) \\
&\quad -\frac{2}{3}y^3-2L^2y+2\sqrt{-L^2}^3\tan^{-1}\frac{y}{\sqrt{-L^2}}\Big)\Big]- \\
&\quad L^2\Big[y\ln(y^2-L^2)-2y+2\sqrt{-L^2}\tan^{-1}\frac{y}{\sqrt{-L^2}}\Big]+\ln(q^2)(y^2-L^2)\Bigg)\Bigg]\Bigg|_{y=-S}^{y=1-S} \\
&\quad +C_{\rho\pi V}\Bigg] \\
\mathrm{Im}F^{vac}_{\rho\pi\pi'} &= \frac{g^2_{\rho\pi\pi'}\mathcal{F}^2_{\rho\pi\pi'}q^4\pi\theta(q-M_X-M_R)}{2m(4\pi)^2}\Bigg[\Big(M_R^2+M_X^2\Big)\frac{y^2}{2}-\frac{q^2}{6}(y^2-y^3)\Bigg]\Bigg|_{y=S-L}^{S+L}
\end{aligned}
\tag{4.30}
$$

The constant C_{xyz} is fixed such that $\mathrm{Re}F^{vac}(q^2=m_\rho^2)=0$ where m_ρ is the bare mass. This choice makes the bare mass the vacuum mass of the ρ.

For (4.8) the calculation is done in [11] and we quote

$$
\begin{aligned}
F^{vac}_{\rho\pi\pi} &= \frac{g^2_{\rho\pi\pi}M^2}{48\pi^2}\Bigg(\Big(1-4m_\pi^2/M^2\Big)^{3/2}\Bigg[\ln\Bigg|\frac{\sqrt{1-4m_\pi^2/M^2}+1}{\sqrt{1-4m_\pi^2/M^2}-1}\Bigg| \\
&\quad i\pi\theta(M^2-4m_\pi^2)\Bigg]+\frac{8m_\pi^2}{M^2}+C\Bigg)
\end{aligned}
\tag{4.31}
$$

where $M^2=q^2$ is the ρ invariant mass and we fix C such that $\mathrm{Re}F^{vac}(M^2=m_\rho^2)=0$, m_ρ is the bare ρ mass.

For $f_1\rho$ loop, we notice that due to the presence of the $\theta(q-M_X-M_R)$ function, $\mathrm{Im}F^{vac}_{\rho f_1\rho}(q)$ will be zero for M between 0 MeV to 2155 MeV, where $M^2=q^2$ is ρ invariant mass. For our calculation we consider M upto 1200 MeV; furthermore the quantity of interest is the ρ spectral function which is dependent primarily on $\mathrm{Re}F^{vac}_{\rho f_1\pi}(q)$ near $q=m_\rho$ where in fact by choice $\mathrm{Re}F^{vac}(M^2=m_\rho^2)=0$. Thus we can exclude the $f_1\rho$ loop altogether.

For the fermion loop (4.10) we have similar but more involved experessions. But again the phase space restriction $q-M_X-M_R>0$ guarantees that $\mathrm{Im}F^{vac}_{\rho NN}, \mathrm{Im}F^{vac}_{\rho NR}=$

0 for the range of ρ invariant mass we are interested in $(0-1200)$ MeV and by the same argument above we can exclude the fermions at zero temperature.

4.2.2 Finite Temperature Contribution

For computing self-energy coming from NN and NR loop, we need to find $\tilde{S}_l$ for l up to 6 whereas loops with mesons require evaluating S_l for l up to 4. For free theory $S_0, S_1(\tilde{S}_0, \tilde{S}_1)$ is given by (2.68). For the rest we use the following identity:

$$w_l^n \triangle_F(iw_n, E) = w_n^{l-2}\Big[1 - \frac{E^2}{w_n^2 + E^2}\Big] \tag{4.32}$$

$$T\sum_n w_n^l \triangle(iw_n, E) \rightarrow \begin{cases} i^l E^{l-1} n(E) & l \text{ even} \\ 0 & l \text{ odd} \end{cases} \tag{4.33}$$

where the arrow indicates we only take the temperature dependent part. The above is easily proven as $\triangle_F(iw_n, E) = 1/(w_n^2 + E^2)$ is the free scalar propagator; a similar identity holds for $\tilde{\triangle}_0^f$ as defined in (2.64) with $n(E) \rightarrow -\tilde{n}(E)$, $n(E), \tilde{n}(E)$ as defined in (2.55, 2.69). Note the temperature dependent part is finite due to the presence of the Fermi-Dirac distribution functions, $n(E)$ or $\tilde{n}(E)$ and there is no renormalization issue. Using the above identity we arrive at the following temperature dependent terms for the $S_l(\tilde{S}_l)$

$$\begin{aligned}
S_2^{\pm} &\rightarrow E_X^2 S_0 - \frac{n(E_R)}{E_R} \\
\tilde{S}_2^{\pm} &\rightarrow E_N^2 \tilde{S}_0 + \frac{\tilde{n}(E_R)}{E_R} \\
S_3^{\pm} &\rightarrow E_N^2 \tilde{S}_1 + (\pm iw)\frac{n(E_R)}{E_R} \\
\tilde{S}_3^{\pm} &\rightarrow E_N^2 \tilde{S}_1 - (\pm iw)\frac{\tilde{n}(E_R)}{E_R} \\
S_4^{\pm} &\rightarrow E_N^4 \tilde{S}_0 - (E_R^2 + E_N^2 - w^2)\frac{n(E_R)}{E_R} \\
\tilde{S}_4^{\pm} &\rightarrow E_N^4 \tilde{S}_0 + (E_R^2 + E_N^2 - w^2)\frac{\tilde{n}(E_R)}{E_R} \\
\tilde{S}_5^{\pm} &\rightarrow E_N^4 \tilde{S}_1 - (\pm iw)(3E_R^2 + E_N^2 - w^2)\frac{\tilde{n}(E_R)}{E_R} \\
\tilde{S}_6^{\pm} &\rightarrow E_N^6 \tilde{S}_0 + (-6w^2 E_R^2 + E_R^4 + w^4 + E_N^2 E_R^2 \\
&\quad -E_N^2 w^2 + E_N^4)\frac{\tilde{n}(E_R)}{E_R}
\end{aligned} \tag{4.34}$$

Using the above expressions for the temperature dependent part of the frequency sums and the expressions (4.23, 4.13) for the numerator of the integrand of the self energies, we can compute it's real and imaginary part provided we know the parameters of the theory:the coupling constants.

4.2.3 The Parameters

We compute the coupling constants that appear in (4.6) by computing the theoretical decay rates and comparing with the experimental value. We consider the decay process $R \rightarrow N\rho$. In the rest frame of the decaying resonance, the decay rate becomes

$$\Gamma_{R\rightarrow\rho N} = \frac{\mathcal{P}}{32\pi^2 m_R^2}\int d\omega |M_{R\rightarrow\rho N}|^2 \tag{4.35}$$

where $|M_{R\rightarrow\rho N}|^2$ represents matrix elements squared summed over initial and averaged over final spin and isospin states, $\mathcal{P}$ is the three momentum of the decay products in center of mass frame i.e. resonance rest frame. With the interaction Lagrangian 4.6, the matrix elements can be computed to be

$$\begin{aligned} |M_{R^{3/2^\pm}\rightarrow\rho N}|^2 &= \frac{IF(2I_{R,\rho}+1)}{(2J_R+1)(2I_R+1)} T^{\pm}_{(3/2)\alpha\beta}(p,k) \\ &\quad \Big(-g^{\alpha\beta}+\frac{q^\alpha q^\beta}{q^2}\Big) \end{aligned} \tag{4.36}$$

$$\begin{aligned} |M_{R^{5/2^+}\rightarrow\rho N}|^2 &= \frac{IF(2I_{\rho}+1)}{(2J_R+1)(2I_R+1)} T^{+}_{(5/2)\alpha\beta}(p,k) \\ &\quad \Big(-g^{\alpha\beta}+\frac{q^\alpha q^\beta}{q^2}\Big) \end{aligned} \tag{4.37}$$

where $k = q + p$ and for (4.36) we use $(2I_R + 1)$ for N resonances and $(2I_\rho + 1)$ for R resonances. For the decay process in the resonance rest frame $\overrightarrow{k} = 0, p^2 = m_N^2, p\cdot k = E_N m_R$ where $E_N = \sqrt{m_N^2 + \overrightarrow{p}^2}$. Using these relations and (34), (36) for the expressions for $T^{\pm}_{(3/2)\alpha\beta}(p,p+q), T^{+}_{(5/2)\alpha\beta}(p,p+q)$, we have

$$\begin{aligned} |M_{R^{3/2^\pm}\rightarrow\rho N}|^2 &= \frac{IF(2I_{R,\rho}+1)}{(2J_R+1)(2I_R+1)}\Big((\frac{-8}{3})q^2\Big((1+\frac{E_N}{m_R}) \\ &\quad (-m_N^2+\frac{(E_N m_R - m_N^2)^2}{q^2}) + 3(m_N^2 + m_N m_R - \end{aligned}$$

$$\frac{(E_N m_R - m_N^2)^2}{q^2} - E_N \frac{(q^2 + E_N m_R - m_N^2)^2}{m_R q^2})\Big)\Big) \tag{4.38}$$

$$\begin{aligned}
|M_{R^{5/2^+}\to\rho N}|^2 = {} & \frac{IF(2I_\rho+1)}{(2J_R+1)(2I_R+1)}\Big(\frac{-8}{5}q^2\Big(\\
& [\frac{2(q^2+E_N m_R - m_N^2)^2 + 2(q^2+E_N m_R - m_N^2)q^2 - 3E_N m_R q^2}{4m_R^2} \\
& -(1-\frac{m_N}{4m_R})q^2 + (q^2+E_N m_R - m_N^2)^2\frac{E_N}{m_R^3}] \\
& (-m_N^2 + \frac{(E_N m_R - m_N^2)^2}{q^2}) + 3[\frac{3m_N}{4m_R}(q^2+E_N m_R - m_N^2)^2 - \\
& (q^2+E_N m_R - m_N^2)^4 E_N \frac{m_R}{m_R^4 q^2} \\
& -\frac{q^2}{4}\Big[3m_N^2 + 3m_N m_R - 2\frac{(E_N m_R - m_N^2)^2}{q^2} + E_N m_R - m_N^2\Big] \\
& +\frac{7(q^2+E_N m_R - m_N^2)^2 E_N m_R q^2}{4m_R^2 q^2} \\
& -\frac{2(q^2+E_N m_R - m_N^2)^3(E_N m_R - m_N^2)}{4m_R^2 q^2}]\Big)\Big)
\end{aligned} \tag{4.39}$$

For the computation of the coupling constants we must consider the finite width of the ρ meson in computing the decay rate and compare that rate to the experimental value. In terms of the decay rate given by (4.35), the decay rate considering finite ρ width becomes

$$\Gamma_{R\to\rho N}^{\text{finite width}} = \int_{2m_\pi}^{m_R - m_N} \frac{qdq}{\pi} S(q)\Gamma_{R\to\rho N} \tag{4.40}$$

where S (q) is the spectral function taken as relativistic Breit-Wigner function

$$S(q) = \frac{2m_\rho \Gamma(q^2)}{(q^2 - m_\rho^2)^2 + (m_\rho \Gamma(q^2))^2} \tag{4.41}$$

where we include the phase space angular momentum dependence for the ρ decay into two pions [48] with

$$\Gamma(q^2) = \Gamma^{\text{vac}}\Big(\frac{\sqrt{q^2/4 - m_\rho^2}}{\sqrt{m_\rho^2/4 - m_\pi^2}}\Big)^3 \tag{4.42}$$

where $\Gamma^{\text{vac}} = 150\text{MeV}$. Table 1 shows the computed coupling constants along with the coupling constants for meson interactions taken from [15] which are also computed in similar fashion i.e. fixing the coupling constant to reproduce experimental width.

Table 4.1: List of the resonances along with their experimental widths and the computed coupling constants obtained by fitting with the experimental widths.f_{JP} is unitless ; $g_{\rho HR}$ have units of GeV^{-2} for f_1 and π' interactions and GeV^{-1} for the rest of the interactions

R	J^P	I	IF	$\Gamma^{vac}_{R\to\rho H}$ (MeV)	f_{JP} or $g_{\rho HR}$	ρH decay
N (1520)	$3/2^-$	1/2	2	25	10.20	ρN
N (1720)	$3/2^+$	1/2	2	100	7.26	ρN
$\triangle(1700)$	$3/2^-$	3/2	2	120	4.00	ρN
$\triangle(1905)$	$5/2^+$	3/2	2	210	12.91	ρN
$\omega(782)$	1^-	0	1	3.5	25.80	$\rho\pi$
$h_1(1170)$	1^+	0	1	300	11.37	$\rho\pi$
$a_1(1260)$	1^+	1	2	400	13.27	$\rho\pi$
$K_1(1270)$	1^+	1/2	2	60	9.42	ρK
$f_1(1285)$	1^+	0	1	3	35.70	$\rho\rho$
$\pi'(1300)$	0^-	1	2	300	9.67	$\rho\pi$

For $\pi\pi$ loop $g_{\rho\pi\pi} = 6.06$ [11] and for the NN loop we use $f_{\rho NN} = 2.63, \kappa = 6.1$ [42]. Note that in (4.40) $\Gamma^{\text{finite}}_{R\to\rho N}$ width is taken to be the experimental value $\Gamma^{\text{vac}}_{R\to\rho N}$ listed in the table.

4.2.4 Thermal Mass and Spectral Functions

The real part of the self energies described in the above sections contribute to the bare mass of the rho meson and in the limit $\vec{q} \to 0$ i.e. three momentum of the ρ going to zero, gives the thermal mass of the ρ meson, $m_\rho(T) = \sqrt{m_\rho^2 + Re\Pi}$. Note that in this limit transverse and longitudinal self energies are equal and we have $F = G$. Thus plotting one is enough.

Using the expressions (2.54), (2.68), (4.34) for the free theory frequency sums we can compute the temperature dependent part of (4.8, 4.9, 4.10). Adding this to the

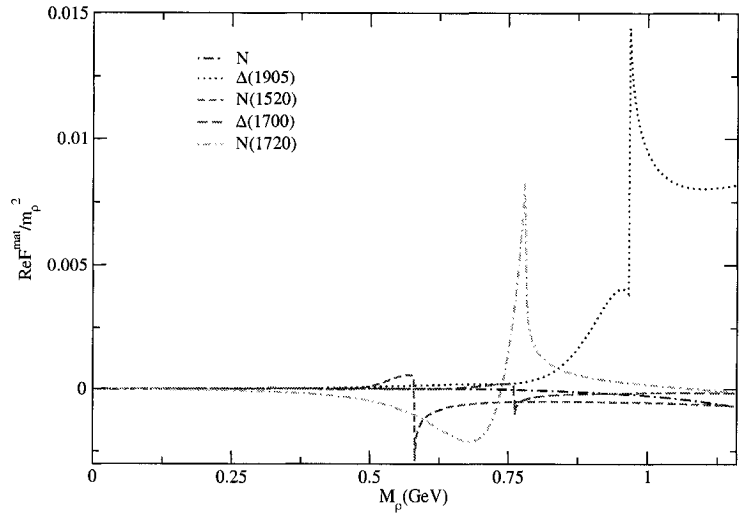

Figure 4.2: Real self-energy for zero three momentum of ρ due to baryons and baryon resonances at T=120 MeV

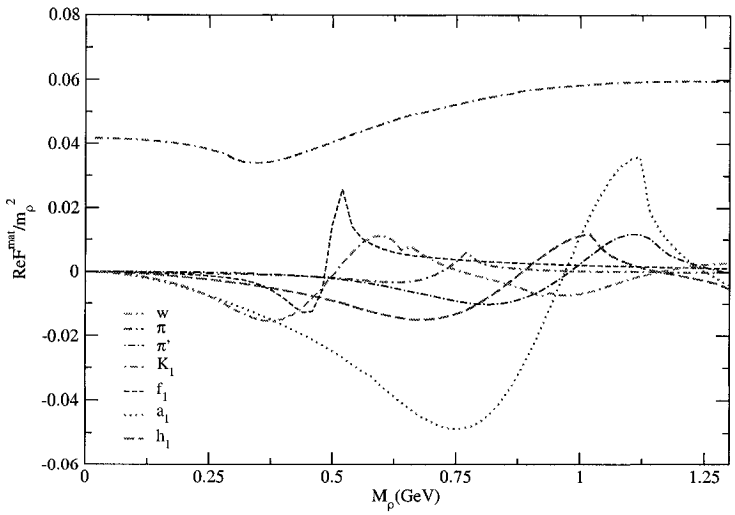

Figure 4.3: Real part of self-energy for zero three momentum of ρ due to free mesons at T=120 MeV

vacuum contributions gives the self-energy in imaginary frequency. We analytically continue $iw \rightarrow q_0 + i\epsilon$ where q_0 is real energy, to get self-energy for real values of energy i.e. we obtain the real time self-energy which has both real and imaginary part. After the analytic continuation we find the self energies which are integrals over three momentum $\vec{p}$. The integrand has singularities and the Cauchy principle value of the integral is evaluated. On the other hand the integrand for the imaginary part contains delta functions and are easily evaluated. As mentioned in section 4.2.1, the decomposition (2.73) is also valid for the temperature dependent part of the self-energy. Thus after the integral is done, we can find $F^{mat}(q,T), G^{mat}(q,T)$ using (2.76) where the superscript 'mat' indicates temperature dependence. Also in computing thermal mass, we note that in the limit $\vec{q} = 0$, $F^{mat} = G^{mat} = \Pi^{11}$.

To find the thermal mass we need to find solution of the following equation

$$m_\rho(T) = q_0(T) = \sqrt{m_\rho^2 + \mathrm{Re}\Pi(q_0, T)} \tag{4.43}$$

In figures 4.2, 4.3 we plot $\mathrm{Re}F^{mat}$ as a function of M for T=120 MeV due to baryon and meson loop. From here on $M^2 = q^2 = M_\rho^2$ is the ρ invariant mass unless otherwise specified.

We see that the contributions due to real part of the self-energy is quite small and varies slightly as q_0 changes for a fixed temperature. Thus it is justified to use $q_0 \sim 770$ MeV when evaluating $\mathrm{Re}\Pi(q_0, T)$ in (4.43) and that determines $m_\rho(T)$. Note that we have to add all the real part of the self energies coming from NN, NR loops and the loops involving the mesons to get $\mathrm{Re}\Pi_{11}(T) = \mathrm{Re}\Pi(T)$. Finally we get the thermal mass using (4.43) as a function of temperature and observe that a decrease of 30 MeV is possible between T=120 MeV and T=180 MeV.

Now repeating the same procedure for nonzero ρ three momentum, using (2.76) and (4.8, 4.9, 4.10) with explicit expressions for the tensors along with the temperature dependent frequency sums and coupling constants in 4.2.3, we evaluate F^{mat}, G^{mat} and obtain the plots 4.4, 4.5, 4.6. We observe that real part of the self-energies have kinks and the imaginary part is non vanishing only for a particular range of M. This is because for an invariant mass range of the ρ meson

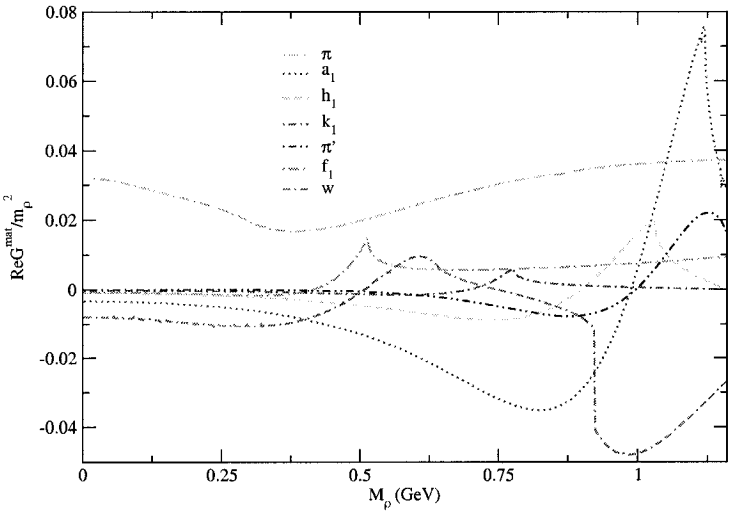

Figure 4.4: Real transverse self-energy due to free mesons at ρ three momentum 300 MeV, T=120 MeV

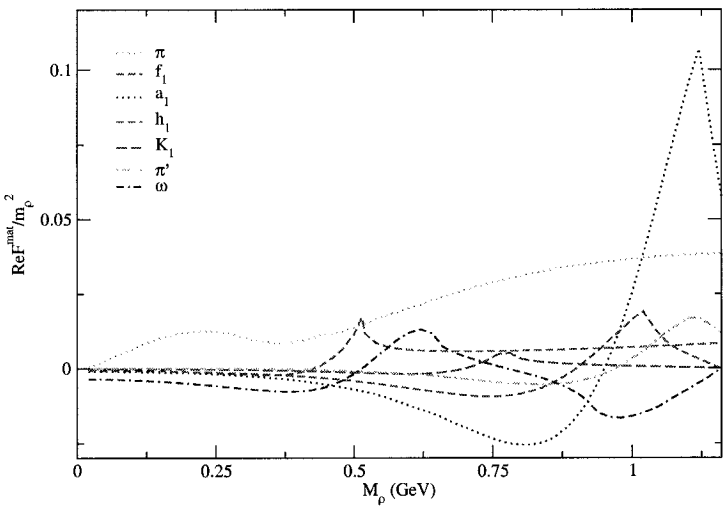

Figure 4.5: Real longitudinal self-energy due to free mesons at ρ three momentum 300 MeV, T=120 MeV

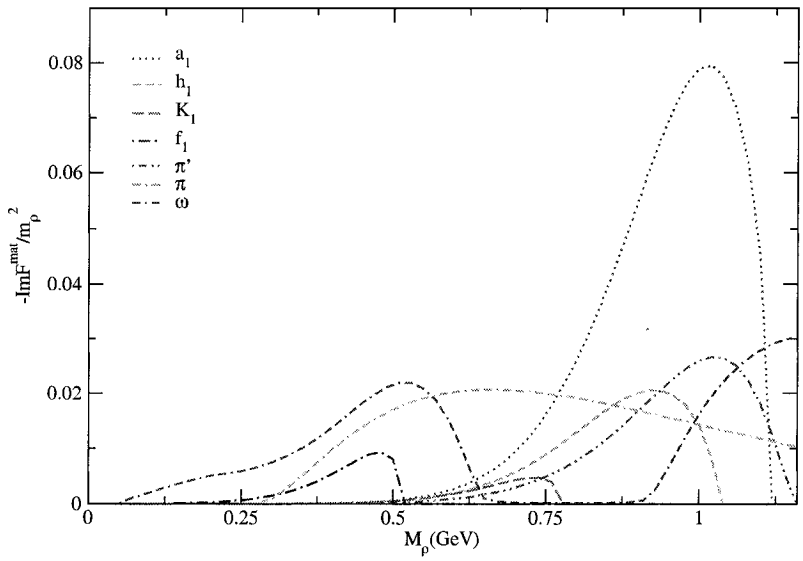

Figure 4.6: Imaginary longitudinal self-energy due to free mesons at ρ three momentum 300 MeV, T=120 MeV

$M = \sqrt{q_0^2 - \vec{q}^2}$, the integrands in the self-energy expressions (4.9,4.10) are singular. In particular, after the frequency sum and analytic continuation, the integrand goes like $f(p)/(q_0 + i\epsilon + s_1 E_X + s_2 E_R)$,$s_1 = \pm, s_2 = \pm$, where the function $f(p)$ depends on the numerator in (4.9,4.10), E_X, E_R are as defined in section 4.2. Thus for the domain $M_{min} < M < M_{max}$ for which $q_0 + s_1 E_X + s_2 E_R = 0$, the real part of the self-energies are Cauchy Principle value integral. Otherwise, for $M < M_{min}, M > M_{max}$, we have a regular integrand. The kinks in the self-energies appear at M_{min}, M_{max}. On the other hand, imaginary part of the self-energies which contain $\delta(q_0 + s_1 E_X + s_2 E_R)$, will be non-zero for $M_{min} < M < M_{max}$. We denote that the ρ self-energy coming from πa_1 loop is the dominant contribution among all the mesons. This is most likely due to the strong coupling $g_{\rho\pi a_1}$ and the domination of the Cauchy Principle value. The interpretation of the imaginary self-energies will be discussed in the following section.

We observe that for the imaginary part there is hardly any difference between

longitudinal and transverse components, so we only plot the longitudinal one. Furthermore the baryon contribution is significantly smaller than the meson contribution; thus we exclude the plots due to baryons for this section. One also notes that the baryon resonances have quite large width and for the treatment in this section we consider zero width, thus zero width baryons are not quite indicative of the true picture. Thus their exclusion is justified. We will in fact include the baryons when considering width in section 4.3.

We also plot the spectral functions (in Fig.4.7 and Fig.4.8) using the expressions (2.79) for ρ_L, ρ_T with $F = \sum_{\rho AB} F^{mat}_{\rho AB} + F^{vac}_{\rho AB}, G = \sum_{\rho AB} G^{mat}_{\rho AB} + G^{vac}_{\rho AB}$. Here $F^{vac}(G^{vac})$ are given by (4.30, 4.31), AB refers to the meson pair or the baryon pair considered in the ρ self-energy loop. One notes that the spectral functions have kinks; this is due to the kinks in the real part of the self-energies. We observe a shift from vacuum mass towards a lower mass, which is also the case for ρ having zero three momentum. Of course in medium, particles in the self-energy loop obtain widths which are not considered here. Thus the shift should not be taken as indicative characteristic of the medium and this calculation is only an approximation. The medium effects are dealt more carefully in section 4.3.

4.2.5 Self-Energy and Scattering Amplitude for Vector Particles

Just like the scalar case considered in section 2.2.2, we can demonstrate the relation between imaginary self-energy and matrix elements for vector particles. From the interaction Lagrangians (4.1-4.6) using Feynman rules for external legs of Feynman graphs, the matrix element squared summed over all possible spin configuration for a three body scattering process is

$$\mathcal{M}^2(p,q,k) = g^2 H^{\mu\nu}(k,p)\mathcal{D}^0_{\mu\nu}(q) = g^2 H^{\mu\nu}(k,p)Q_{\mu\nu}(q) \tag{4.44}$$

where $\mathcal{D}^0_{\mu\nu}(q)$ is the ρ propagator as in (2.63) with $iw_n \rightarrow q_0$ where q_0 is real, $H^{\mu\nu}$ are the tensors appearing in the numerators of (4.9, 4.10) given by (4.11) and (4.19). We

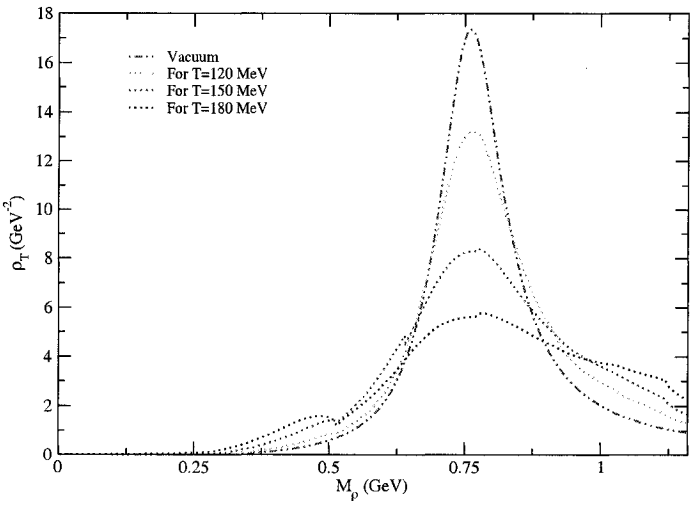

Figure 4.7: Transverse Spectral Function due to mesons as a function of M_ρ for various temperature and the vacuum value at ρ three momentum 300 MeV

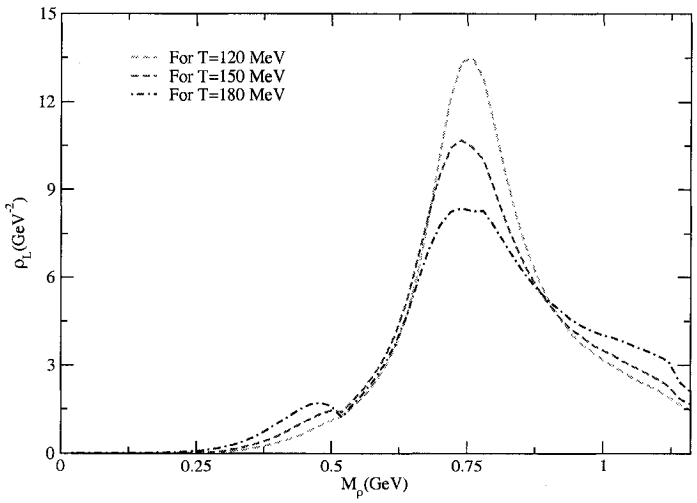

Figure 4.8: Longitudinal Spectral Function due to mesons as a function of M_ρ for various temperature at ρ three momentum 300 MeV

have also used the transversality of $H^{\mu\nu}$ in replacing $\mathcal{D}^0_{\mu\nu}(q)$ with $Q_{\mu\nu}$ above. Now writing the self energy as in (2.73), using the properties (2.75) of $P^{\mu\nu}_{L,T}$ and the generic form of (4.9, 4.10) we have

$$\begin{aligned} Q_{\mu\nu}\Pi^{\mu\nu} &= F + 2G \\ &= -IFg^2T\sum_n \int \frac{d^3p}{(2\pi)^3}\frac{H^{\mu\nu}Q_{\mu\nu}}{[w_n^2+E_X^2][(w_n+w)^2+E_R^2]} \end{aligned} \tag{4.45}$$

The numerator above $H^{\mu\nu}Q_{\mu\nu} = \mathcal{M}^2$ will be a polynomial in iw_n. We denote by A^l the coefficient of of $(iw_n)^l$ in the polynomial; then taking imaginary part, using (4.44) and the frequency sums (2.66) with expression for the free spectral functions we have,

$$\begin{aligned} &\mathrm{Im}F(q_0+i\epsilon) + \mathrm{Im}2G(q_0+i\epsilon) = -g^2IF\pi\int\frac{d^3p}{(2\pi)^3}\int_{-\infty}^{\infty}dp_0\int_{-\infty}^{\infty}dk_0\frac{1}{4w_kw_p}\varepsilon(p_0)\varepsilon(k_0) \\ &(\sum_l A^l p_0^l\delta(q_0-p_0-k_0)\delta(p_0-w_p)\delta(k_0-w_k)(1+f(p_0)+f(k_0)) \\ &+\sum_l A^l p_0^l\delta(q_0-p_0-k_0)\delta(p_0-w_p)\delta(k_0+w_k)(1+f(p_0)+f(k_0)) \\ &+\sum_l A^l p_0^l\delta(q_0-p_0-k_0)\delta(p_0+w_p)\delta(k_0-w_k)(1+f(p_0)+f(k_0)) \\ &+\sum_l A^l p_0^l\delta(q_0-p_0-k_0)\delta(p_0+w_p)\delta(k_0-w_k)(1+f(p_0)+f(k_0))) \\ = \; &-IF\pi\int\frac{d^3p}{(2\pi)^3}\int d^3k\int_{-\infty}^{\infty}dp_0\int_{-\infty}^{\infty}dk_0\frac{1}{4w_kw_p}\varepsilon(p_0)\varepsilon(k_0) \\ &(\mathcal{M}^2_{\rho\to\phi_1\phi_2}\delta^4(q-p-k)\delta(p_0-w_p)\delta(k_0-w_k)(1+f(p_0)+f(k_0)) \\ &+\mathcal{M}^2_{\rho\phi_1\to\phi_2}\delta^4(q+p-k)\delta(p_0+w_p)\delta(k_0+w_k)(-f(p_0)+f(k_0)) \\ &-\mathcal{M}^2_{\rho\phi_1\phi_2\to 0}\delta^4(q+p+k)\delta(-p_0+w_p)\delta(k_0+w_k)(1+f(p_0)+f(k_0)) \\ &+\mathcal{M}^2_{\rho\phi_2\to\phi_1}\delta^4(q-p+k)\delta(p_0+w_p)\delta(-k_0-w_k)(f(p_0)-f(k_0))) \\ = \; &-IF\pi\int\frac{d^3p}{(2\pi)^3}\frac{1}{4w_kw_p}(\mathcal{M}^2_{\rho\to\phi_1\phi_2}\delta(q_0-w_p-w_k)(1+n(w_k)+n(w_p)) \\ &+\mathcal{M}^2_{\rho\phi_2\to\phi_1}\delta(q_0-w_p+w_k)(-n(w_p)+n(w_k)) \\ &+\mathcal{M}^2_{\rho\phi_1\to\phi_2}\delta(q_0+w_p-w_k)(n(w_p)-n(w_k)) \\ &+\mathcal{M}^2_{\rho\phi_2\phi_1\to 0}\delta(q_0+w_p+w_k)(-1-n(w_p)-n(w_k))) \end{aligned} \tag{4.46}$$

where ϕ_1, ϕ_2 are particles in the loop with momentum p, k respectively, q is the momentum of the ρ. We have just demonstrated the relation between self-energy and scattering amplitude for vectors using free propagators. This result in fact helps us explain our plot in figure 4.6. We note from (4.46) that for regions in q_0 phase space where none of the arguments of the delta functions become zero, $\mathrm{Im}F + 2\ \mathrm{Im}G = 0$. Also note that all the $\mathcal{M}^2$ values are positive as they indicate probability and in the range of $q_0 > 0$ where the argument of the delta function obtains zero value, factors $1+n(w_k)+n(w_p), n(w_p)-n(w_k))$ are also positive and thus $\mathrm{Im}F+2\ \mathrm{Im}G < 0$. Figure 4.6 shows $\mathrm{Im}F < 0$ and goes to zero for certain range of q_0; furthermore our calculation for $\mathrm{Im}G$ shows same behavior i.e. $\mathrm{Im}G < 0$ and goes to zero in the same range of q_0 as $\mathrm{Im}F$ does. The negative sign and the range in q_0 for which $\mathrm{Im}F + 2\ \mathrm{Im}G = 0$ is precisely consistent with (4.46) and thus the relationship between imaginary self-energy and scattering amplitude explains our results for $\mathrm{Im}F$ and $\mathrm{Im}G$.

In fact we can comment on the relative strengths of the different contribution to imaginary self-energy plotted in figure 4.6. For a given loop containing $P = \phi_1, A = \phi_2$, where $A = a_1, h_1, k_1, f_1, \omega, \pi'$or π, $P = \pi$ or K, there are four processes as shown by the four matrix elements in (4.46). From figure 4.6, we observe that $a_1\pi$ loop has the highest contribution. Using (4.46), we conclude that $\rho\pi \rightarrow a_1$ is the dominant process among all the scattering processes involving ρAP contained in the self-energy loops.

4.3 Self-Energy at Higher Orders in the Interaction

Having calculated the free theory self-energy, we now want to approximate what happens in an interacting medium. We restrict to the case when one particle in the loop interacts; for meson loop, the π, K propagators are free while a_1, h_1, K_1, w, f_1 interacts with the medium. For the fermion loop the nucleon propagator is free while the resonance interacts. In vacuum π, K and the nucleons only have weak interactions and the width is small enough to neglect; at nonzero temperature they will acquire

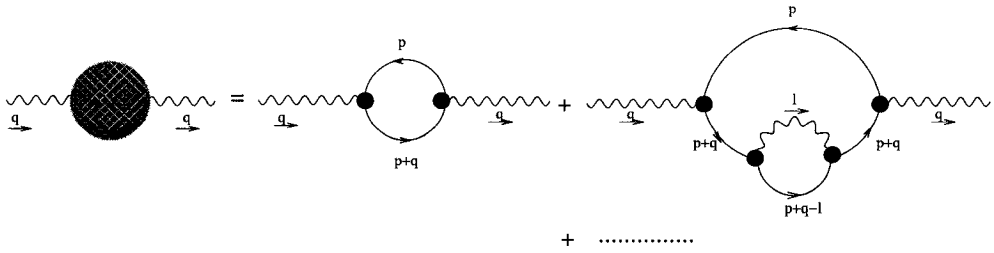

Figure 4.9: Feynman Diagram for the interaction theory

collisional width which will come from diagrams higher order in loop topology and will be suppressed. Thus taking π, K and the nucleon propagator to be free is a good enough approximation for our treatment. The expression for the self-energy is

$$\begin{aligned}
\Pi^{0^-(n=1)}_{\mu\nu}(iw,\overrightarrow{q}) &= -IF\ T\sum_n\int\frac{d^3p}{2\pi^3}\Gamma^{0(n=1)^-}_{\mu}\triangle_F(iw_n,\overrightarrow{p}) \\
&\quad \triangle_{\pi'}(i(w_n+w),\overrightarrow{p}+\overrightarrow{q})\Gamma^{0(n=1)^-}_{nu} \\
\Pi^{1^\pm(n=1)}_{\mu\nu}(iw,\overrightarrow{q}) &= -IF\ T\sum_n\int\frac{d^3p}{2\pi^3}\Gamma^{1(n=1)^\pm}_{\mu\alpha}\triangle_F(iw_n,\overrightarrow{p}) \\
&\quad \triangle^{\alpha\beta}(i(w_n+w),\overrightarrow{p}+\overrightarrow{q})\Gamma^{1(n=1)^\pm}_{\beta\nu} \\
\Pi^{1^+(n=2)}_{tf}(iw,\overrightarrow{q}) &= -IF\ T\sum_n\int\frac{d^3p}{2\pi^3}\Gamma^{1(n=2)^+}_{\mu\alpha t}\triangle^{\mu\nu}_F(iw_n,\overrightarrow{p})\Gamma^{1(n=2)+}_{\nu\beta f} \\
&\quad \triangle^{\beta\alpha}(i(w_n+w),\overrightarrow{p}+\overrightarrow{q}) \qquad (4.47)
\end{aligned}$$

$$\begin{aligned}
\Pi^{\pm}_{(J)\mu\nu}(iw',\overrightarrow{q}) &= -IF\,T\sum_n\int\frac{d^3p}{2\pi^3} \\
&\quad -\mathrm{Tr}[\tilde{\triangle}_F(p)\Gamma^{\pm}_{\mu\alpha}(q)\tilde{\triangle}^{\alpha\beta}_{(2m+1)/2}(p+q)\Gamma^{\pm}_{\nu\beta}(-q)] \qquad (4.48)
\end{aligned}$$

with Γ is as in (4.12, 4.20) but $\triangle^{\alpha\beta}, \triangle_{\pi'}, \tilde{\triangle}^{\alpha\beta}_{(2m+1)/2}$ are the dressed propagators, $m = 1, 2$ representing spin $3/2, 5/2$; $\triangle_F(iw_n,\overrightarrow{p}) = 1/(w_n^2+\overrightarrow{p}^2+m^2)$ is the free scalar propagator, $\triangle^{\mu\nu}_F(iw_n,\overrightarrow{p})$ is as in (2.63) and $\tilde{\triangle}_F(p)$ is defined by (2.64). In computing (4.47, 4.48) we will encounter frequency sums of the form (2.53) and (2.52); using (2.80) for the dressed boson and the free spectral representation for the π, K propagator (2.64) with ρ^v_0 given by (2.67) we can evaluate (4.47) provided we know ρ_A thus according to (2.72), the self energies Π_A's. We approximate Π_A with the vacuum value Π^{vac}_A as that is the leading order contribution. In vacuum there is no difference

between three dimensionally transverse and longitudinal components, $F^{vac} = G^{vac}$ and we obtain (2.81). For the fermion loop (4.48) we use (2.82) for the dressed fermion and free theory spectral representation of the nucleon propagator (2.64) with ρ_0^f given by (2.67). Note that after all these substitutions the numerators in both (4.47, 4.48) are exactly given by (4.13, 4.23) once we factor out $\rho_A, \rho_0^{v,f}$. Thus we have all the necessary expressions and after writing the numerator as a polynomial in iw_n, iw_n', computing the frequency sum gives us (2.84) and the corresponding equation for the fermions. All we need to know now are ρ_A, ρ^f.

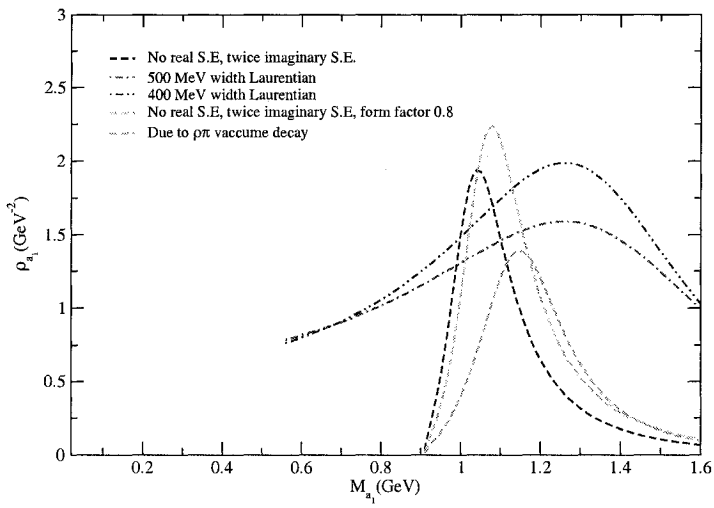

Figure 4.10: Comparisons of a_1 spectral functions

We can obtain ρ_A by using (4.30) with replacing M_R with m_ρ and M_X with m_π or m_K to get F_A^{vac} with setting the form factor to be one. This is valid as the couplings for A loop are exactly same as ρ loop; i.e. $g_{\rho PA} = g_{A\rho P}$ and we ignore form factor for the A loop for simplification. ρ_{a_1} such obtained is plotted in figure 4.10. One notes that here we are only considering one interaction as shown in the Feynman diagram; as we are using vacuum self-energy, we expect the pole mass to be the bare mass and the the spectral function resembling the vacuum quantity as tabulated by Particle Data Group (PDG). Our spectral function is only an approximation coming from a single interaction. When all interactions are considered we expect our spectral

function to agree with the PDG data.

We note that our explicitly derived spectral function using (4.30) is similar to a Lorentzian-like distribution. As we consider more interactions, the imaginary part always grows from our single interaction calculation but the real part can increase or decrease; to see the effect we also plot the a_1 spectral function obtained by multiplying the imaginary part of a_1 self-energy coming from the $\rho\pi$ vacuum loop, taking real self-energy to be zero and varying the form factor. Note that if we consider $a_1 \rightarrow \pi\pi\pi$ decay we would have non vanishing spectral function starting from three pion mass that is 560 MeV. Taking this calculation as an indicator, we approximate that the effect of all the interactions will result in ρ_A, ρ^f being a Lorentzian having the corresponding experimental width and the pole mass given by PDG. That is we take ρ_A, ρ^f to be

$$\rho(M) = \frac{4\Gamma_{\text{exp}} m \theta(L)}{(M^2 - m^2)^2 + (2\Gamma_{\text{exp}} m)^2} \tag{4.49}$$

where m is the observed mass, Γ_{exp} is experimental width, M is invariant mass. We use this Lorentzian spectral function having a cutoff given by $\theta(L)$ with L given by (4.28) in the rest of the calculation. In (4.28) we choose M_X, M_R to be the lowest two masses the particle can decay to. The Lorentzian spectral function for a_1 is also plotted for two widths. The experimental widths are taken from PDG with picking $\Gamma^{a_1}_{\text{exp}} = 400$ MeV, $\Gamma^{\pi'}_{\text{exp}} = 400$ MeV as these widths have a range and the rest of the widths are taken to be PDG's best estimated values. It turns out that for the cases where we have a range of widths, the result for the self-energies do not vary significantly and thus picking an intermediate width in the range is justified.

We recognize that in giving this interaction representation to the spectral function we have given width to the particle meaning that the on shell condition has been relaxed. In the following plots we present imaginary and real parts of the self-energy with the choice (2.76); we also plot transverse and longitudinal spectral function of the ρ meson using (2.79) with $F(G) = \sum F_{\rho AB}(G_{\rho AB})$, AB denoting the pair of mesons or baryons of the ρ self-energy loop and $F(G) = F^{vac}(G^{vac}) + F^{mat}(G^{mat})$. In all the plots ρ meson's three momentum is 300 MeV and just as a comparison

we have also included $\rho\pi\pi$ self energies in the plots which is in fact a free theory calculation. For the baryon loop we have omitted plotting NN contribution as it is insignificant. Also note we take F^{vac}, G^{vac} here as computed in 4.2.1 which will be the leading contribution.

Comparing Fig. 4.11 and Fig. 4.12 with Fig. 4.4 and Fig.4.5 respectively, we observe that the kinks have smoothened out and magnitude of each channel $a_1, h_1, k_1, f_1, \omega, \pi'$ has decreased. We also observe that the amplitude has gone down more for the channels given higher width. We can explain this behaviour by looking at (2.84), the expression for frequency sum, which we obtain in evaluating the self-energies (4.47, 4.48). The Cauchy Principle value integral for a finite domain in M which generates the kink (at the boundary of that finite domain) and dominates the overall magnitude of the self-energies, is now weighted by the spectral functions ρ_A, ρ^f which are Lorentzians. As we increase the width of a Lorentzian, the magnitude of it's peak goes down, resulting in a decrease in the self-energy. Also from (2.84) with $k_1 = p, k_2 = p + q, iw \to q_0 + i\epsilon$, we observe that $q_0 \pm E_1 - y = 0$ is possible for all $M > 0$ as $-\infty < y < \infty$. Thus, Cauchy Principle value is present in (2.84) for all $M > 0$ and there is no boundary point M_{min}, M_{max} and thus no kink. Of course if we make the width of the Lorenztian to go to zero, we end up with a delta function. This will force $y = \pm E_2$ and again we have the kinks. The Lorenztians with finite width have effectively replaced the kinks with smooth peaks. But note that as f_1 has very small width, the peak is quite sharp.

In Fig.4.13 and Fig.4.14 we have plotted real self-energy of ρ due to baryons. As baryons have large width, we have smooth peaks (compared to Fig.4.2) and overall magnitude is quite small compared to the meson contributions. This is possibly due to zero chemical potential and small couplings f_{JP}'s. From Fig.4.15-Fig.4.18, we plot the imaginary parts of the self-energies in interaction theory. Again due to weighting by the Lorentzian spectral functions, the imaginary parts go smoothly to small values but not zero as in the free theory case. This is because $\delta(q_0 \pm E_1 - y)$ always contributes nontrivially as $q_0 \pm E_1 - y = 0$ for all $M > 0$. Comparing Fig.4.16 with Fig.4.6, we observe that the magnitude has gone down in the interaction theory case (Fig.4.16)

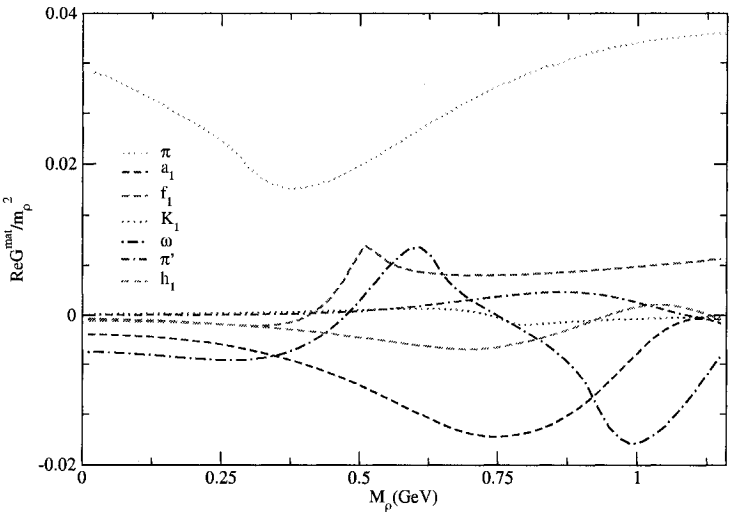

Figure 4.11: Real part of transverse self-energy as a function of M for T=120 MeV including mesons with width

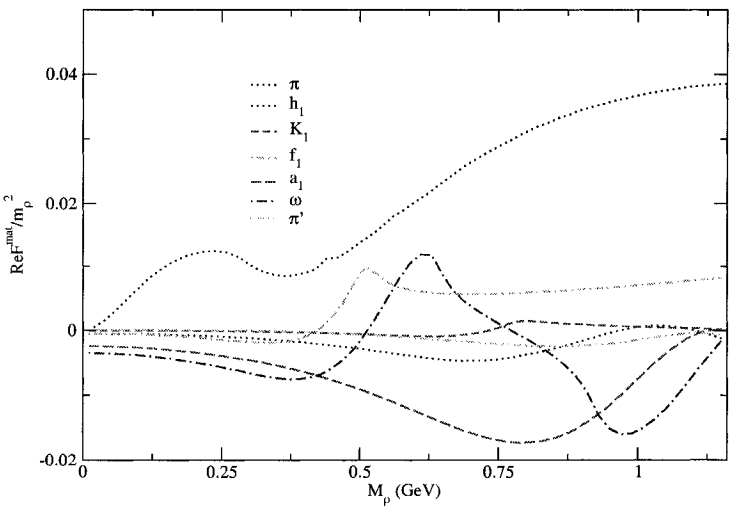

Figure 4.12: Real part of longitudinal self-energy as a function of M for T=120 MeV including mesons with width

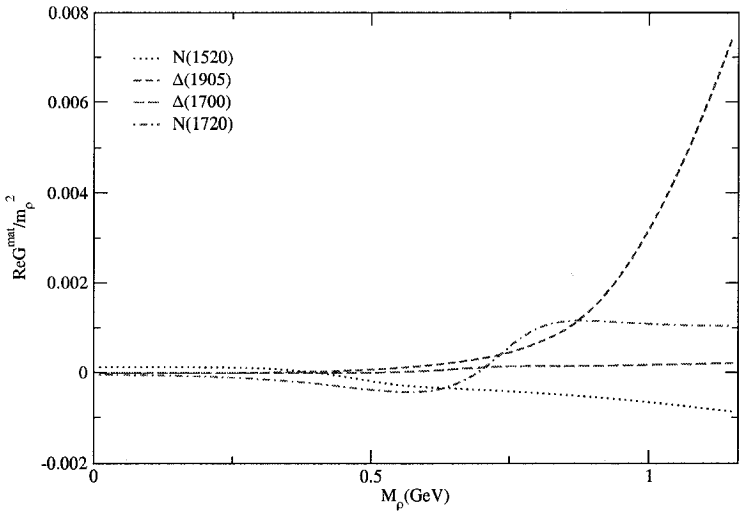

Figure 4.13: Real part of transverse self-energy as a function of M for T=120 MeV including baryons with width

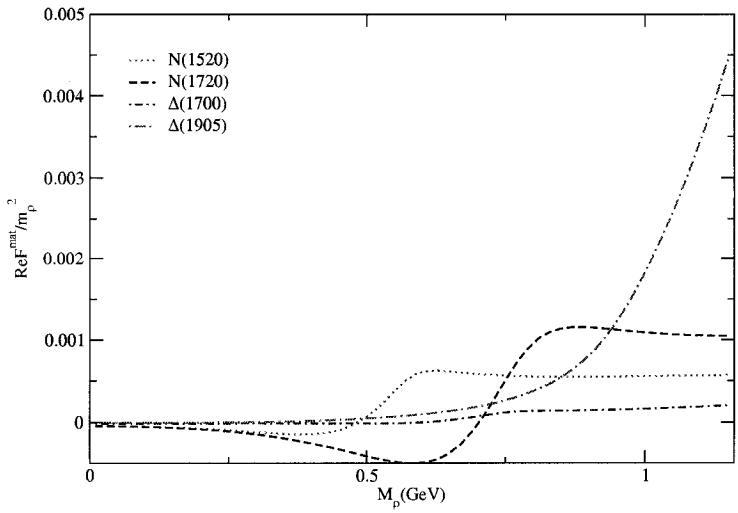

Figure 4.14: Real part of transverse self-energy as a function of M for T=120 MeV including baryons with width

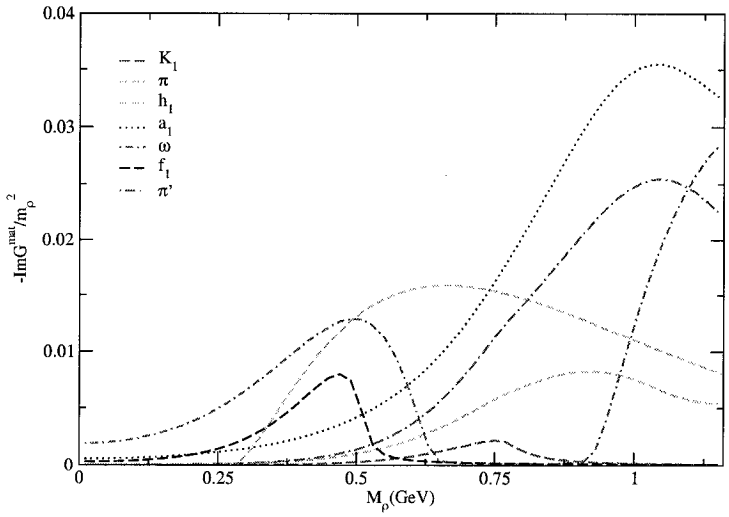

Figure 4.15: Imaginary part of transverse self-energy as a function of M for T=120 MeV including mesons with width

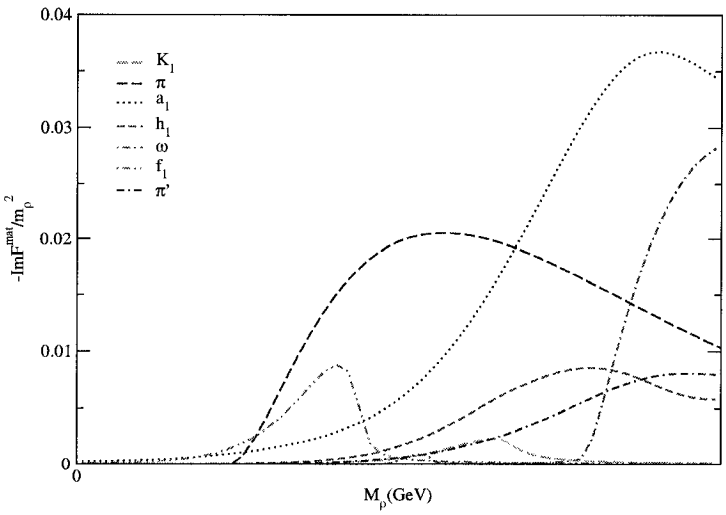

Figure 4.16: Imaginary part of longitudinal self-energy as a function of M for T=120 MeV including mesons with width

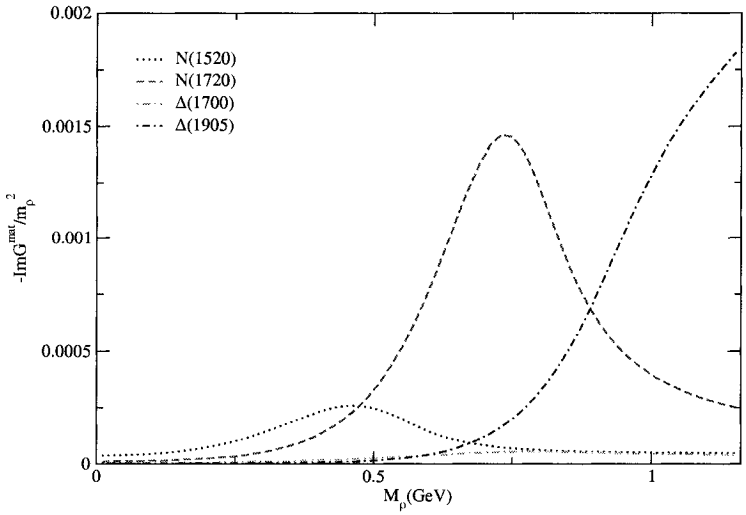

Figure 4.17: Imaginary part of transverse self-energy as a function of M for T=120 MeV including baryons with width

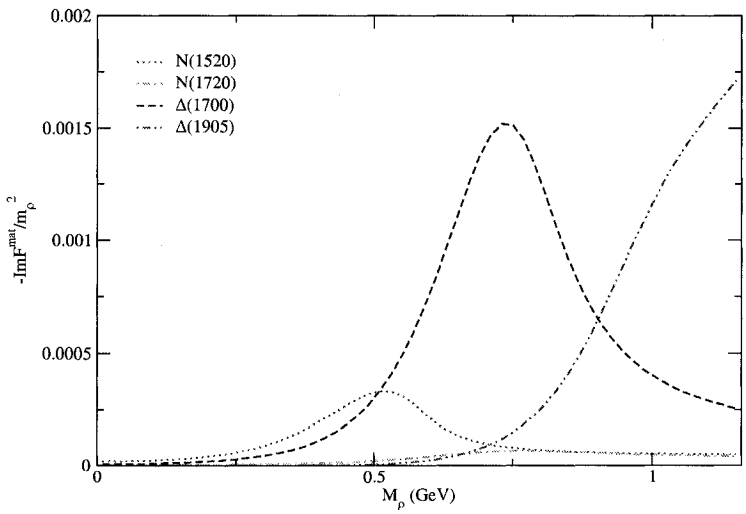

Figure 4.18: Imaginary part of longitudinal self-energy as a function of M for T=120 MeV including baryons with width

which is expected due to the non zero width of the Lorenzian.

Finally we plot the spectral functions for interaction theory. The longitudinal spectral function indicates a shift of the location of the peak towards higher mass (compared to vacuum mass) while the transverse spectral function peak location remains almost unchanged. Both functions broaden as temperature goes up while the kink at high invariant mass appearing in the vacuum spectral function have disappeared. This is because the real self-energy for interaction theory has no kinks and smooth structure for high ρ invariant mass. There is still a kink at around 515 MeV which is due to the sharp peak in the real self-energy due to $\rho f_1 \pi$. Comparing Fig.4.19, Fig.4.20 with Fig.4.7 and Fig.4.21, Fig.22 with Fig.4.8, we observe that while the heights of the peaks are quite comparable, location of the peaks in interaction picture has shifted towards higher mass instead of lower mass as in free theory. The location of the peak is sensitive to the real part of the self-energy around vaccum value of ρ mass,$M \sim 0.77GeV$. Comparing real parts of the sum of all self-energies around $M \sim 0.77GeV$, we see that in the interaction case, the real part is positive and for free theory it is negative. Thus we have mass incease in interaction thoery while a decrease in free theory.

The self energies thus obtained in both 'free' and 'interaction' theory are transverse which is required by current conservation. (3.21) implies that the ρ field is proportional to a conserved current and thus ρ self-energy is a current current correlator which must be conserved too. Our calculation also satisfies transversality. For the 'free' theory case it is easily seen by looking at explicit expressions (4.13, 4.23) for the numerators of (4.9, 4.10); as $q_\mu Q^{\mu\nu}(q) = q_\mu K^{\mu\nu}(q) = 0$, the presence of $Q^{\mu\nu}, K^{\mu\nu}$ guarantees transversality. For 'interacting' theory boson loop (4.47), we first make the observation that in (4.11) the terms which are proportional to $1/m_R^2$ do not get any contribution from other terms as particles are not on shell. So after tensors are contracted the terms proportional to $1/m_R^2$ still remain unaffected. Now using the first equation in (2.81) we see that the numerator in (4.47) will have terms proportional to $1/k^2$ or $1/m_R^2$ and terms which are proportional to neither, with denominator having four powers of momentum. We see that the terms proportional to $1/k^2$ and the non

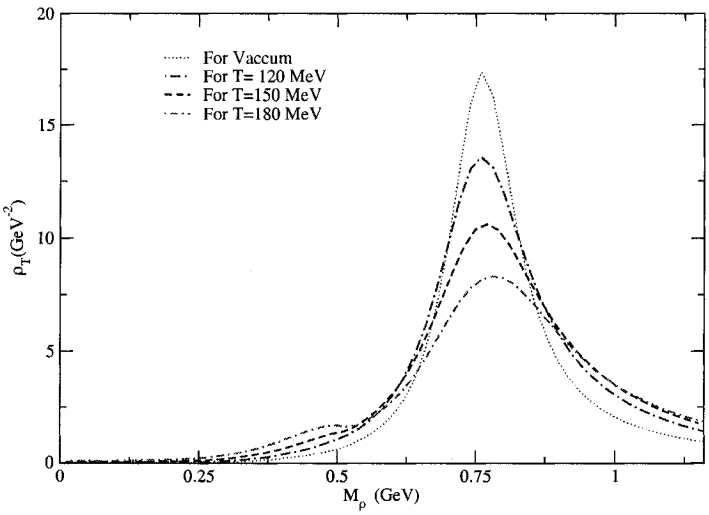

Figure 4.19: Transverse Spectral Function including interacting mesons

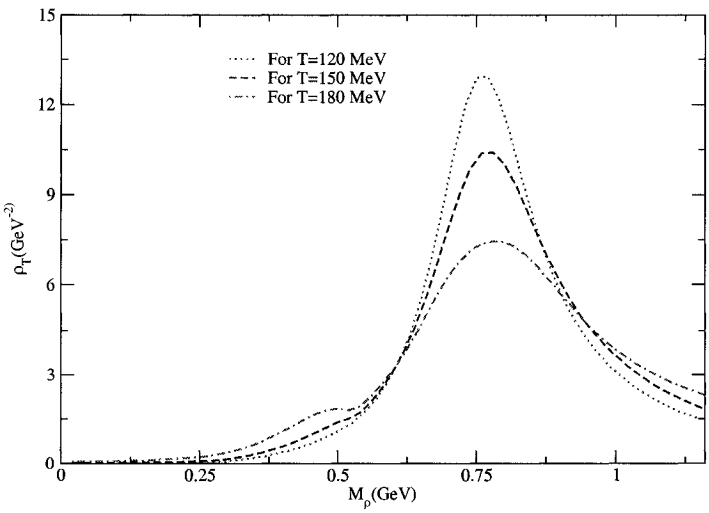

Figure 4.20: Transverse Spectral Function including interacting mesons and baryons

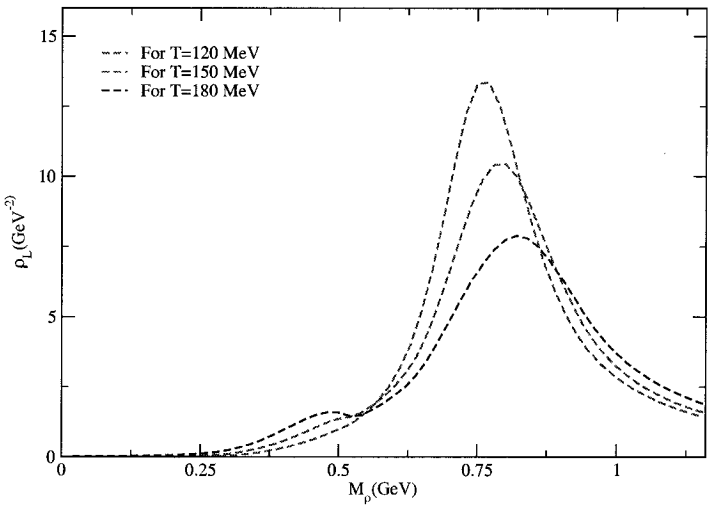

Figure 4.21: Longitudinal Spectral Function including interacting mesons

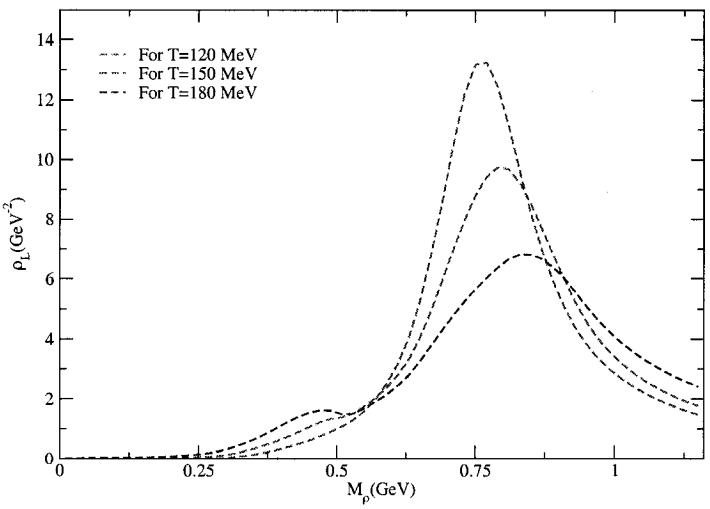

Figure 4.22: Longitudinal Spectral Function including interacting mesons and baryons

proportional terms, after taking out the common factor ρ^V are exactly those in (4.11, 4.13). Also the terms proportional to $1/m_R^2$ are exactly negative of those which are proportional to $1/m_R^2$ in (4.11, 4.13). This is precisely due to our observation mentioned above. Note that all the terms in (4.13) are either proportional to $Q^{\mu\nu}$ or $K^{\mu\nu}$ thus all the terms in the numerator of (4.47) will be proportional to these tensors and the self-energy (4.47) will be transverse. For the fermion loop (4.48) using (2.82) we see that once we take out the common factor ρ^f the tensor in the numerator of (4.48) is exactly equal to (4.19, 4.23) which is is transverse and so is (4.48).

Chapter 5

Conclusions

In this thesis we have applied effective field theory techniques to obtain the self-energy for the vector meson ρ in thermal environments where temperature reaches up to 180 MeV. Our approach is an independent one which relies on computing the ρ propagator using the path integral formalism aided by Feynman diagrams. Firstly we compute the one loop self-energy with propagators in the loop being free. Next we consider the case when one propagator is dressed and the other is free. We note that the spectral functions for the dressed propagator is similar to a Lorentzian and thus we use Lorentzian spectral functions for the 'dressed' particle in the loop.

Our treatment is independent from that of [15] which relies on computing scattering amplitudes. They have restricted to the case where the interaction is with the mesons only whereas we extend the analysis to include baryons. The overall shape of the self-energy and the spectral function of the ρ when including dressed propagators in the loop is in agreement with their result but we observe a shift towards higher mass when considering interaction with the mesons only. When including the baryons, we have computed the coupling constants which are consistent with experimental decay rates. With this inclusion, the mass shift gets slightly higher and the width of the spectral function grows. This is to be expected as adding baryons increases the imaginary part of the self-energy resulting in the broadening. For the case when we have free propagators in the loop, real self-energy is not a smoothly behaving function of invariant mass with kinks coming from the threshold effect of the Cauchy Principle

Value integral. In particular there are big kinks at 1120 MeV coming from $a_1\pi$ loop and at 515 MeV coming from $f_1\pi$ loop. This in turn results in threshold effect in the spectral function at 515 MeV, 770 MeV and 1120 MeV. The kink at 770 MeV is due to the non smooth behavior of real self-energy around 770 MeV. All the irregularities except the one at 515 MeV disappear when we consider dressed propagator as that treatment results in smoothly behaving real self energies. The kink at 515 MeV remains as a testimony to the small width of f_1. Overall the spectral function broadens and mass gets shifted towards higher values as temperature is increased up to possible chiral symmetry restoration value. This increase is consistent with the results obtained in [24] with a simple model. Considering Weinberg sum rules discussed in chapter three, this would suggest that a_1 spectral function shifts towards lower pole mass and gets flatter for the cancellation to occur. Thus our treatment seems to suggest the scenario where both axial and vector mesons melt away as temperature rises and we essentially get free pions as we reach chiral symmetry.

We have also derived independently 'Matsubara Frequency' sums vital for treating dressed propagators. We have related imaginary self-energy with amplitude of different scattering processes for scalars and vector bosons.

For comparison with experiments, the spectral functions obtained needs to be folded into a time evolution model describing the produced medium in heavy ion collisions to finally compute dilepton production rates. The NA60 experiment [21] at CERN provides dilepton production rates for invariant mass region relevant to our calculation; thus our calculation provides vital tool to compare effective field theory methods with experiments and could prove to be a key element in analyzing the thermal medium.

Bibliography

[1] G.Boyd, et al. Phys. Rev. Lett. **75**, 4169 (1995).

[2] J.W.Harris and B.Muller, Ann. Rev. Nucl. Part. Sci. **46**, 71 (1996).

[3] J.Rafelski and B.Muller, Phys. Rev. Lett. **48** (16), 1066 (1982).

[4] T.Matsui and H. Satz, Phys. Rev. Lett. B **178**, 416 (1986).

[5] C.Gale, Nucl.Phys. A, **698**, 143 (2001).

[6] *http://pauli.uni-muenster.de/latfor/Schmidt.pdf*

[7] C.Gale and K.L.Haglin, Invited review for QGP3, R. Hwa and X.-N. Wang eds.

[8] Joseph I. Kapusta and Charles Gale, *Finite-Temperature Field Theory: Principles and Applications*, Cambridge University Press (Cambridge, 2006).

[9] R.Rapp and J. Wambach, Adv. Nucl. Phys. **25**, 1 (2000).

[10] S.Turbide, R.Rapp and C.Gale, Phys. Rev. C **69**, 014903 (2004).

[11] Charles Gale, Joseph I.Kapusta, Nucl. Phys. B **357**, 65 (1991).

[12] G. Chanfray and P. Schuck, Nucl. Phys. A **545** (1992) 271C.

[13] R. Rapp, G. Chanfray and J. Wambach, Phys. Rev. Lett. **76**, 368 (1996) [arXiv:hep-ph/9508353].

[14] R. Rapp, G. Chanfray and J. Wambach, Nucl. Phys. A **617**, 472 (1997) [arXiv:hep-ph/9702210].

[15] Ralph Rapp and Charles Gale, Phys. Rev. C **60**, 024903 (1999).

[16] V. L. Eletsky, M. Belkacem, P. J. Ellis and J. I. Kapusta, Phys. Rev. C **64**, 035202 (2001) [arXiv:nucl-th/0104029].

[17] T. E. O. Ericson and W. Weise, *Oxford, UK: Clarendon (1988) 479 P. (The International Series of Monographs on Physics, 74)*

[18] R. Rapp and J. Wambach, Nucl. Phys. A **573**, 626 (1994) [arXiv:nucl-th/9311018].

[19] S. Jeon and P. J. Ellis, Phys. Rev. D **58**, 045013 (1998) [arXiv:hep-ph/9802246].

[20] V. L. Eletsky, B. L. Ioffe and J. I. Kapusta, Eur. Phys. J. A **3**, 381 (1998) [arXiv:nucl-th/9807072];V. L. Eletsky and J. I. Kapusta, Phys. Rev. C **59**, 2757 (1999).

[21] R. Arnaldi *et al.* [NA60 Collaboration], Phys. Rev. Lett. **96**, 162302 (2006) [arXiv:nucl-ex/0605007].

[22] Steven Weinberg, Phys. Rev. Lett. **18**, 13 (1967).

[23] J.J. Sakurai, *Lectures on New Mesons, Resonances and Unitary Symmetry*, Tata Institute of Fundamental Research, Bombay, (1963).

[24] Robert D. Pisarski, Phys. Rev. D **52**, 7 (1995).

[25] J.I. Kapusta and E.V. Shuryak, Phys. Rev. D **49**, 9 (1994).

[26] C. Song, Phys. Rev. D **48**, 1375 (1993)

[27] G. Brown and M. Rho, Phys. Rev. Lett. **66**, 2720 (1991).

[28] E.V. Shuryak, Rev. Mod. Phys. **65**, 1 (1993).

[29] J.F.Donoghue, E.Golowich, B.R.Holstein, *Dynamics of Standard Model*, Cambridge University Press (Cambridge, 1992).

[30] M.A. Shifman, A.I.Vainshtein and V.I. Zakharov, Nucl. Phys. B **147**, 385 (1979); B **147**, 448 (1979), B **147**,519 (1979).

[31] Michel Le Bellac, *Thermal Field Theory*, Cambridge University Press (Cambridge, 1996).

[32] Jean-Paul Blaizot, Edmond Iancu, Physics Reports **359**, 355 (2002)

[33] H.Arthur Weldon, Phys. Rev. D **28**, 8 (1983).

[34] J.J.Sakurai, *Modern Quantum Mechanics*, Addison-Wesley (Reading 1994).

[35] W.Rarita and J.Schwinger, Phys. Rev. **60**, 61 (1941)

[36] Michael E.Peskin and DanielV.Schroeder, *An introduction to Quantum Field Theory*, Westview Press (1995).

[37] Ulf-G.Meissner, Phys.Rep.**161, Nos.5** and **6**, 213 (1988).

[38] I.Zahed and G.E.Brown, Phys. Rep. **142**, 1 (1986).

[39] E.Witten, Nucl. Phys. B **223**, 422 (1983).

[40] W.A.Bardeen, Phys. Rev. **184**, 1848 (1969).

[41] C.Itzykson and J.Zuber, *Quantum Field Theory*, McGraw-Hill Book Company (New York, 1980).

[42] R. Machleidt, Adv. Nucl. Phys. **19**, 198 (1989).

[43] Bing Ann Li, Phys. Rev. D **52**, 5165 (1995).

[44] H.Gomm, O.Kaymakcalan and J Schechter, Phys. Rev. D **30**, 594 (1984).

[45] Huang Shi-Zhong, Zhang Peng-Fei, Ruan Tu-Nan, Zhu Yu-Can, Zheng Zhi-Peng, Eur. Phys. J. C **42**, 375 (2005).

[46] Octavian Teodorescu, Abhee K. Dutt Mazumdar, Charles Gale, Phys.Rev. C **66**, 015209 (2002).

[47] D. M. Brudnoy, Phys. Rev. Lett. **14**, 273 (1965).

[48] W.Peters, M.Post, H.Lenske, S.Leupold and U.Mosel, Nucl. Phys. A **632**, 109 (1998).

[49] P.Ramond, *Field Theory:A Modern Primer*, Second Edition, Addison-Wesley Publishing Company, Inc. Redwood City, California (1989).